AD-762 204

FRAGMENT HAZARD STUDY: GRADING AND ANALYSIS OF 15MM YUMA TEST FRAGMENTS

David I. Weinstein

IIT Research Institute

Prepared for:

Department of Defense Explosives Safety Board

October 1972

FRAGMENT HAZARD STUDY: GRADING AND ANALYSIS OF 155mm YUMA TEST FRAGMENTS

Contract DAAB09-72-C-0051

Final Technical Report
IITRI J6272

October 1972

Distribution of this document is unlimited.

Department of Defense Explosives
Safety Board
Forrestal Building, Room GB 270
Washington, D.C. 20314

IITRI

Engineering Mechanics Division
IIT Research Institute
10 West 35th Street
Chicago, Illinois 60616

Final Technical Report IITRI J6272
Contract DAAB09-72-C-0051

FRAGMENT HAZARD STUDY: GRADING AND ANALYSIS OF 155mm YUMA TEST FRAGMENTS

Department of Defense Explosives
Safety Board
Forrestal Building, Room GB 270
Washington, D.C. 20314

Prepared by:

D. I. Feinstein

October 1972

Final Report for Period April 1972 to October 1972

FOREWORD

Under Contract DAAB09-72-C-0051 between IIT Research Institute (IITRI) and the U.S. Army Electronics Command - Washington, IITRI is performing a study of fragmentation hazards to unprotected personnel; specifically the grading and analysis of 155mm Yuma test fragments. This is the final report of the study which was carried out during the period April 1972 to October 1972.

The work was conducted for the Department of Defense Explosives Safety Board and supervised by Col. W. Cameron III, Chairman; Lt. Col. J. H. Coder, Project Manager; and Dr. T. A. Zaker, Explosives Scientist. Principal contributors to the presently reported work included D. I. Feinstein and R. Wlezien. Special acknowledgement is made to Dr. Zaker for providing overall technical direction to this study.

Respectfully submitted,
IIT RESEARCH INSTITUTE

D. I. Feinstein

D. I. Feinstein
Research Engineer

APPROVED:

E. P. Bergmann

E. P. Bergmann, Manager
Civil Engineering Systems
and Explosives

Unclassified
Security Classification

DOCUMENT CONTROL DATA - R & D

(Security classification of title, body of abstract and indexing annotation must be entered when the overall report is classified)

1. ORIGINATING ACTIVITY (Corporate author)	2a. REPORT SECURITY CLASSIFICATION
IIT Research Institute 10 West 35th Street Chicago, Illinois 60616	Unclassified
	2b. GROUP

3. REPORT TITLE

FRAGMENT HAZARD STUDY: GRADING AND ANALYSIS OF 155mm YUMA TEST FRAGMENTS

4. DESCRIPTIVE NOTES (Type of report and inclusive dates)

Final Report

5. AUTHOR(S) (First name, middle initial, last name)

David I. Feinstein

6. REPORT DATE	7a. TOTAL NO. OF PAGES	7b. NO. OF REFS
October 1972	80	6

8a. CONTRACT OR GRANT NO.	9a. ORIGINATOR'S REPORT NUMBER(S)
DAAB09-72-C-0051 b. PROJECT NO.	J6272
c.	9b. OTHER REPORT NO(S) (Any other numbers that may be assigned this report)
d.	

10. DISTRIBUTION STATEMENT

Distribution of this document is unlimited.

11. SUPPLEMENTARY NOTES	12. SPONSORING MILITARY ACTIVITY
	DOD Explosives Safety Board Forrestal Building, Rm. GB 270 Washington, D.C. 20314

13. ABSTRACT

Metal fragments collected from the ground surface following the experimental detonation of 1000 155-mm projectiles were graded and weighed, and the results have been analyzed. The analysis consists of a determination of the resulting fragment size distribution and hazard associated with the test detonation. In addition, results of the analysis have been compared with analytic results for a single munition and test results of another stack of 155-mm projectiles that were detonated within an igloo.

DD FORM 1473 (PAGE 1) REPLACES DD FORM 1473, 1 JAN 64, WHICH IS OBSOLETE FOR ARMY USE.
S/N 0101-807-6801

Unclassified
Security Classification

14. KEY WORDS	LINK A		LINK B		LINK C	
	ROLE	WT	ROLE	WT	ROLE	WT
Fragment Safety						
Fragment Trajectories						
Fragment Velocities						
Projectile Fragmentation						
Stacked Projectiles						
Far Field Fragment Distribution						

ABSTRACT

Metal fragments collected from the ground surface following the experimental detonation of 1000 155-mm projectiles were graded and weighed, and the results have been analyzed. The analysis consists of a determination of the resulting fragment size distribution and hazard associated with the test detonation. In addition, results of the analysis have been compared with analytic results for a single munition and test results of another stack of 155-mm projectiles that were detonated within an igloo.

CONTENTS

ILLUSTRATIONS

ILLUSTRATIONS (Continued)

ILLUSTRATIONS (Continued)

ILLUSTRATIONS (Concluded)

TABLES

GRADING AND ANALYSIS OF 155 mm YUMA TEST FRAGMENTS

1. INTRODUCTION

Working under direction of the Department of Defense Explosives Safety Board, IITRI has been conducting a series of investigations concerning fragment hazards associated with accidental detonation of munitions.

Phase I (Ref. 1) of this study was concerned with establishing quantitative damage criteria in terms of fragment mass, velocity, and attack angle for various targets including standing personnel, vehicles, aircraft, buildings and open weapon stores. In Phase II an analytical model was developed to predict the density of fragments and the probability of damage to the targets considered in Phase I from explosion of individual munitions of various types. These included gun projectiles and general purpose bombs. Here damage probability contours were obtained in polar coordinates for a horizontal orientation of the munition axis in each case. Phase III attempted to extend the fragment hazard model for individual munitions to the case of multiple munitions in open stores (Ref. 2). The result was a limited demonstration that an analytic model could be developed to describe the initial fragment field of a stack of munitions. However, it was also brought out that this initial fragment field was often related to munition case design, stack configuration and mode of initiation.

The most recent study, prior to this investigation, resulted in the development and documentation (Ref. 3) of a computer model which generates the information necessary in establishing minimum separation distances between various munition types and personnel in order to mitigate fragment hazards. The model specifically treats the fragment hazard associated with a single munition and has been utilized to generate single unit fragment hazard data for seven common military munitions. While single unit detonation does not represent a realistically severe accident

situation, previous work indicates that multiple unit (i.e., stacks) fragment hazards may be proportional to single unit results. In support of this hypothesis, the computer model has generated results which compared favorably with experimental results from stacks of 750 lb bombs, obtained in the NWC-China Lake tests of March 1970.

The results generated by the computer model are dependent upon, and quite sensitive to, the munition effectiveness data which are input. These data were originally generated to support munition effectiveness studies and are the result of explosive tests of single unit munitions. This is the only known source of information concerning near field estimates of munition fragment size, number and initial velocity. However, since it has been collected to be utilized in weapon effectiveness studies, it is primarily concerned with the fragments which are effective within the applicable range of the munition. This has normally led to a set of data which has a high degree of resolution, in terms of weight intervals, where the greatest number of fragments are concentrated. This unfortunately is at a rather low fragment weight (e.g., below 300 grains). The remaining fragment weight of the munition is quite substantial, but because it does not break down into very many fragments and is not always projected into the designed zones of munition effectiveness, its recorded resolution is usually quite poor.

Another inadequacy of recorded munition effectiveness data is concerned with its use in representing the basis for multiple unit munitions fragment hazard analysis. Here, the primary concern is whether the munition fragment size, number and initial velocities will be similar for munitions in single and multiple units. As noted previously, results coming out of previous detonation tests of stacked munitions indicate that thin wall "bomb type" munitions tend to fragment into similar size fragemnts for both multiple and single units. However, qualitative appraisal of similar results for thickwall "shell type" munitions indicated marked dissimilarities between multiple and single unit munitions.

The present study is a detailed investigation of one of these shell type stacked munition tests, the AMC-Yuma test, and a comparison of this test with another somewhat similar test, the Eskimo I test.

1.1 Description of AMC-Yuma Experiment

In June 1970, an experiment that included the detonation of a stack of 155-mm projectiles was carried out by the Army Material Command (AMC) at the Yuma Proving Grounds. The AMC-Yuma experiment used two configurations of stacked 155-mm shells as shown in Figure 1. The first experiment consisted of 1000 units of 155-mm shells stacked 10 high and 100 wide in a parallel array with minimum spacing between projectiles. The stack was detonated by a single, centrally located 155-mm projectile with the remainder of the stack initiated by sympathetic detonation. The second experiment consisted of three stacks of 1000 155-mm projectiles; each, 10 projectiles high by 100 projectiles long. The center, or donor, stack was oriented nose-to-nose with respect to one stack and base-to-base with respect to the other. The stacks were 50 in. apart. The 155-mm artillery projectiles used in these experiments incorporated these nominal parameters of interest:

(1) Total assembly weight: 97 lbs.
(2) TNT
(3) Metal component weight: 82 lbs.

The projectiles were provided with ring-type nose plugs and protective grommets on the rotating bands. The stacked projectiles were supported by wooden end structures, and plywood shim dunnage, only as required to maintain stack levelness. Thus all recovered fragments were components of the projectile case material. After each detonation, resulting fragments were collected from preselected sectors and subsequently were weighed in the aggregate and crated for shipment to IITRI. Figure 2 illustrates these preselected collection cell specifications.

A. Yuma 1000 Unit 155mm Projectile Stack Test

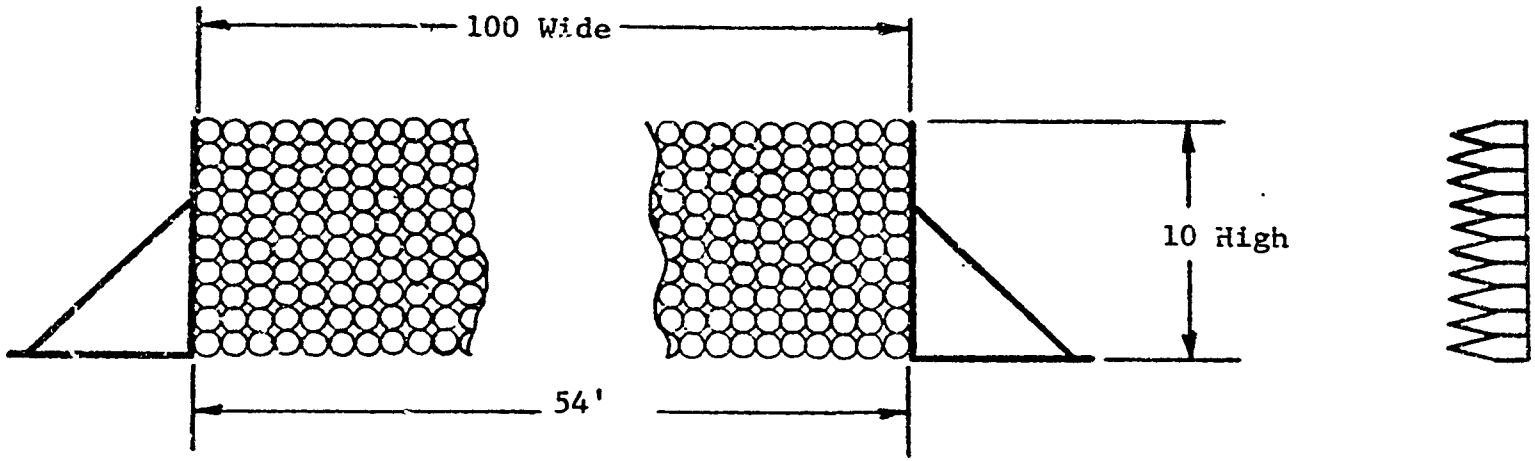

B. Yuma 3000 Unit 155mm Projectile Stacks Test

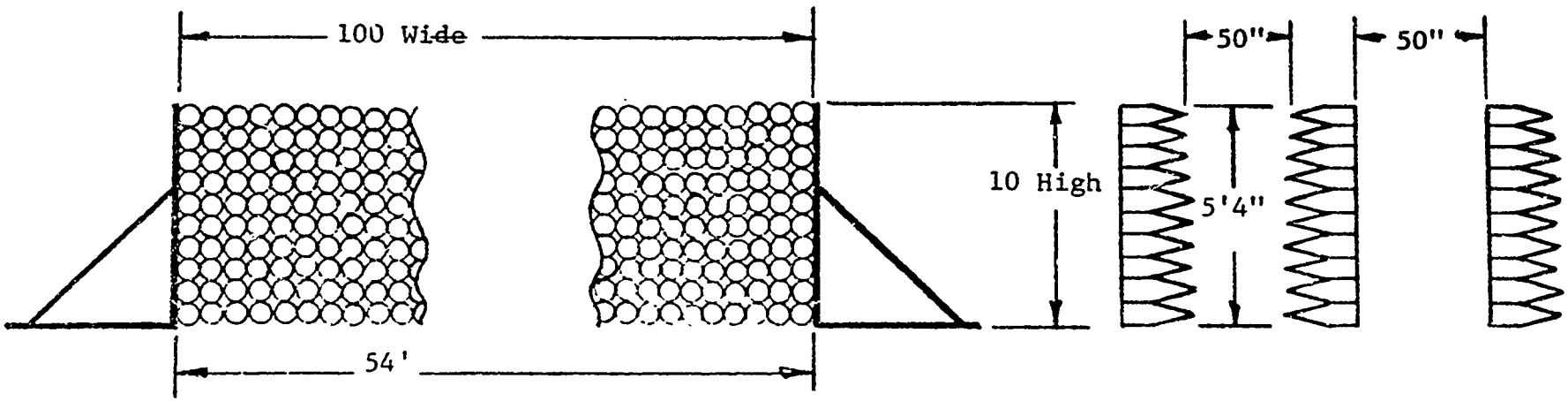

Figure 1 YUMA PROVING GROUND 155mm PROJECTILE STACK TESTS

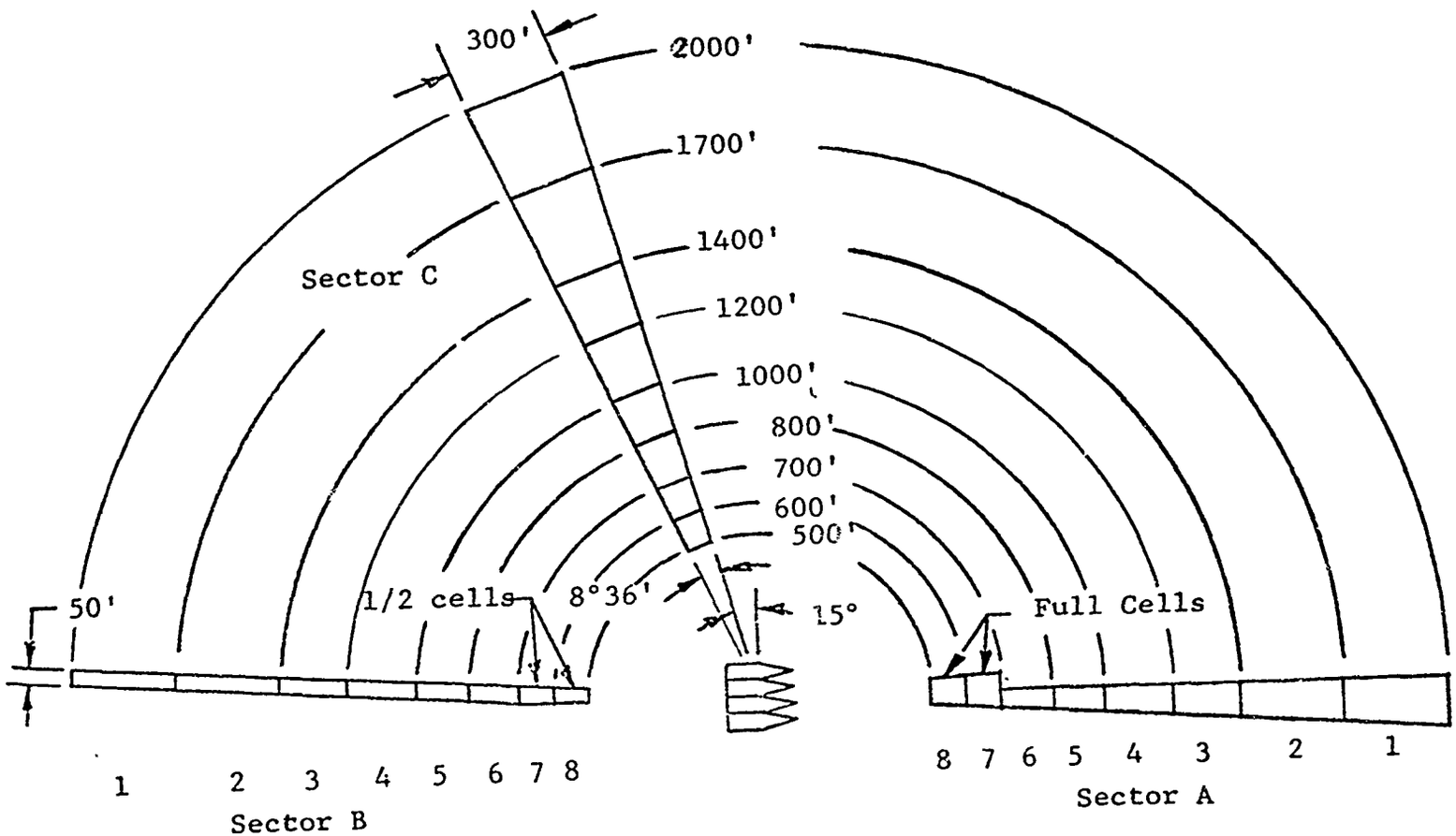

Figure 2 YUMA FRAGMENT COLLECTION CELL SPECIFICATIONS

The present study is a detailed investigation of the data emanating from the 1000 unit array. Fragments from both Yuma tests, capable of being hazardous to unprotected personnel have been aggregated, individually weighed and counted, their corresponding weight and number densities on the ground computed, and an estimate made on fragment hazard using conservative assumptions.

1.2 Description of Eskimo I Test

The Eskimo I Igloo test, conducted at China Lake in December 1971, also utilized the 155-mm projectile as the fragment source. Here, the stack contained a nominal weight of 200,000 lbs of high explosives (i.e., 13,336 units). The projectiles were stacked on end and palletized within a steel arch, earth covered igloo with concrete headwalls in accordance with the applicable AMC standard storage drawing. Primed projectiles were located at eight corners of the palletized stack and at the middle column of projectile pallets. A 15.5 ft high earth barricade was built about 60 ft from the headwall of the donor igloo. Acceptor igloos, approximately 14 ft high were located 161 ft west of the sidewall and 117 ft to the rear of the donor. Figure 3 indicates the relative positions of the donor and acceptor igloos and the barricade.

The fragment distribution, resulting from the test, was measured by surveying and clearing three rays of five degree width extending from 500 ft radii northward, westward, and southward of the donor magazine center, as shown in Figure 4. The west and south rays were cleared to 3000 ft, and the south ray actually was extended along the 171 degree azimuth, to avoid a hill located due south of the donor. The north ray terminated at 1600 ft because of a hill. Additional 100 ft square areas were surveyed and marked, but not cleared, on two lines extending at 30 degrees from the front and 45 degrees from the rear of the donor at 900 ft, 1800 ft, and 2700 ft. Five areas 100 ft square were also marked on the 5000 ft radius and along the north line at 2000 ft, 2500 ft, and 3000 ft. The cleared rays were marked

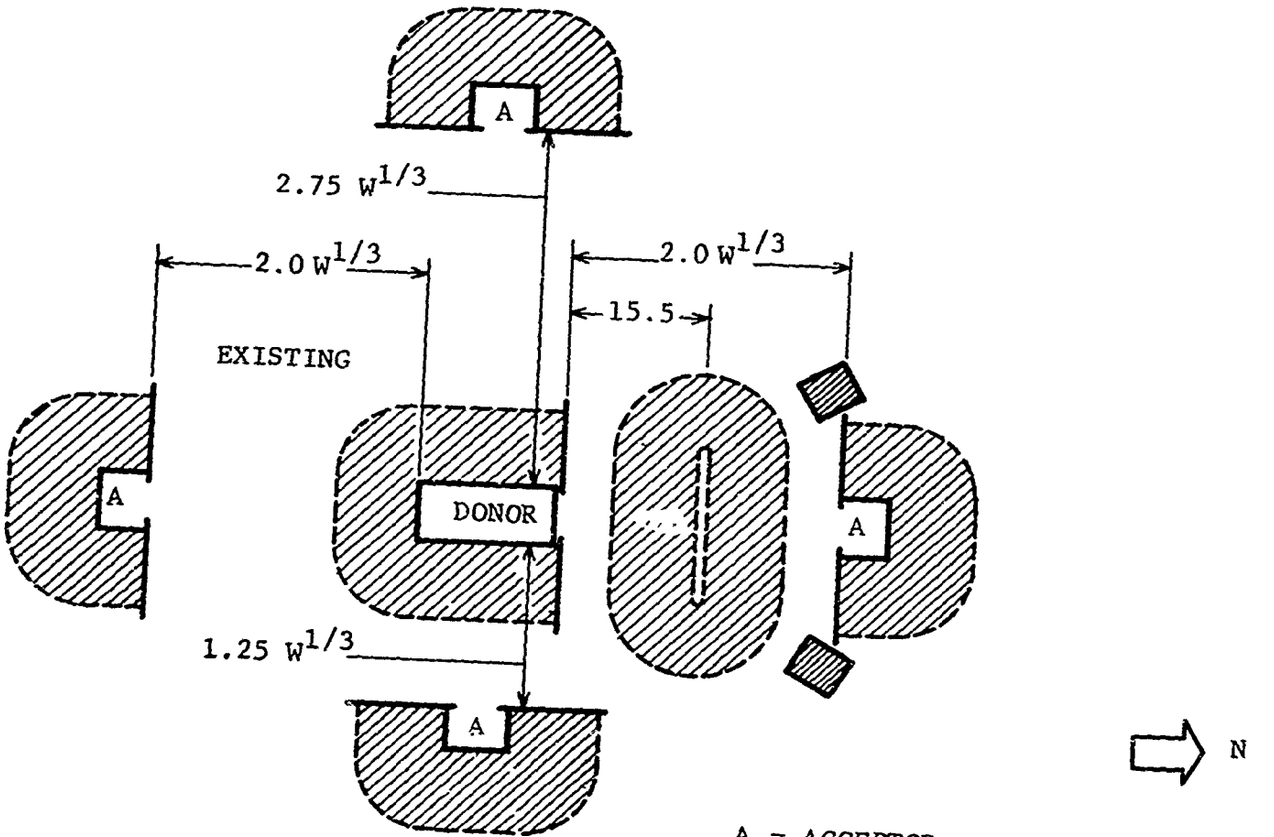

Figure 3 LAYOUT OF TEST AREAS FOR ESKIMO I

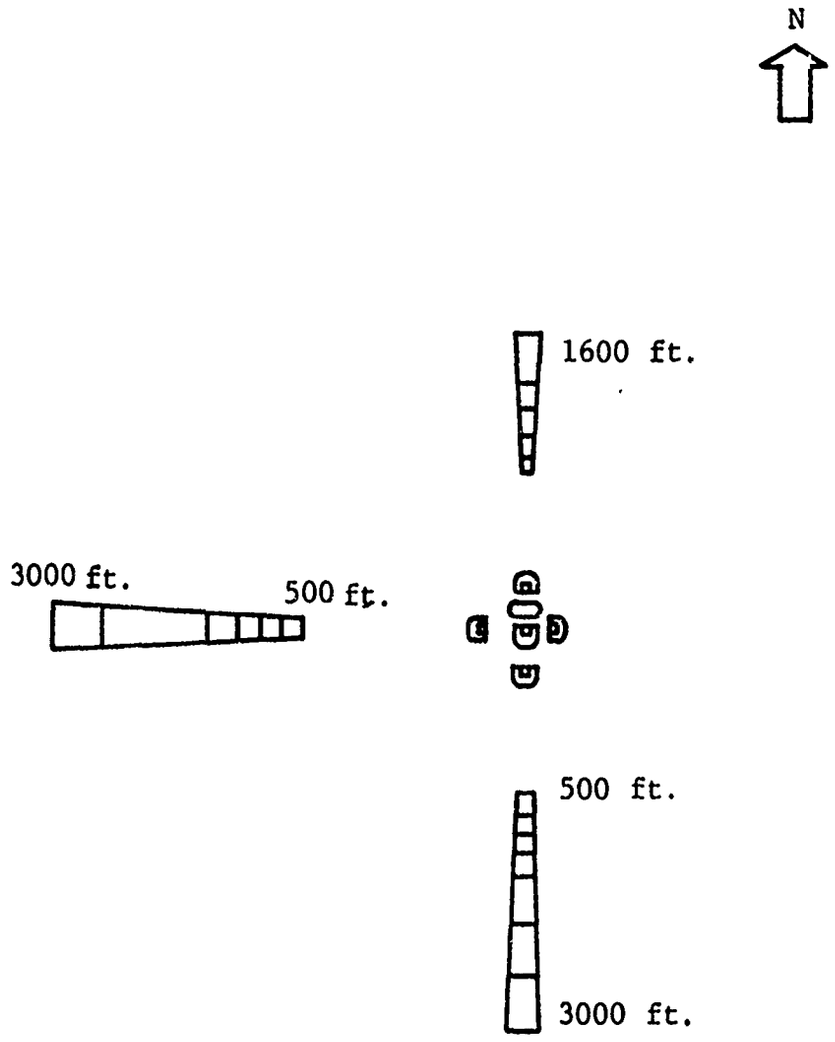

Figure 4 FRAGMENTATION COLLECTION AREAS

in 250 ft and 500 ft sectors, and a magnet truck was used to collect fragments from each sector for subsequent statistical analysis.

The collection, sizing, grading, and analysis of Eskimo I fragment data was conducted at the Naval Weapons Center, China Lake, California under the direction of Mr. F. H. Weals. A preliminary meeting between IITRI and NWC personnel established compatible fragment size categories for Yuma and Eskimo I data.

1.3 Program Accomplishments

The major result of this study was the characterization of the far field fragment hazard associated with the 1000 unit stack of 155-mm projectiles detonated at Yuma Proving Grounds. This included an analysis procedure for determining a minimum weight fragment of interest based upon applicable hazard criteria, the design and utilization of an automatic weighing-counting device to facilitate fragment grading and counting, and an extensive analysis of far field fragment data in terms of number densities, cumulative weight densities and probability of injury. Eskimo I results, obtained by NWC personnel, were put into a form similar to the Yuma results and appropriately compared. These results indicate that even though the two stack configurations are quite different, there are several important similarities that exist. The overall fragment weight distributions for each of the stacks are quite different than for a single unit. This is conclusive quantitative evidence that the fragments emanating from a multiple unit stack detonation tend to be substantially greater in weight than those emanating from a single unit munition. Also both multiple unit stacks showed a similar marked falloff of hazardous fragment density at about 1300 ft from the center of detonation. This result is particularly important in that it may be possible to establish a limiting distance of fragment hazard based upon a maximum expected fragment size and the number of units in a stack.

1.4 Program Highlights

The following sections of this report are organized to first present the analysis upon which the fragments were separated into nonhazardous and potentially hazardous categories. Next, a description of the automatic weighing-counting device is presented and this is followed by a presentation of results obtained for the Yuma test and a comparison of these results with similar results coming out of the Eskimo I test. Finally, the study is summarized in the form of conclusions reached and recommendations pertaining to future multiple unit tests based upon these conclusions. An appendix is included that outlines the computational steps involved in deriving the program results.

2. SELECTION OF APPROPRIATE WEIGHT INTERVALS

To minimize the effort required in weighing and counting over 2 tons of Yuma fragments, the first task was directed toward establishing a minimum weight fragment. This task also involved an estimate of the amount of material above and below the chosen minimum weight.

Based on study objectives to characterize the fragment hazard at Yuma, and to then compare this hazard to the Eskimo I hazard, expedience dictates that detailed weighing and counting of fragments be directed at only those fragments which result in a hazard to unprotected personnel.

The criteria for hazardous fragments to unprotected personnel have been established as:

- A hazardous fragment has a kinetic energy of 58 ft-lbs or greater, and
- An acceptable density of hazardous fragments is not more than one per 600 sq ft

Utilizing the first of these criteria together with previously developed analytic relationships (Refs. 3,4), it is possible to establish a minimum fragment weight of interest.

Figure 5 depicts the relation between two energy criteria, terminal velocity and fragment weight for fragments in free fall (i.e., upper register fragments). Figures 6 and 7 depict a similar relationship for lower register fragments and show the fragment weight-range necessary to exceed the given energy criteria (i.e., 11 or 50 ft-lbs). In each figure there is a separate curve corresponding to a particular initial fragment velocity.

Documentation of the Yuma test results (Ref. 5) indicates that fragments had an initial velocity of about 5000 ft/sec. Current quantity-distance tables indicate an 990 ft required distance for 15,000 lbs explosive. Table 1 is a summary of the critical fragment size for the two criteria in both the upper and lower registers.

TABLE 1

CRITICAL FRAGMENT WEIGHT (grains)

	Energy Criteria	
	58 ft-lbs	11 ft-lbs
Lower Register	1000	590
Upper Register	1983	570

Based upon the weights shown in Table 1 the stored fragments were divided into three size categories: those remaining on a 1 in. sieve, those remaining on a 5/8 in. sieve, and the material passing through the 5/8 in. sieve. Table 2 is a correspondence between the sieve size categories and approximate weight in grains.

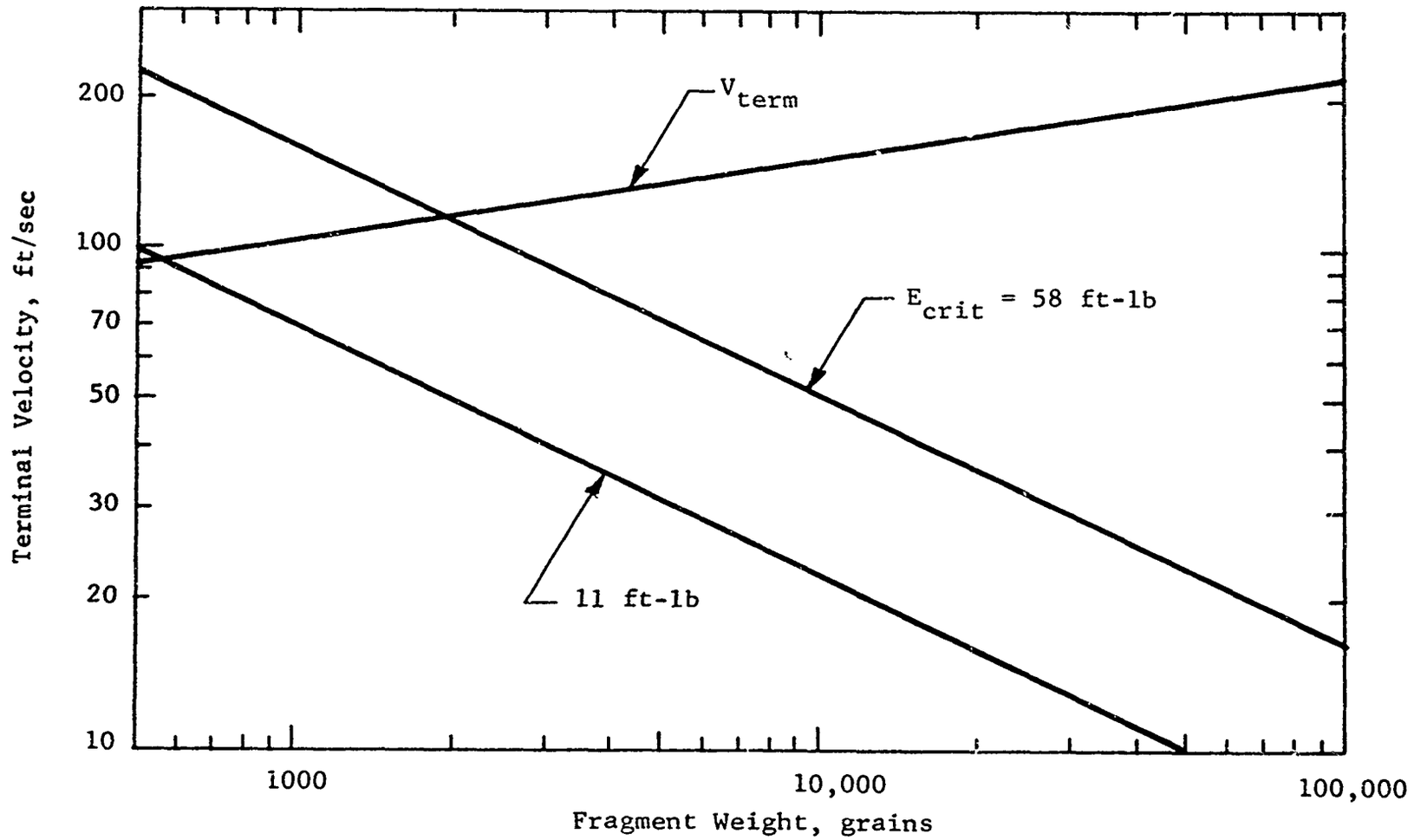

Figure 5 INJURY CRITERIA AND TERMINAL VELOCITIES FOR UPPER REGISTER FRAGMENTS

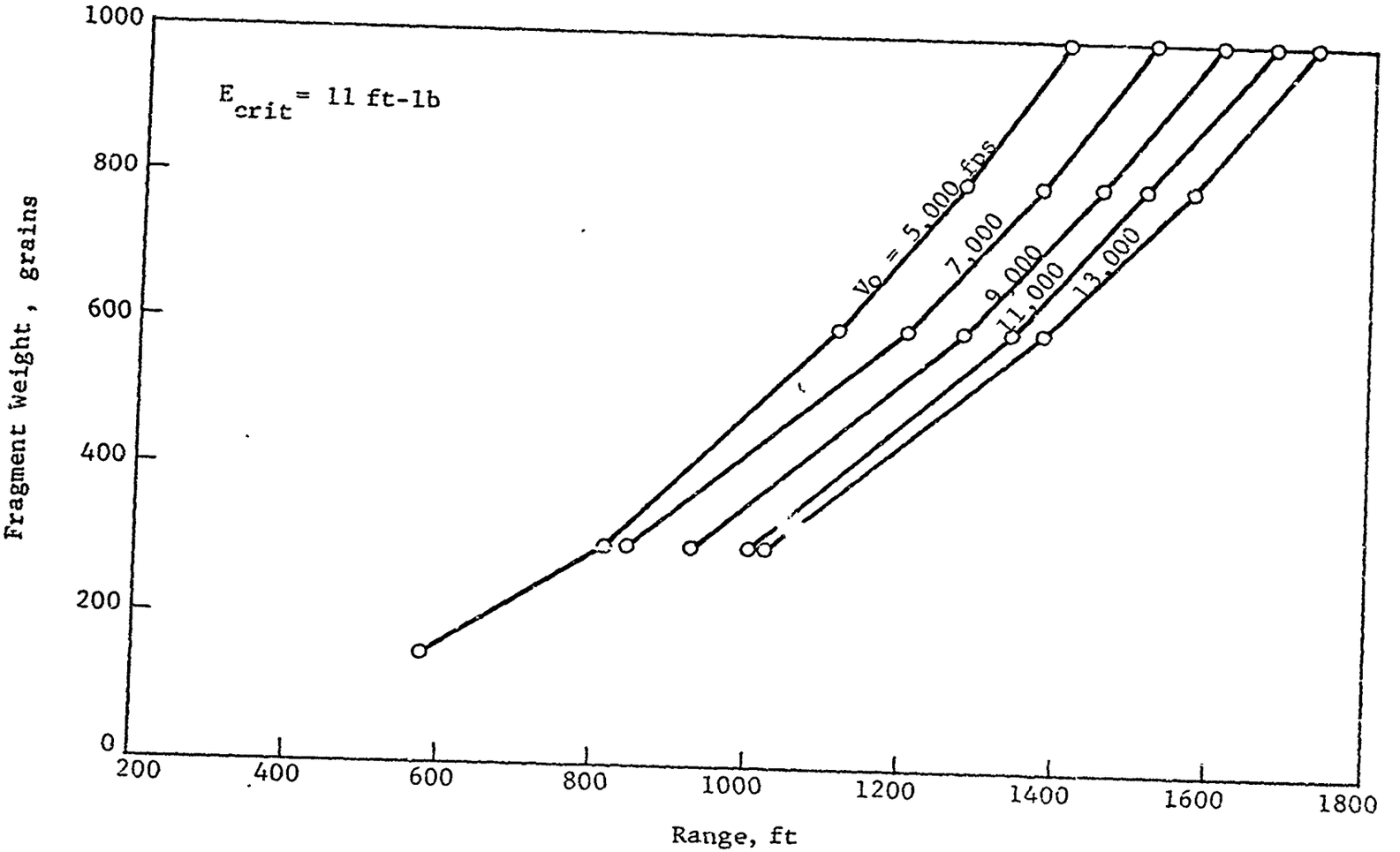

Figure 6 FRAGMENT WEIGHTS AND RANGES FOR LOWER REGISTER FRAGMENTS WITH A CRITICAL ENERGY OF 11 FT-LB

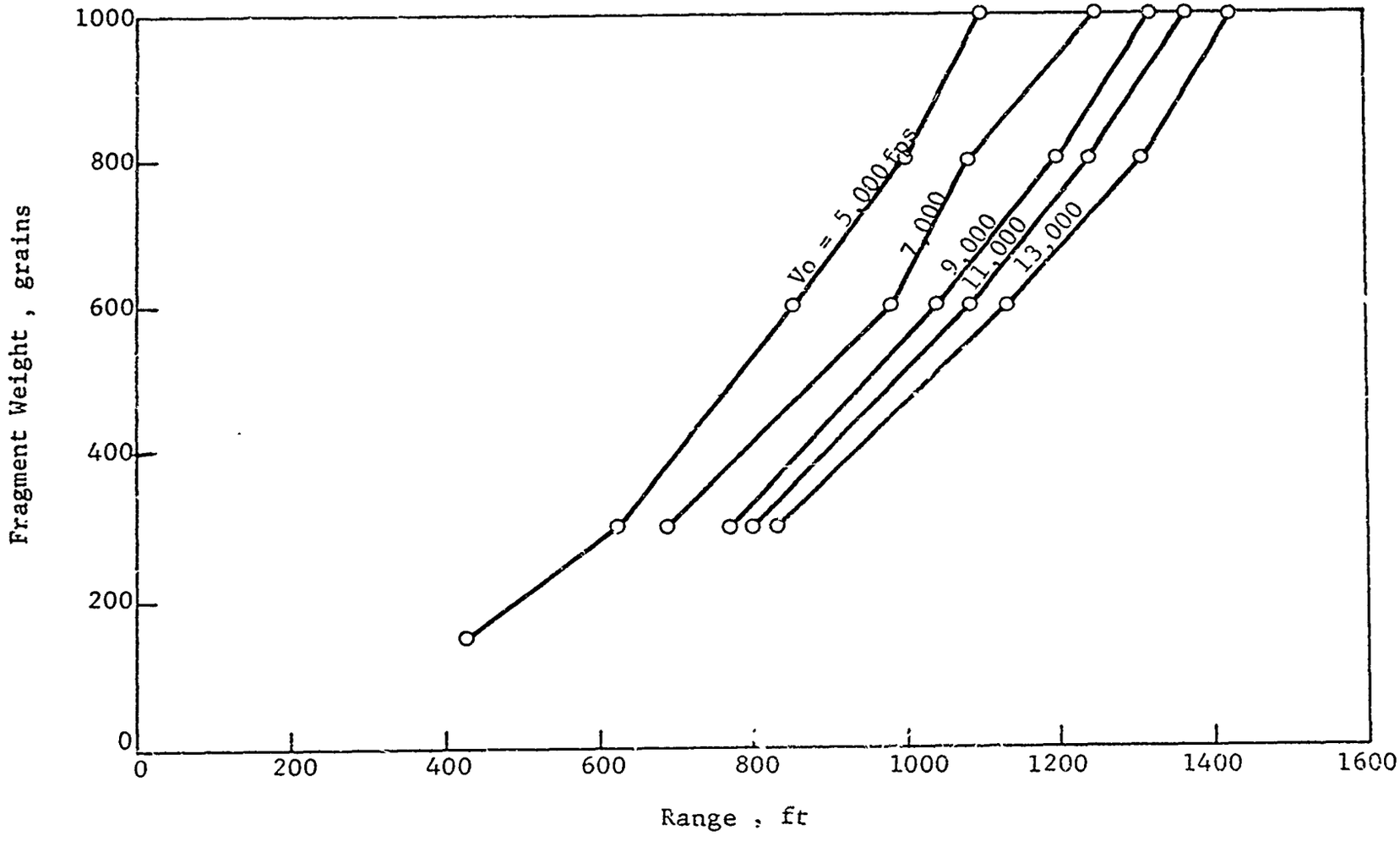

Figure 7 FRAGMENT WEIGHTS AND RANGES FOR LOWER REGISTER FRAGMENTS WITH A CRITICAL ENERCY OF 58 FT-LB

TABLE 2

SIEVE SIZE - FRAGMENT WEIGHT CORRESPONDENCE

Sieve Size (in.)	Average Fragment wt (grains)
1	over 1000
5/8	over 400
< 5/8	less than 400

Figures 8, 9 and 10 present the percent of material in each of the three collection rays. (i.e., the nose, base and side rays). Each figure has three curves corresponding to the three size categories and relating percent of total material to ground range from the explosion. It is evident that the smallest size category (those passing through the 5/8 sieve) begins to fall off considerably at 900 ft and represents only about 20 percent, by weight, of the total material at 1100 ft from the explosion. Table 3 summarizes the weight distribution for all the material out to a 2000 ft range and for the material between 1000 and 2000 ft. This latter category is the primary zone of hazardous fragments.

TABLE 3

SUMMARY OF TOTAL WEIGHT DISTRIBUTION

Ground Range	0-2000 ft		1000-2000 ft	
Sieve Size (in.)	Fragment wt (lbs)	Percent	Fragment wt (lbs)	Percent
1	1840	42.1	1118	57.3
5/8	1027	23.5	600	30.8
< 5/8	1504	34.4	232	11.9

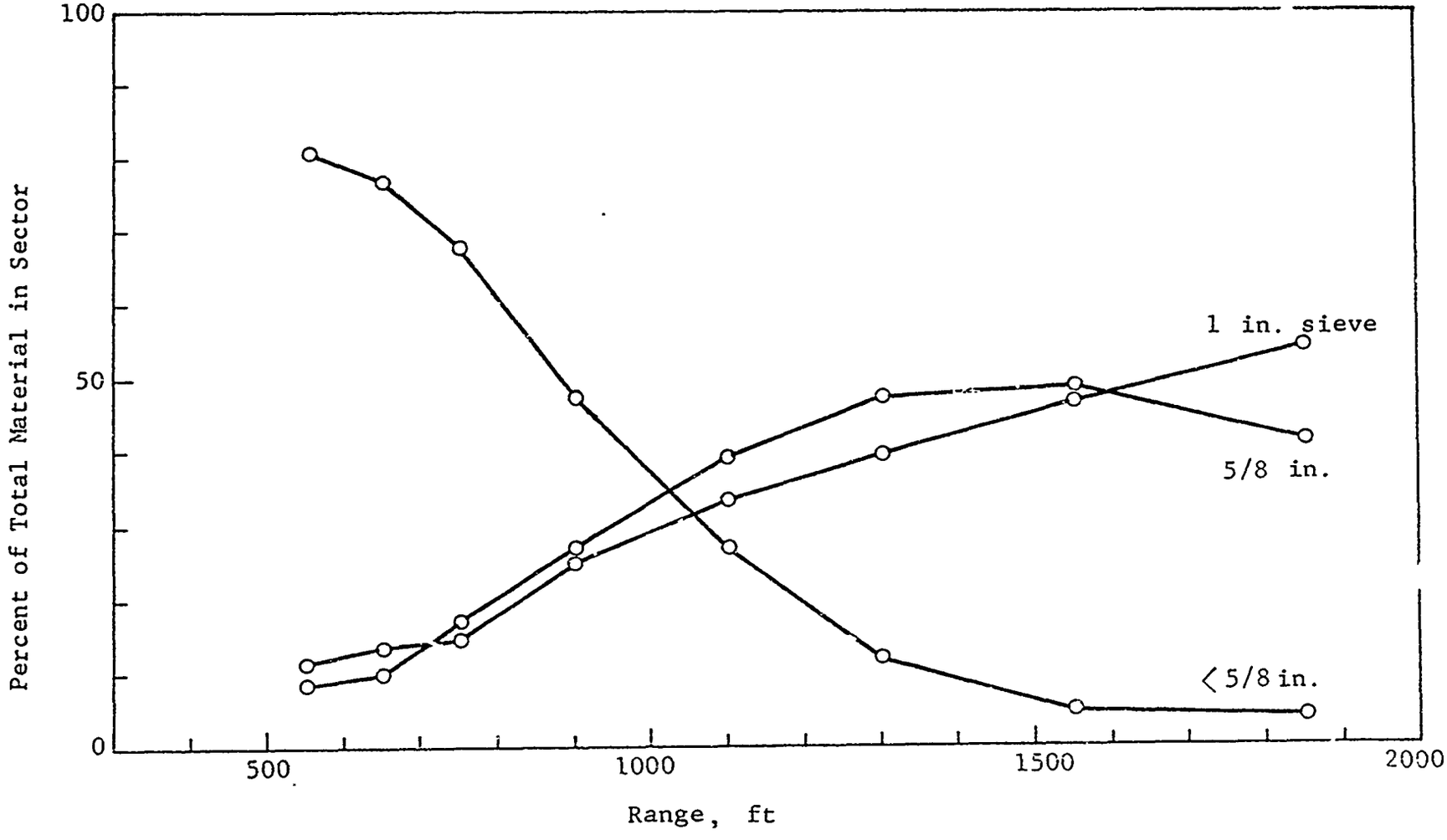

Figure 8 PERCENT OF TOTAL SECTOR MATERIAL AS A FUNCTION OF RANGE - NOSE RAY

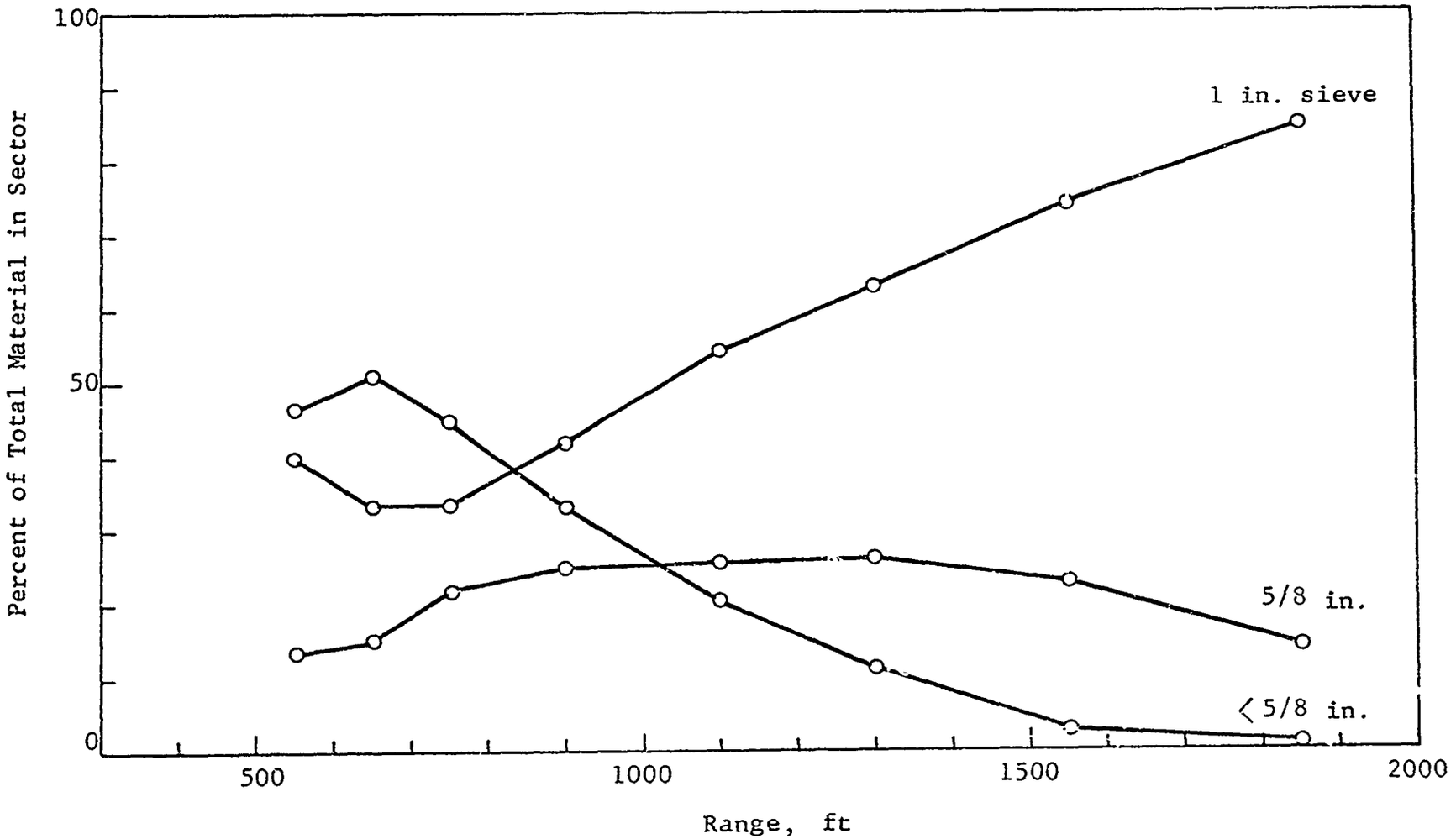

Figure 9 PERCENT OF TOTAL SECTOR MATERIAL AS A FUNCTION OF RANGE - BASE RAY

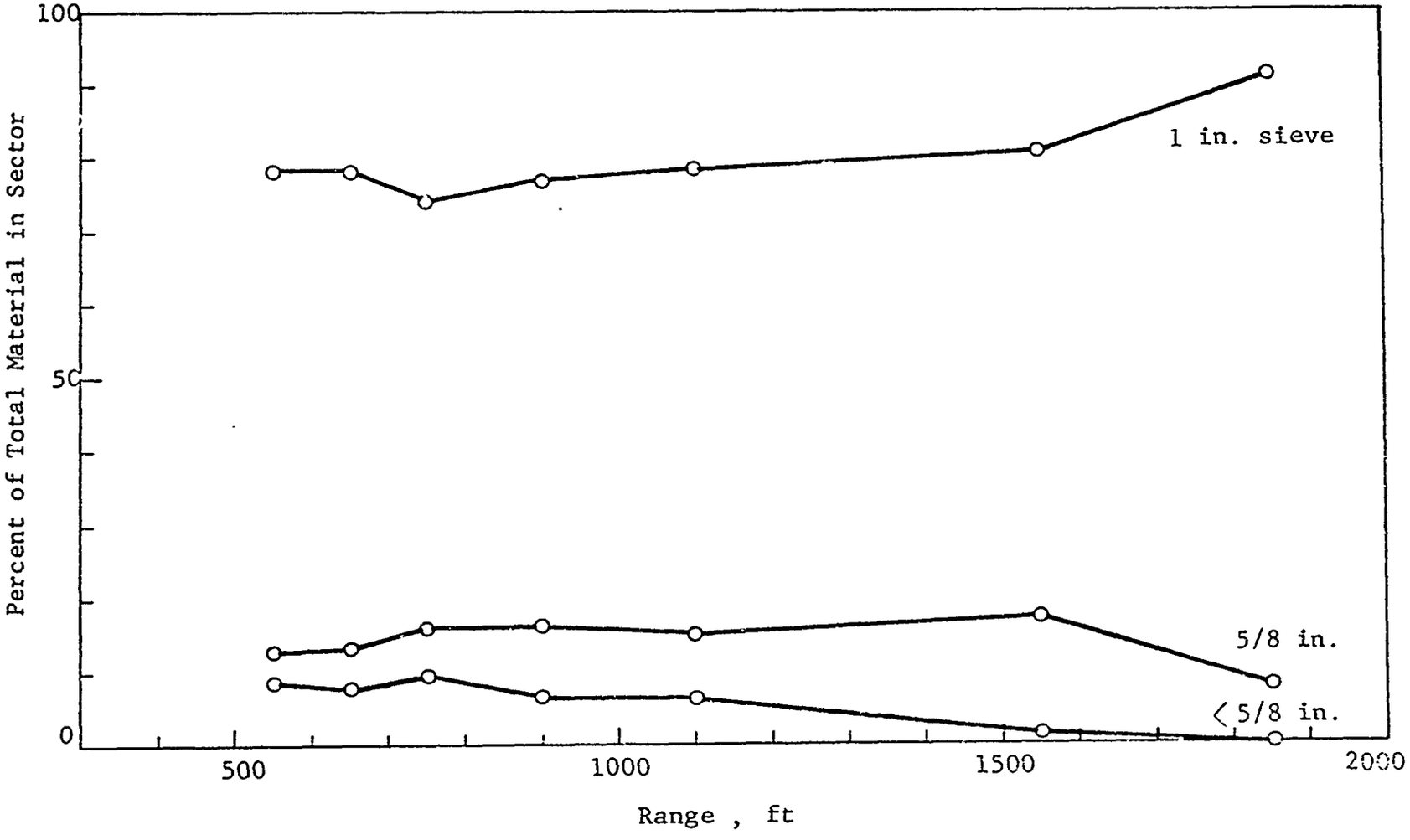

Figure 10 PERCENT OF TOTAL SECTOR MATERIAL AS A FUNCTION OF RANGE - SIDE RAY

The above results indicate a twofold justification for disregarding fragments passing through the 5/8 in. sieve. That is, they are well below the critical weight required of hazardous fragments and they represent less than 12 percent of the total material in the major area of concern.

If these small fragments are disregarded, the effort required to weigh and count the remaining fragments is reduced such that this can be done on an individual fragment basis. This is desirable since it will now be possible to characterize the fragment hazard, associated with the Yuma test, with maximum resolution.

3. DESCRIPTION OF IITRI AUTOMATIC WEIGHING-COUNTING DEVICE

A load cell mechanically coupled to a weighing pan was used to weigh the fragments. The load on the cell was directly proportional to the weight of the fragment. The output voltage of the cell was directly proportional to the load. This voltage is recorded on paper tape and, through a linear relationship, was converted to the weight.

The weighing apparatus, shown schematically in Figure 11, consists of a lever arm, a base, a pan, and a load cell. The lever arm is a 30 in. aluminum bar resting upon a fulcrum 10 in. from one end. The pan can be hung at a distance of 6 in. or 10 in. from the fulcrum. These positions are denoted as (x) and (y) respectively. The base rests upon four tubular aluminum legs and has three positions countersunk for the load cell. These holes are located at 18, 12, and 2 in. from the fulcrum and are labeled A, B, and C respectively.

The load cell is a circular diaphragm resting upon four strain gauges. These gauges are located about the rim of the diaphragm, 90 degrees apart. A load is applied through a ball bearing resting axially upon the diaphragm, and the diaphragm is consequently deformed. The strain gauges convert this deformation to an output voltage and they are balanced by a Wheatstone bridge. The output is increased through a differential amplifier and is

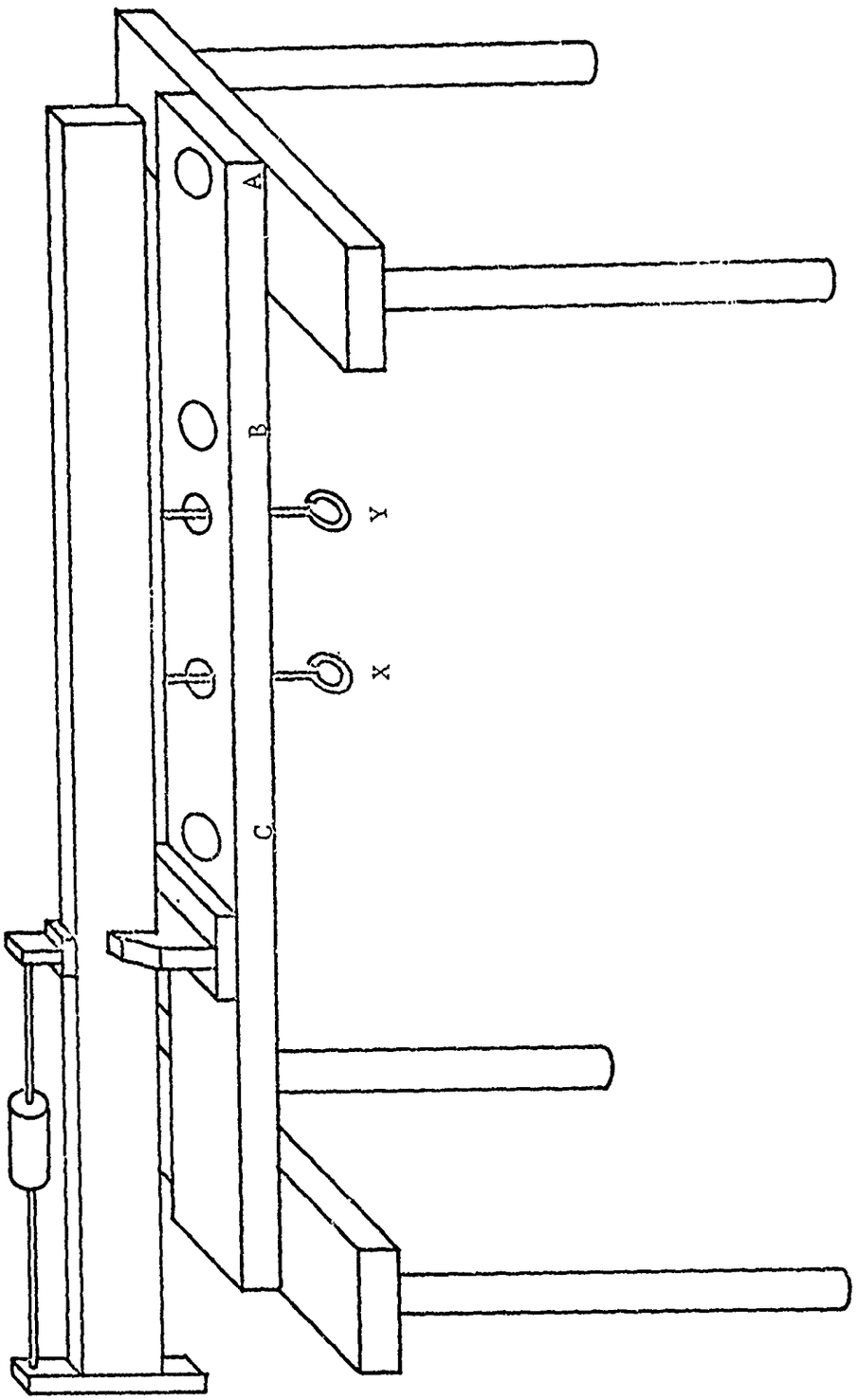

Figure 11 WEIGHING APPARATUS

displayed on a digital voltmeter. When the system reaches equilibrium, the voltage is punched on paper tape. The tape punch is programmed to punch four digits plus appropriate carriage control and live feed symbols so as to be compatible with the data analysis equipment. Figure 12 is a system diagram of this arrangement. Figure 13 is a series of three photographs displaying the total system, the weighing apparatus and the lever arm-load cell respectively.

Since the pan and load cell have multiple positions, it is possible to have six different weighing modes. Each mode corresponds to a different ratio of lever arms, hence a different mechanical advantage. It is possible, therefore, to have six different ranges on the instrument. As the load/weight ratio increases the degree of precision also increases. However, the range of the instrument decreases with increased precision. Although the load cell can withstand a load of 10 lbs, it was not loaded to a point greater than that which would cause a 10 volt reading on the digital voltmeter. In readings over 10 volts one digit is lost in the final tape, and precision drops sharply. It is possible to weigh from 0 to 67,720 grains in the series of modes shown in Table 4.

TABLE 4

CORRESPONDENCE OF CELL-PAN POSITIONS TO MEASURED WEIGHTS

Cell Position	Pan Position	Load/Weight Ratio	Maximum Based on 10 v (grains)	Maximum Based on 10 lb Load Cell (lbs)	Precision (grains per 10 millivolt)
A	X	0.33	67,720	30	72.7
A	Y	0.56	43,120	18	44.2
B	X	0.50	46,200	20	49.0
B	Y	0.83	27,720	12	28.4
C	X	3.00	7,200	3.33	7.9
C	Y	5.00	4,620	2	4.7

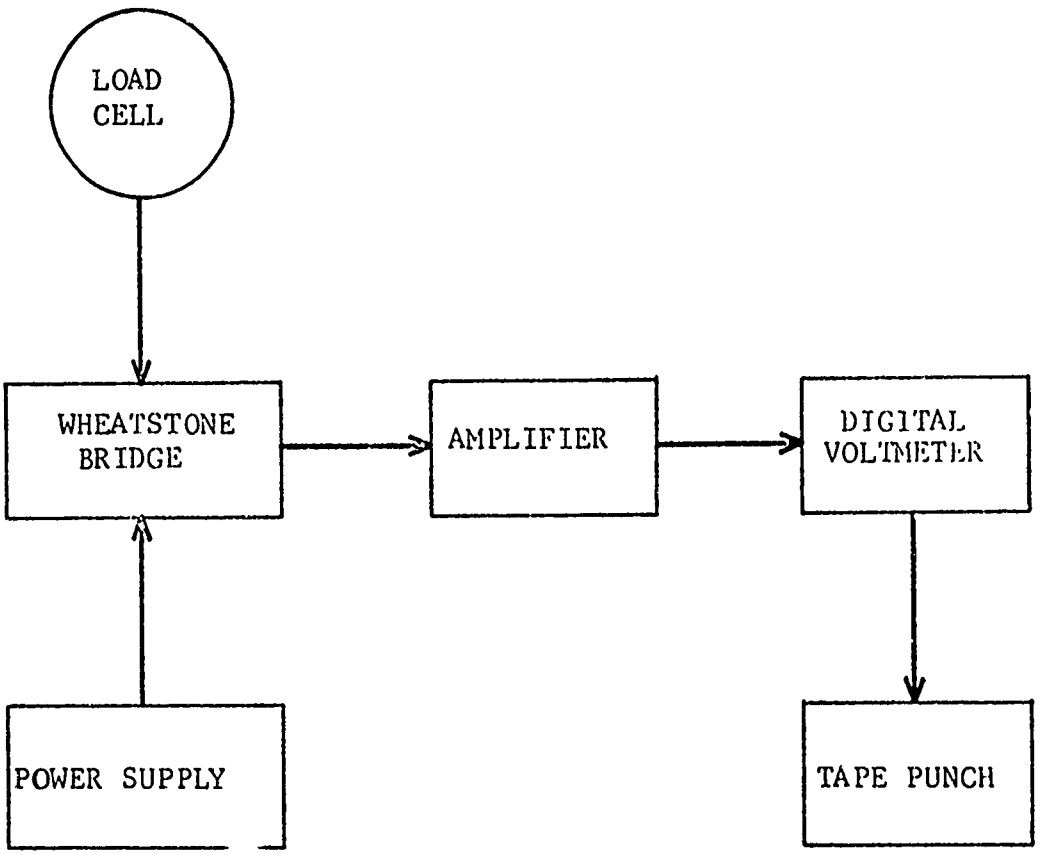

Figure 12 SYSTEM DIAGRAM

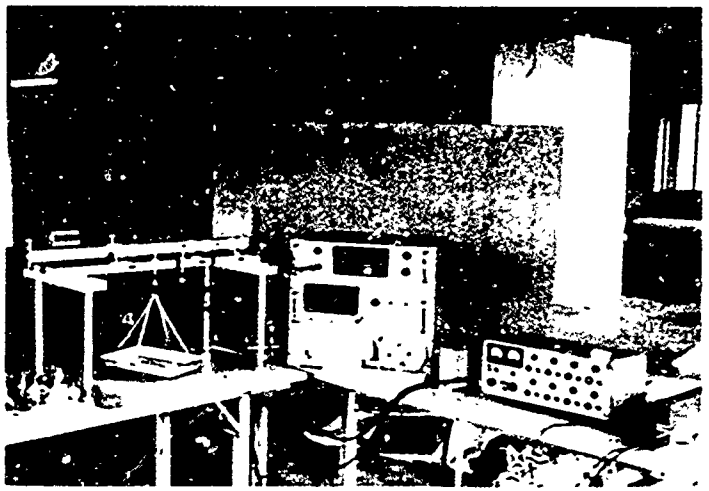

A. Complete System

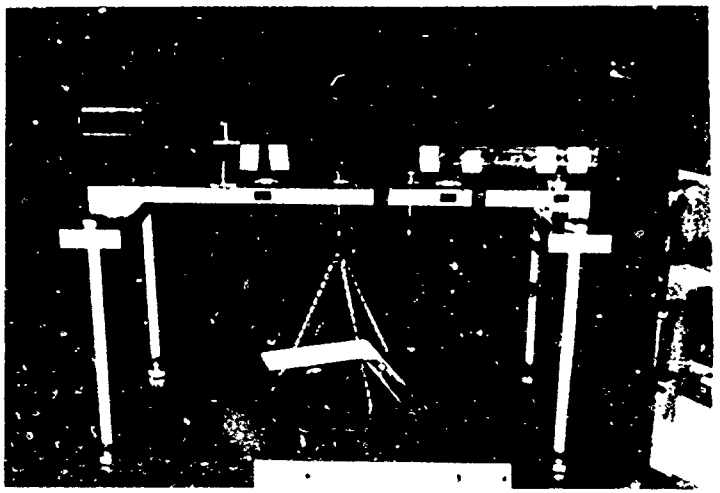

B. Weighing Apparatus

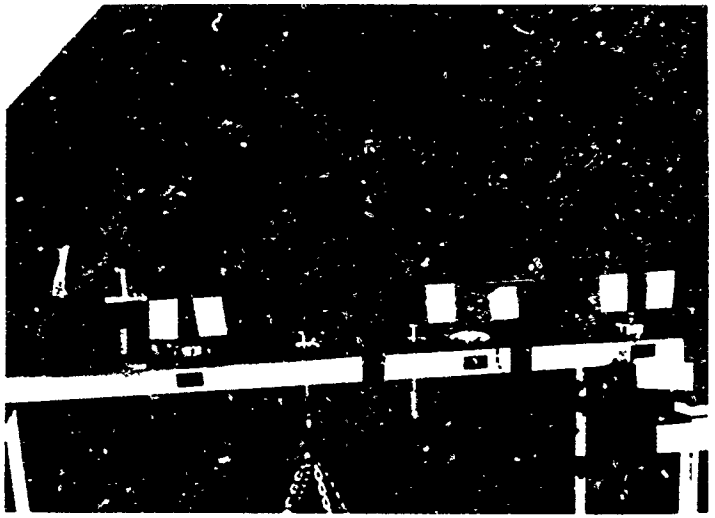

C. Lever Arm-Load Cell Arrangement

Figure 13 THE IITRI AUTOMATIC WEIGHING-COUNTING DEVICE

Due to the linear relationship between the voltage and the weight, the apparatus was calibrated by using a series of test masses and graphing mass as dependent on voltage. A very good linear relationship, illustrated in Figures 14, 15 and 16, was found to exist and a least-squares approximation to these relationships is incorporated into a computer routine for direct conversion of the voltages into weights.

4. YUMA TEST RESULTS

The first step in analyzing the fragments collected at Yuma was to screen out those fragments falling through a 5/8 in. sieve. This left 18,655 potentially hazardous fragments having a total weight of 19,299,759 grains. Thus, the mean weight of those fragments was 1,035 grains, well above the 76.3 mean weight of published munition effectiveness data.

Figure 17 depicts the cumulative weight distributions for (1) a single 155-mm projectile as reported in munition effectiveness data, (2) all fragments collected in the Yuma 1000 unit experiment and (3) the potentially hazardous fragments collected at Yuma. This figure gives the percentage of total weight consisting of fragments lighter than a given individual weight. It is obvious from this illustration that the fragments emanating from the Yuma experiment are considerably heavier than those reported for the case of a single unit munition detonation. For example, 50 percent of fragments fall below 320 grains for the single unit, below 650 grains for the entire set of Yuma fragments and below 2,050 grains for the set of Yuma fragments retained by a 5/8 inch sieve.

4.1 Cumulative Fragment Density as a Function of Weight

The cumulative number density as a function of fragment weight has been compiled for all collected fragments, broken down by rays, and then by sectors within rays. This is a convenient format in that if all fragments are considered to have upper register trajectories, then fragment weight, W, can be directly related to fragment energy, E, by using the following

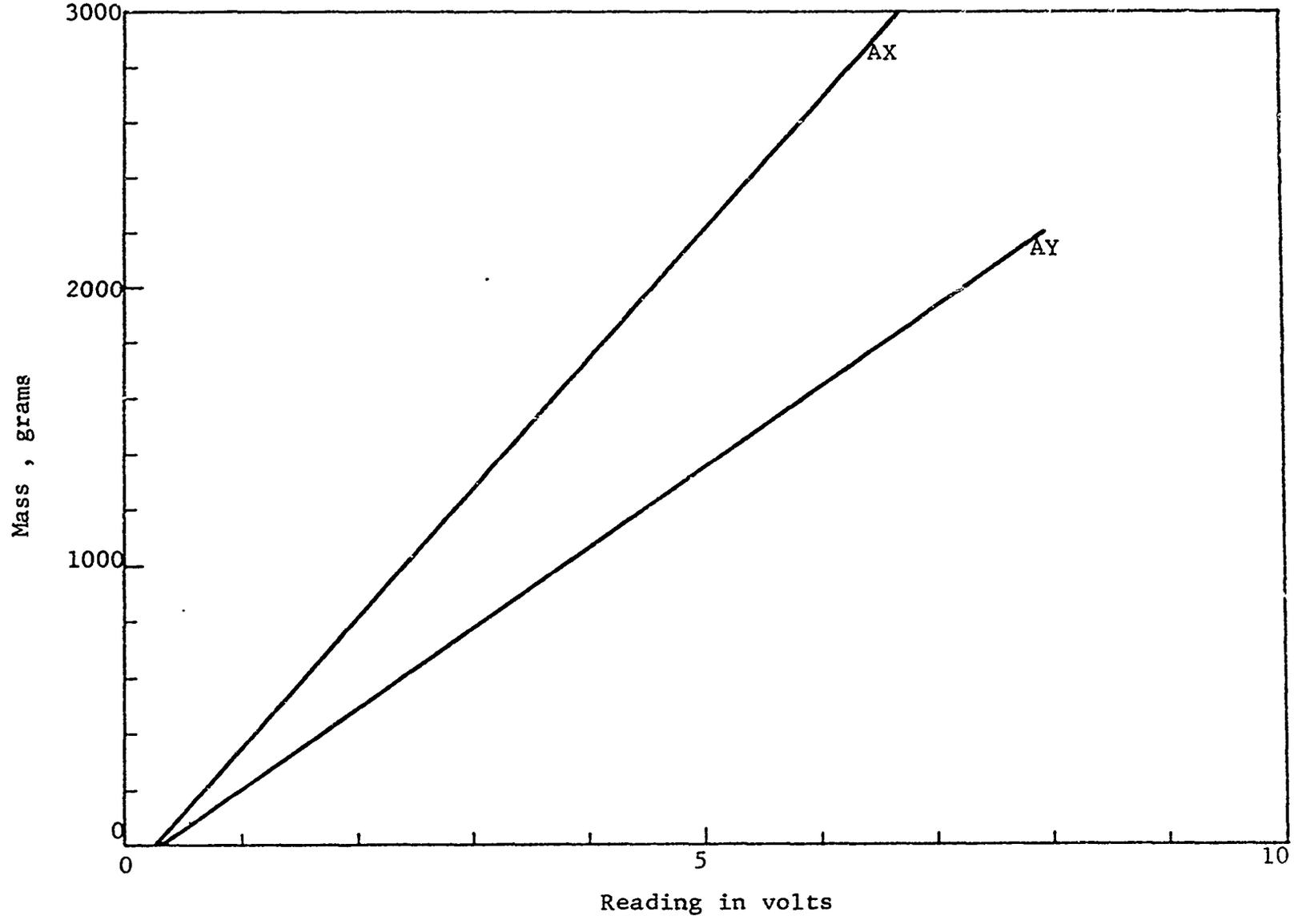

Figure 14 CALIBRATION CURVE FOR LOAD CELL POSITION A AND PAN POSITIONS X AND Y

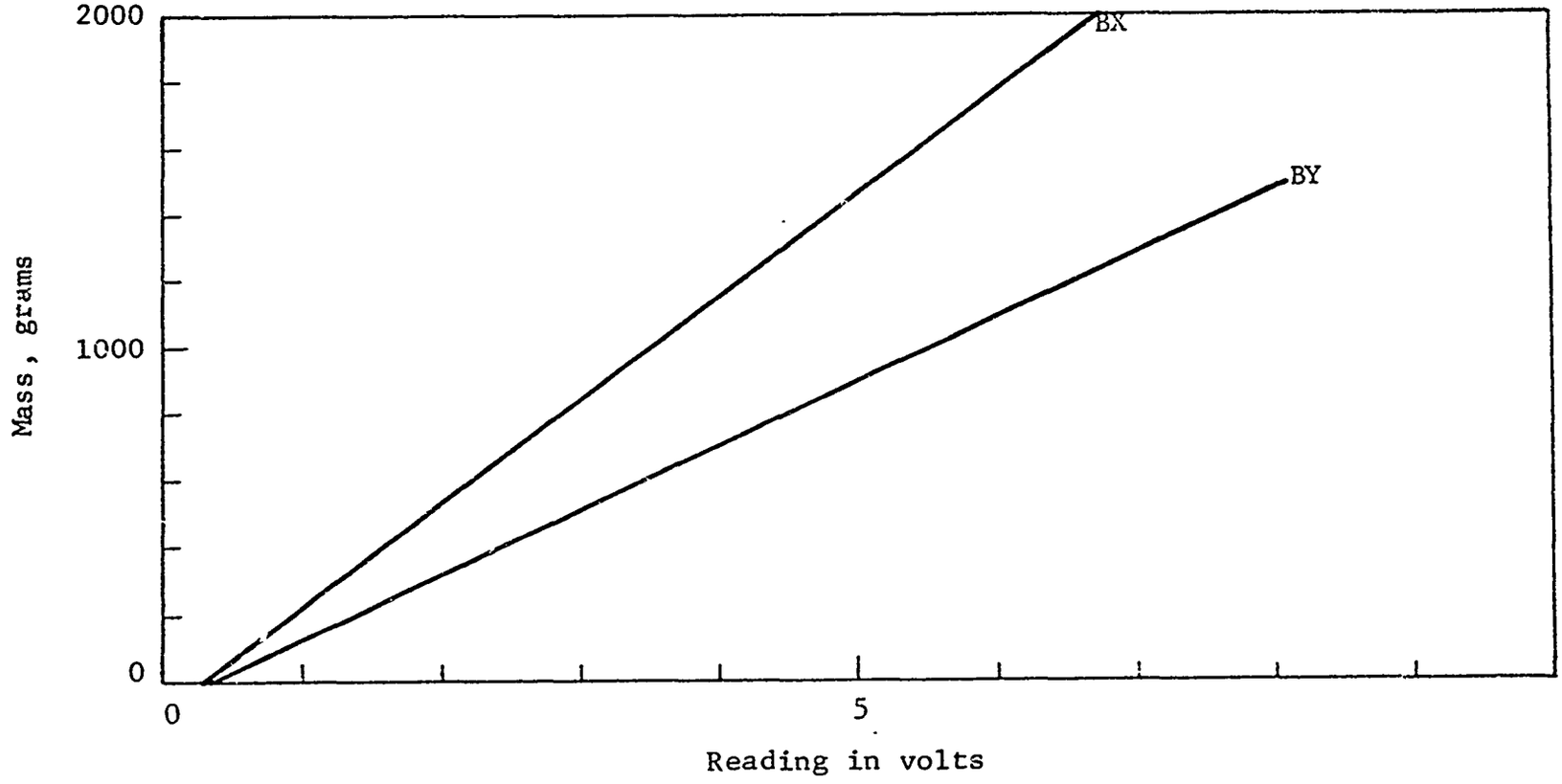

Figure 15 CALIBRATION CURVE FOR LOAD CELL POSITION B AND PAN POSITIONS X AND Y

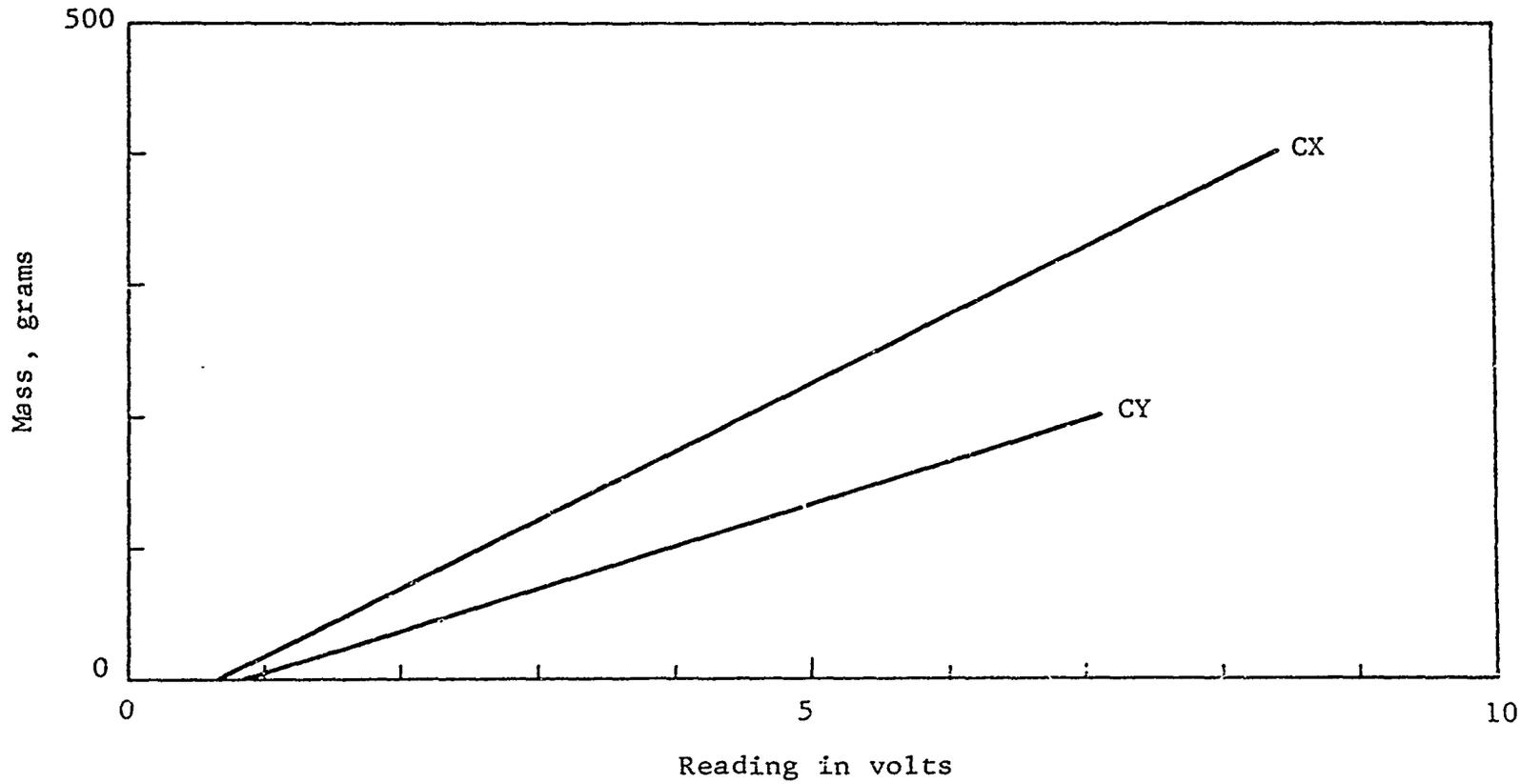

Figure 16 CALIBRATION CURVE FOR LOAD CELL POSITION C AND PAN POSITIONS X AND Y

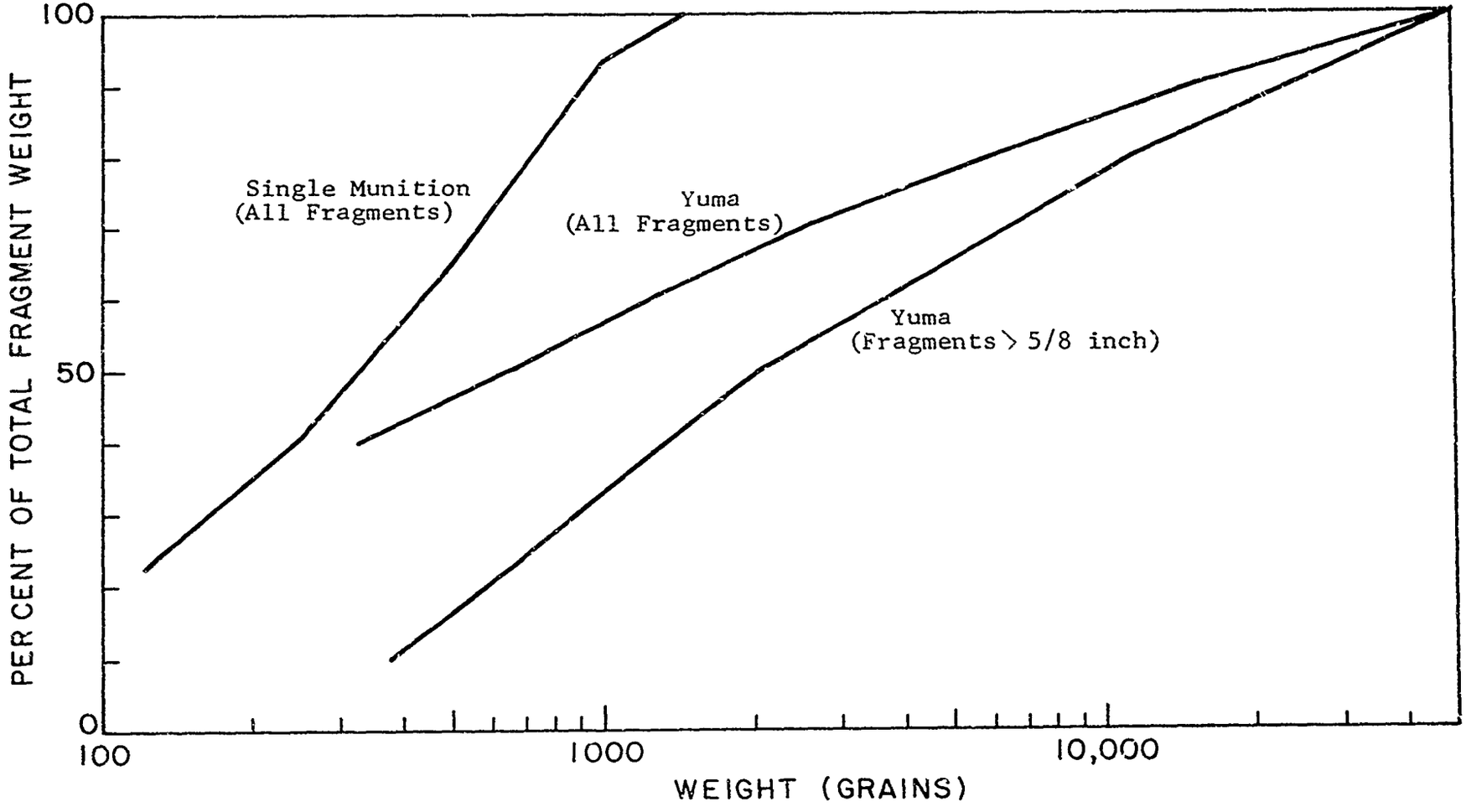

Figure 17 CUMULATIVE WEIGHT DISTRIBUTIONS

expression:

$$E = kW^{4/3} \qquad (1)$$

where $k = 0.0023269$ ft-lbs/(grains)$^{4/3}$ for the 155-mm projectile. Thus, utilizing equation (1) E = 1.08, 23.27 and 501.31 ft-lbs for a fragment size of W = 100, 1,000 and 10,000 grains respectively. Conversely, W = 570 and 1983 grains for respective energies of 11 and 58 ft-lbs; these energy levels are alternative fragment hazard criteria for serious injury to unprotected personnel.

Figure 18 is the distribution of fragment density as a function of weight for all Yuma fragments collected and weighed. Figure 19 breaks this total distribution down by rays. As previously noted, in a qualitative manner, the base ray, B, contains the greatest density and weight of fragments. This is closely followed by the nose ray and to a lesser extent by the side ray C, however, displays a generally exponential fall in number in excess of 8500 grains, the side ray has a higher number density per sq ft than the nose ray. Figures 20, 21, 22, 23, and 24 break down the fragment densities by sectors within each ray. Here it is interesting to note that for the nose and base rays the fragment number densities build to a peak at sector 6, (i.e., 750 ft) then fall off gradually through sector 3 (i.e., 1,300 ft) and finally fall off rapidly beyond sector 3. Side ray C, however, displays a generally exponential fall in number density as a function of sector.

4.2 Fragment Density as a Function of Range

The fragment number density as a function of range for all fragments remaining on the 5/8 in. sieve is shown in Figure 25 separately by ray. Figures 26 and 27 are a subset of Figure 25 and show the fragment number density as a function of range for those fragments having terminal energies in excess of 11 and 58 ft-lbs respectively in each ray. Here fragment energies were taken as the greater value of an upper and lower register assumption.

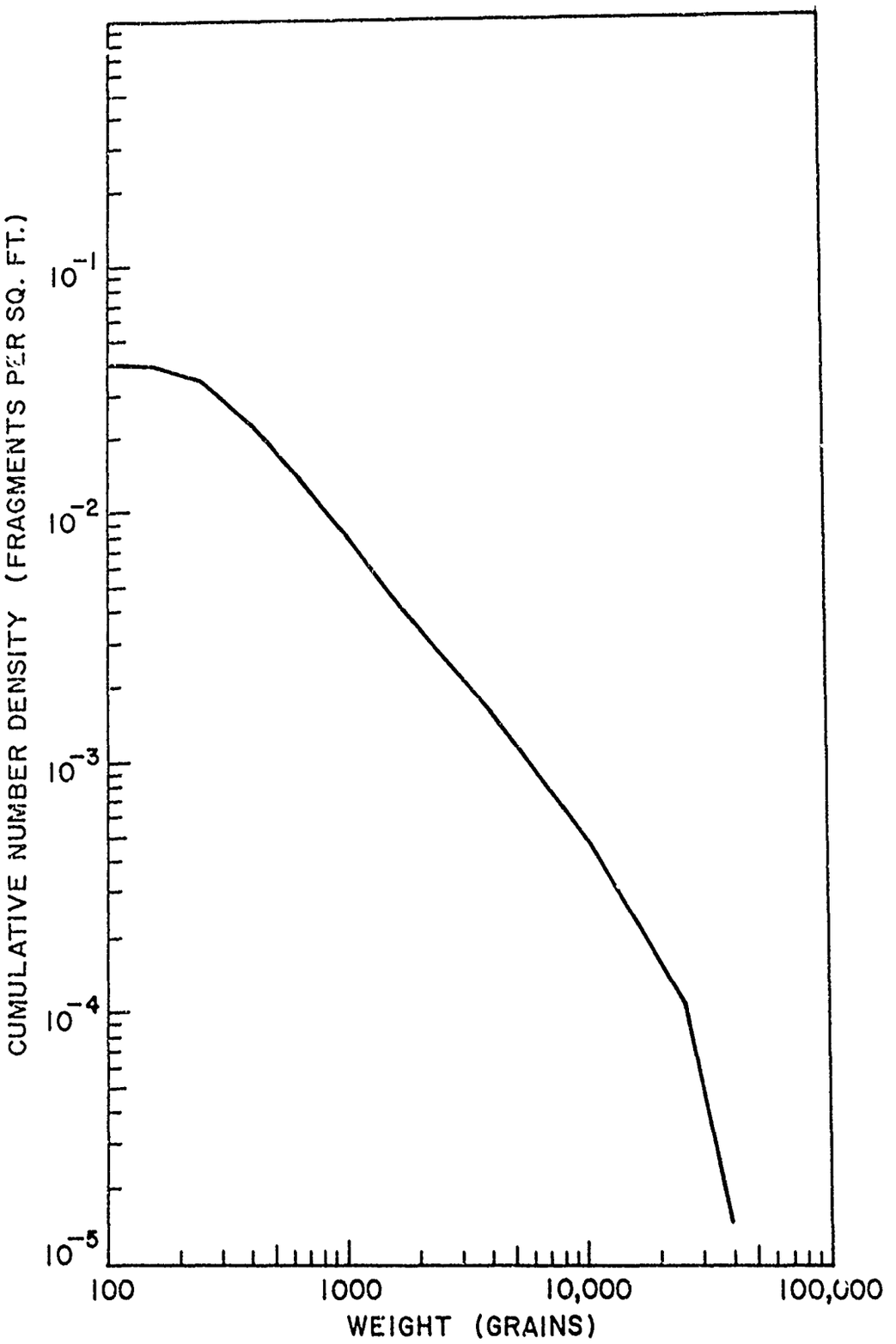

Figure 18 NUMBER DENSITY OF FRAGMENTS WITH WEIGHT GREATER THAN W - TOTAL DISTRIBUTION

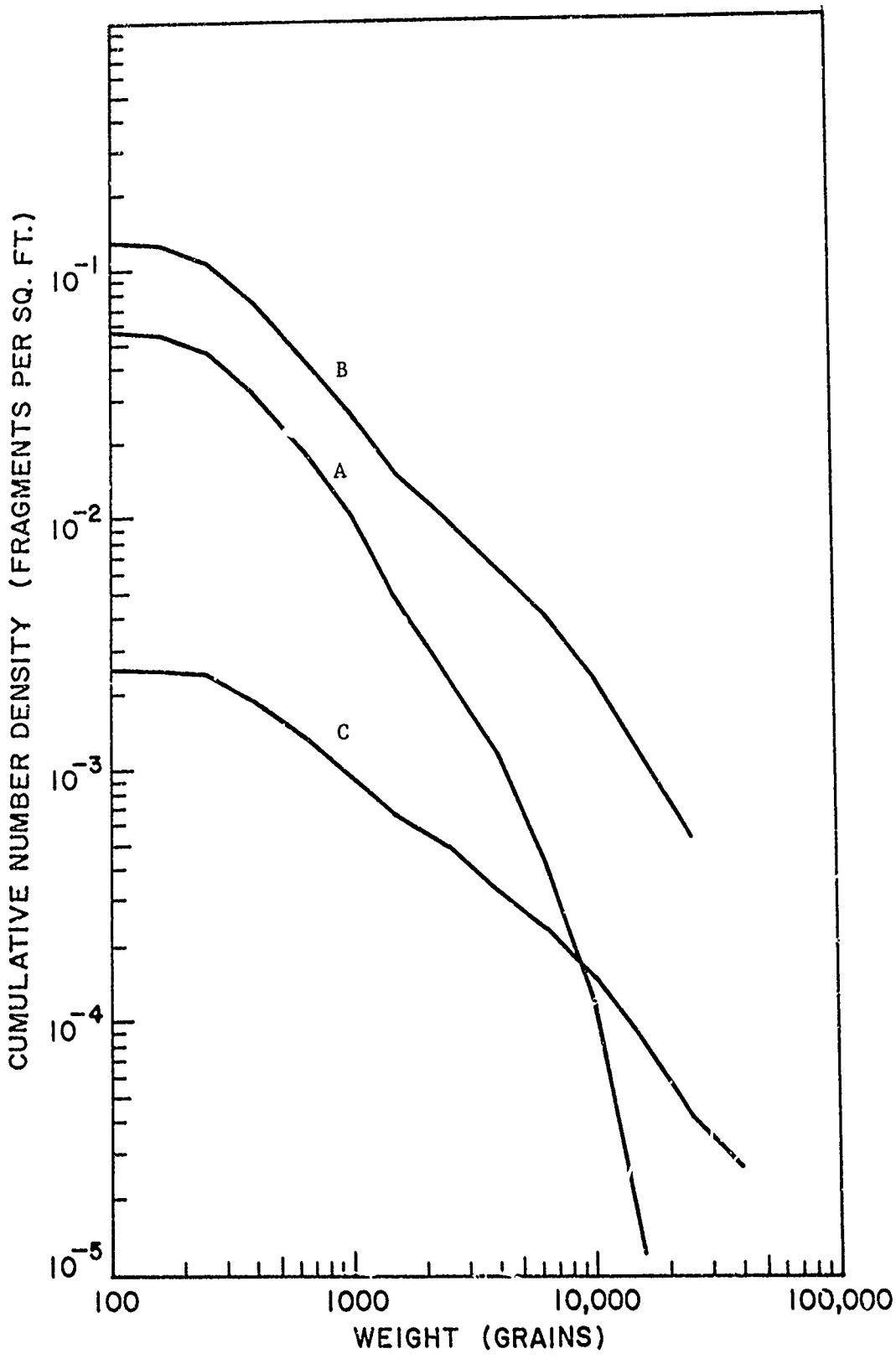

Figure 19 NUMBER DENSITY OF FRAGMENTS WITH WEIGHT GREATER THAN W - RAYS A, B, C

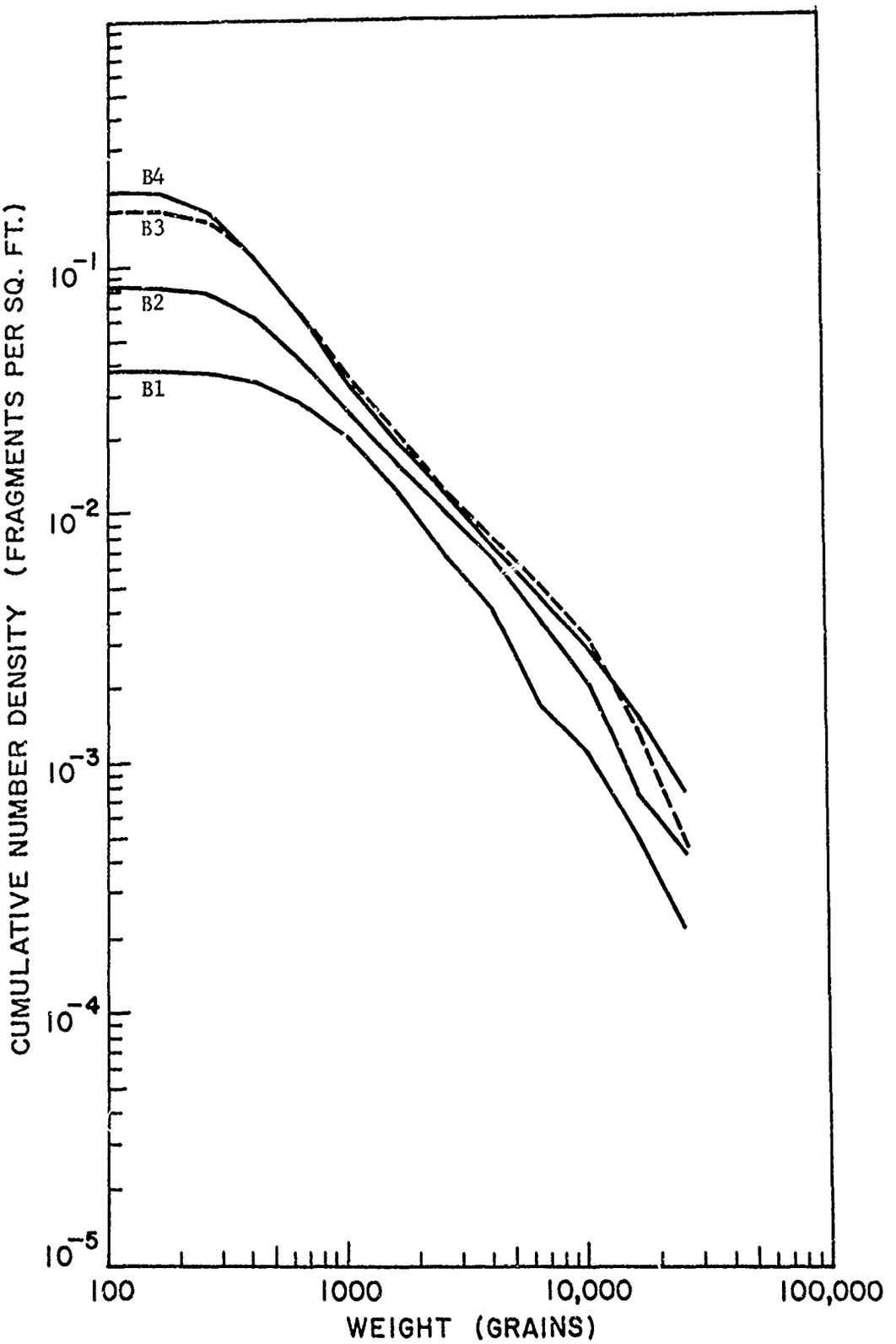

Figure 20 NUMBER DENSITY OF FRAGMENTS WITH WEIGHT GREATER THAN W - RAY B SECTORS 1, 2, 3, 4

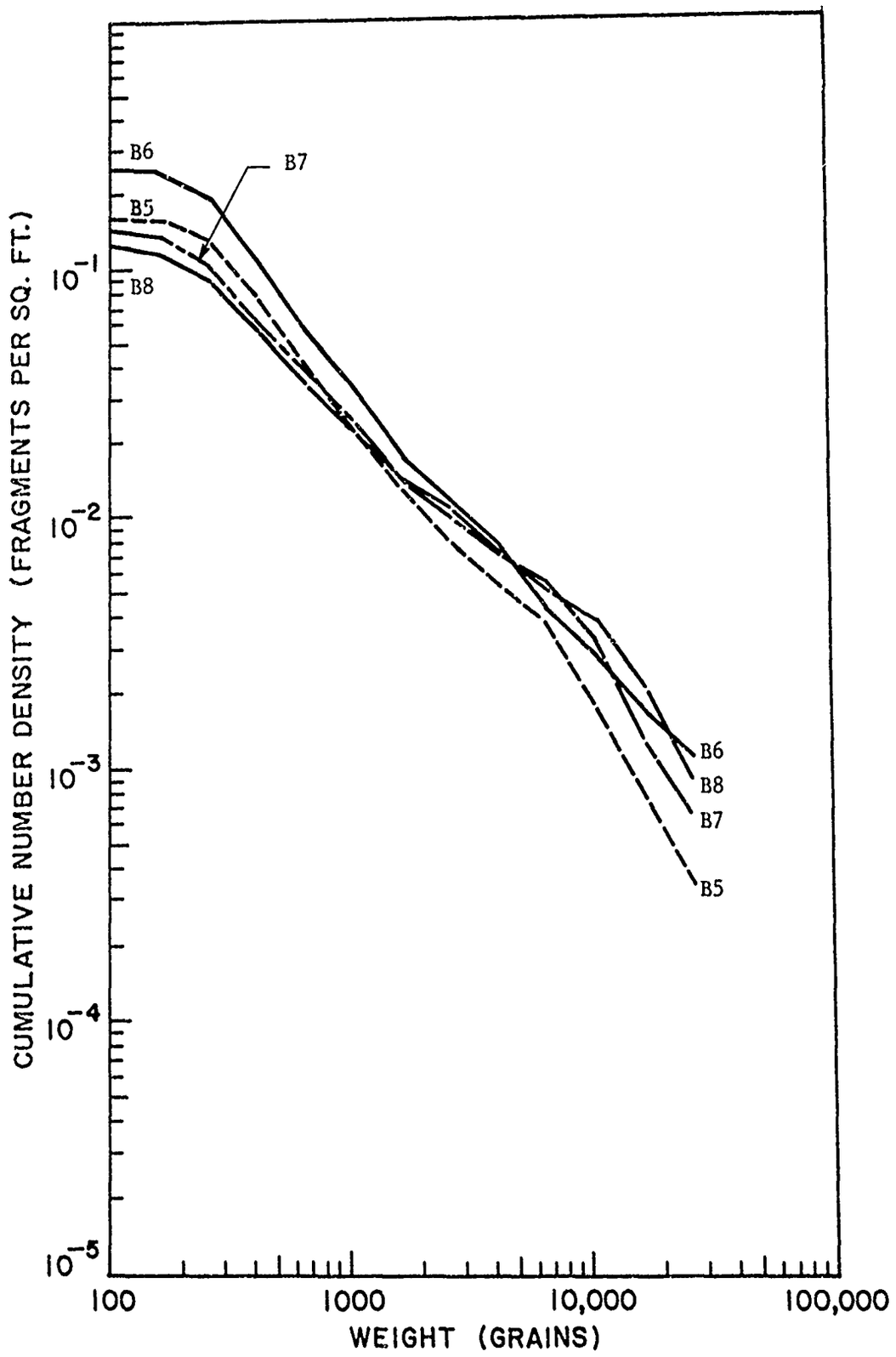

Figure 21 NUMBER DENSITY OF FRAGMENTS WITH WEIGHT GREATER THAN W RAY B SECTORS 5, 6, 7, 8

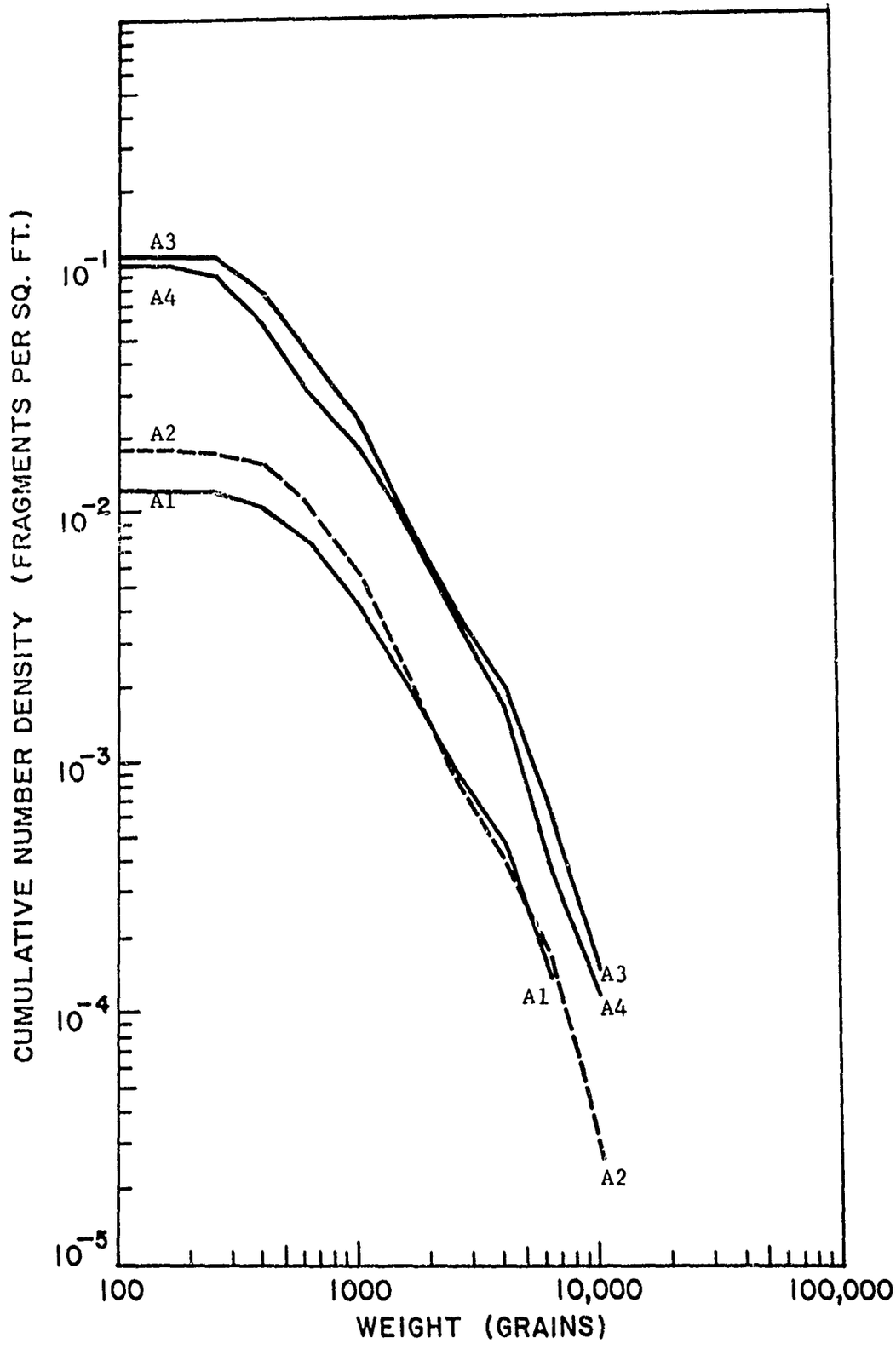

Figure 22 NUMBER DENSITY OF FRAGMENTS WITH WEIGHT GREATER THAN W RAY A SECTORS 1, 2, 3, 4

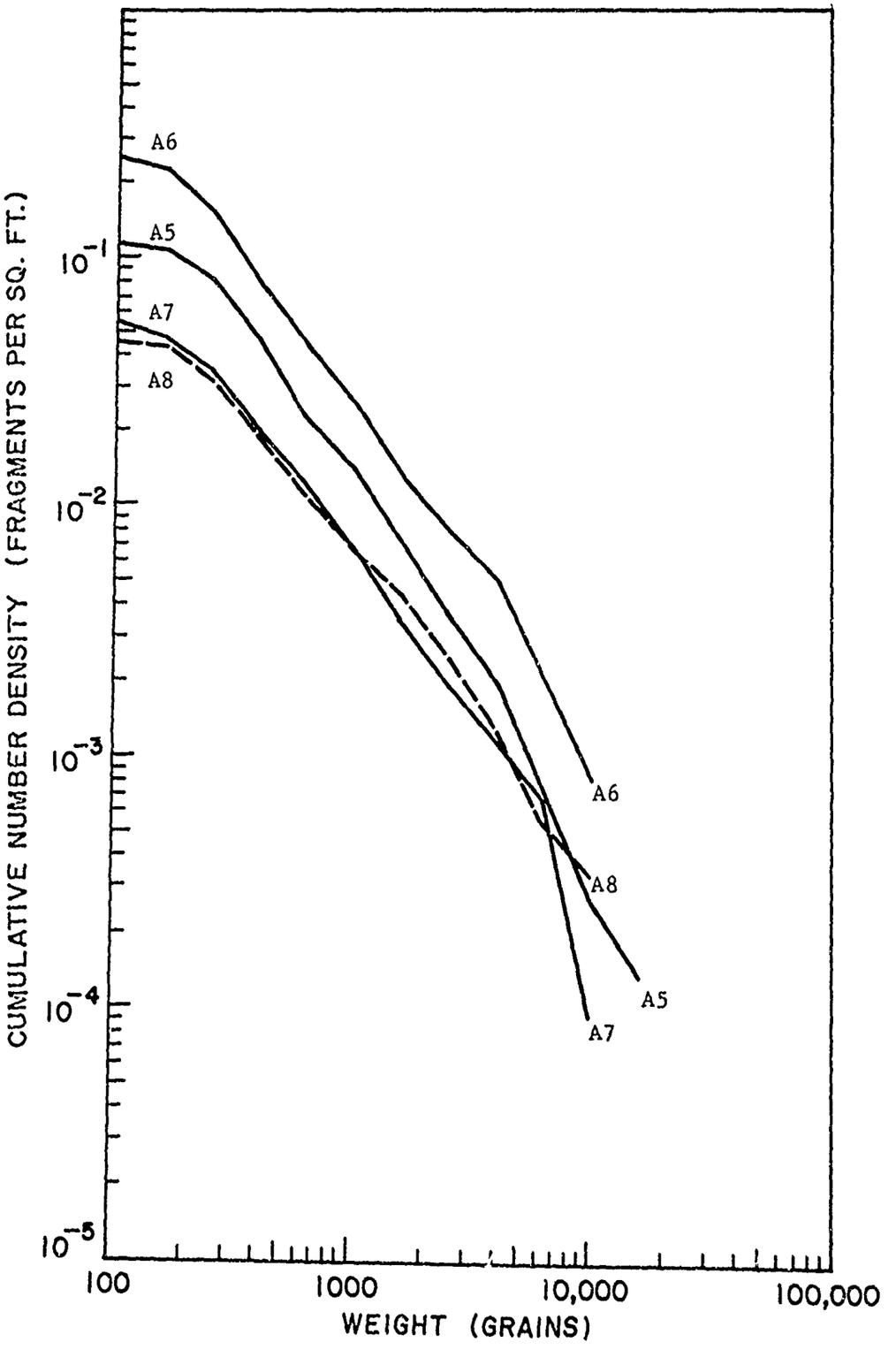

Figure 23 NUMBER DENSITY OF FRAGMENTS WITH WEIGHT GREATER THAN W RAY A - SECTORS 5, 6, 7, 8

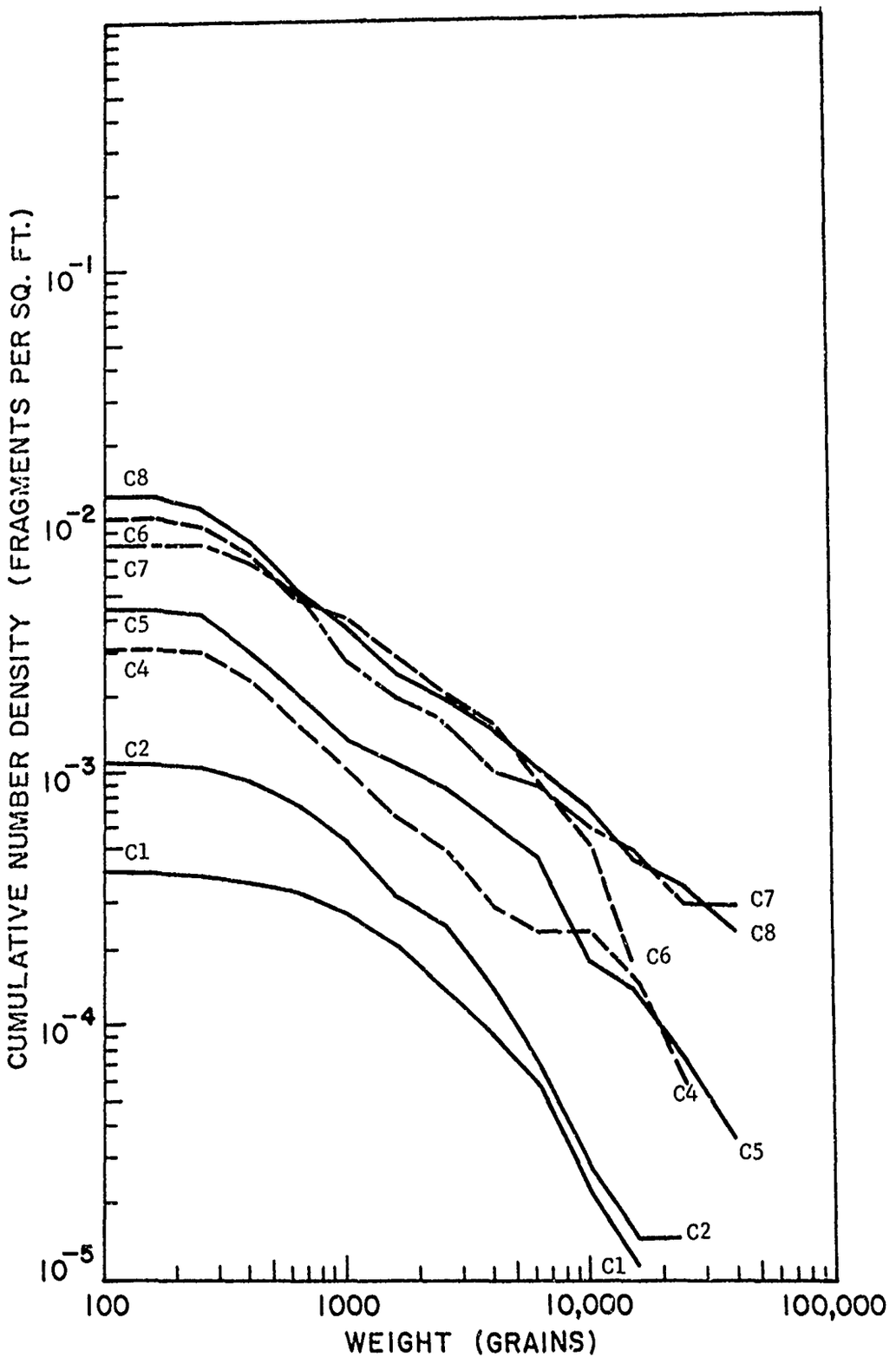

Figure 24 NUMBER DENSITY OF FRAGMENTS WITH WEIGHT GREATER THAN W RAY C - SECTORS 1, 2, 4, 5, 6, 7, 8

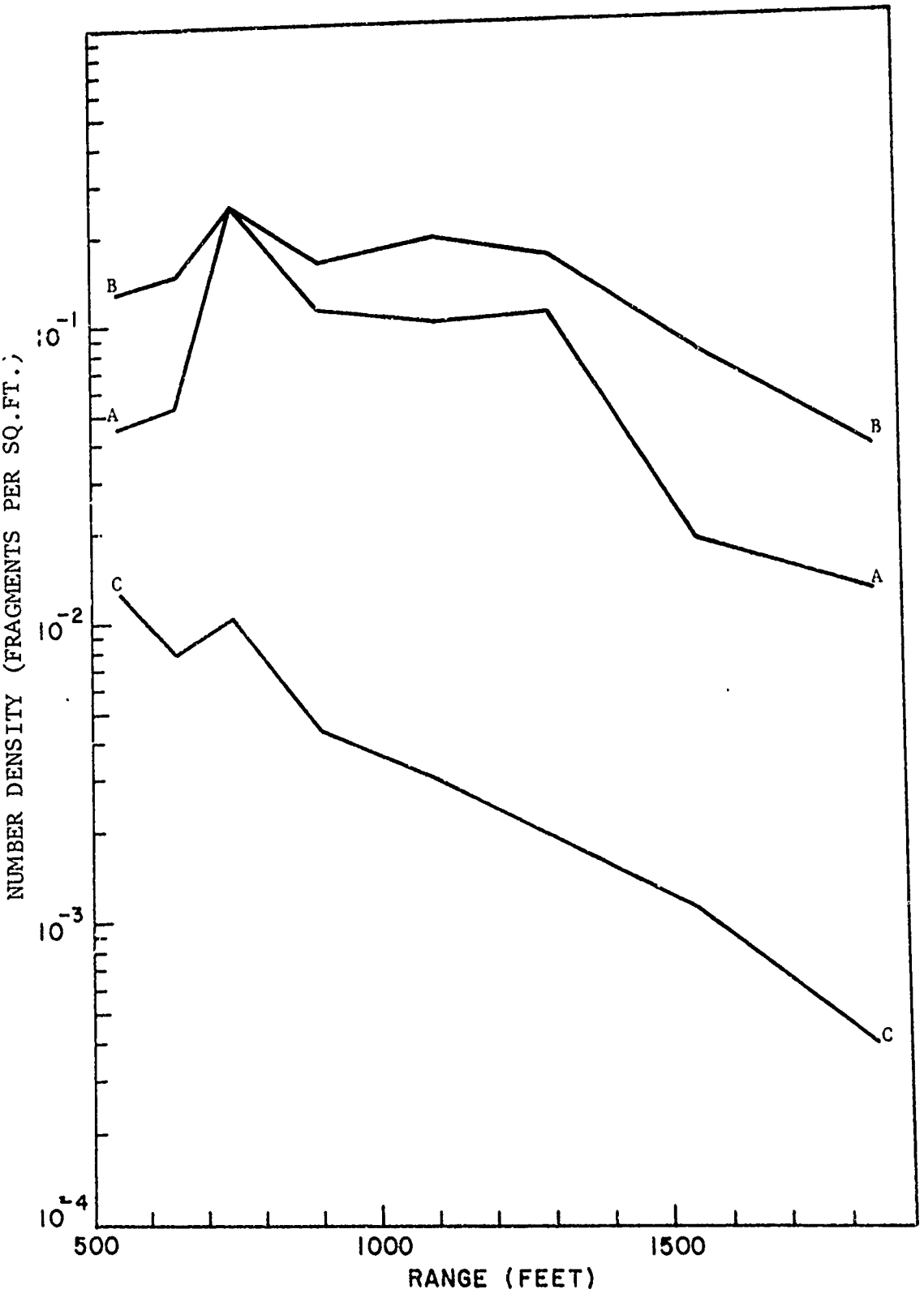

Figure 25 TOTAL FRAGMENT NUMBER DENSITY - RAYS A, B, C

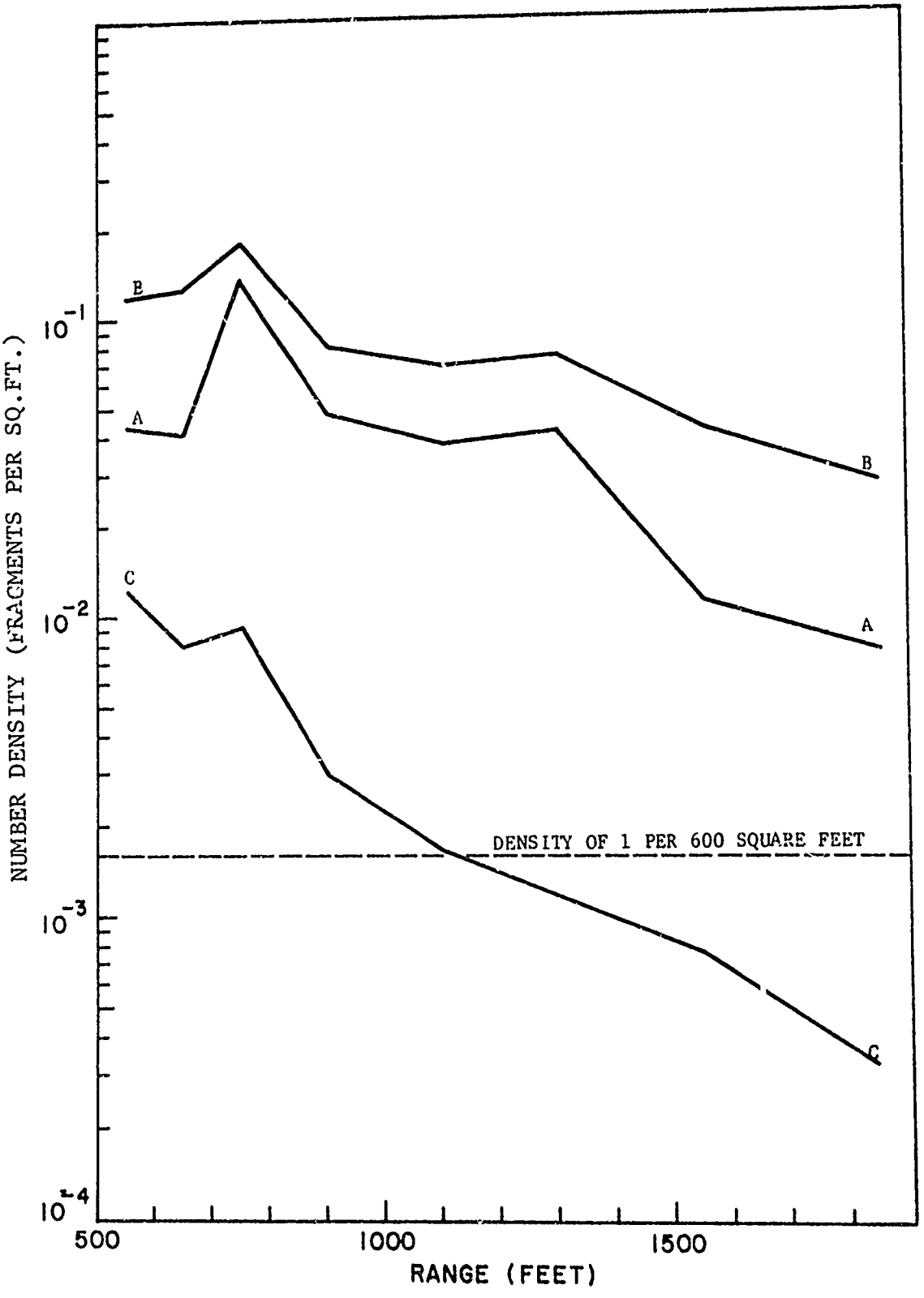

Figure 26 HAZARDOUS FRAGMENT NUMBER DENSITY FOR 11 ft-lb ENERGY CRITERIA - RAYS A, B, C

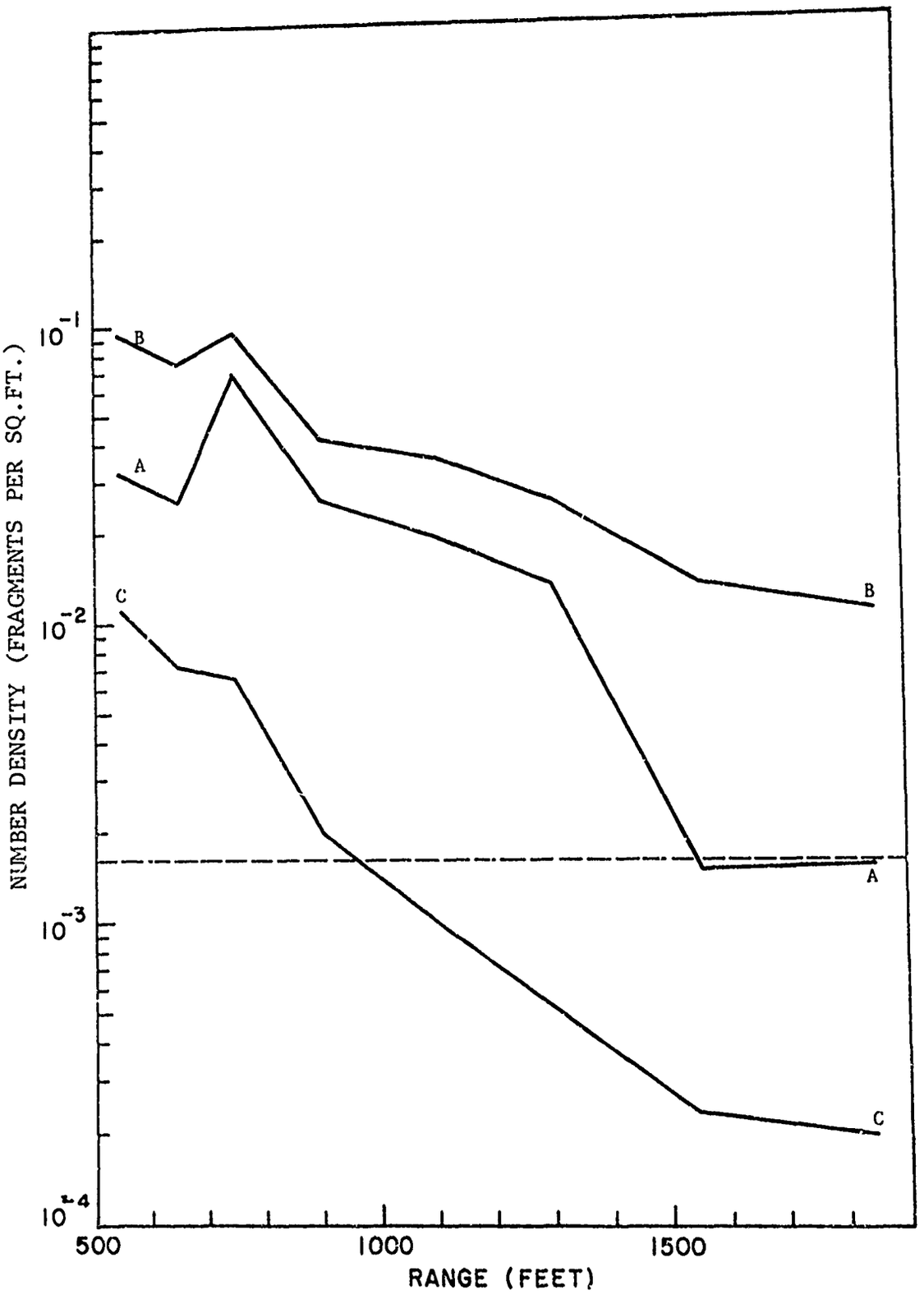

Figure 27 HAZARDOUS FRAGMENT NUMBER DENSITY FOR 58 ft-lb ENERGY CRITERIA - RAYS A, B, C

Figures 28, 29 and 30 show the upper and lower register fragment densities as a function of range, for the 11 ft-lb energy criteria and an initial fragment velocity of 5000 ft/sec, for rays A, B and C respectively, These distributions have been combined on the basis of the areal distribution of a standing man under upper and lower register fire (see Appendix). Figure 26 illustrates this combined distribution. Figures 31, 32, 33 and 27 illustrate similar characteristics for the 58 ft-lb energy criteria.

As noted in the previous section rapid falloff in fragment number density takes place at about 1300 ft from detonation. Examination of Figures 28 through 33 indicates that lower register fragments predominate as the more serious hazard up to about 1300 ft. Beyond this range, the upper register fragments are usually the most serious threat. Since the probability of serious injury is dependent upon a target area and the target area is a function of the terminal fragment elevation angle, a lower register fragment will almost always pose a more serious threat. An upper register fragment impacts a standing man with a presented area of 1.33 sq ft while a lower register fragment can hit a standing man that varies anywhere from 1.33 to 9.0 sq ft.

Figures 34 and 35 illustrate the probability of serious injury as a function of range from detonation for an 11 and 58 ft-lb injury criteria for each ray. The previous point pertaining to target area is shown by the absence of a rapid falloff of injury probability beyond a 1300 ft range, especially for the base sector. (See Appendix).

4.3 Variation of Fragment Pickup within Sectors

Examination of cumulative weight distributions for individual bags within a given sector was made to investigate the variability of pickup by a magnet truck within a sector. Figures 36, 37, and 38 illustrate this degree of variability in sector A4. Here eight bags were picked up and, while there was a close similarity in distributions for bags A and B, there was significant variation between bags C and F. Thus, the manner in which the magnet truck picks up fragments within a sector presently precludes anything but complete pickup within the sector.

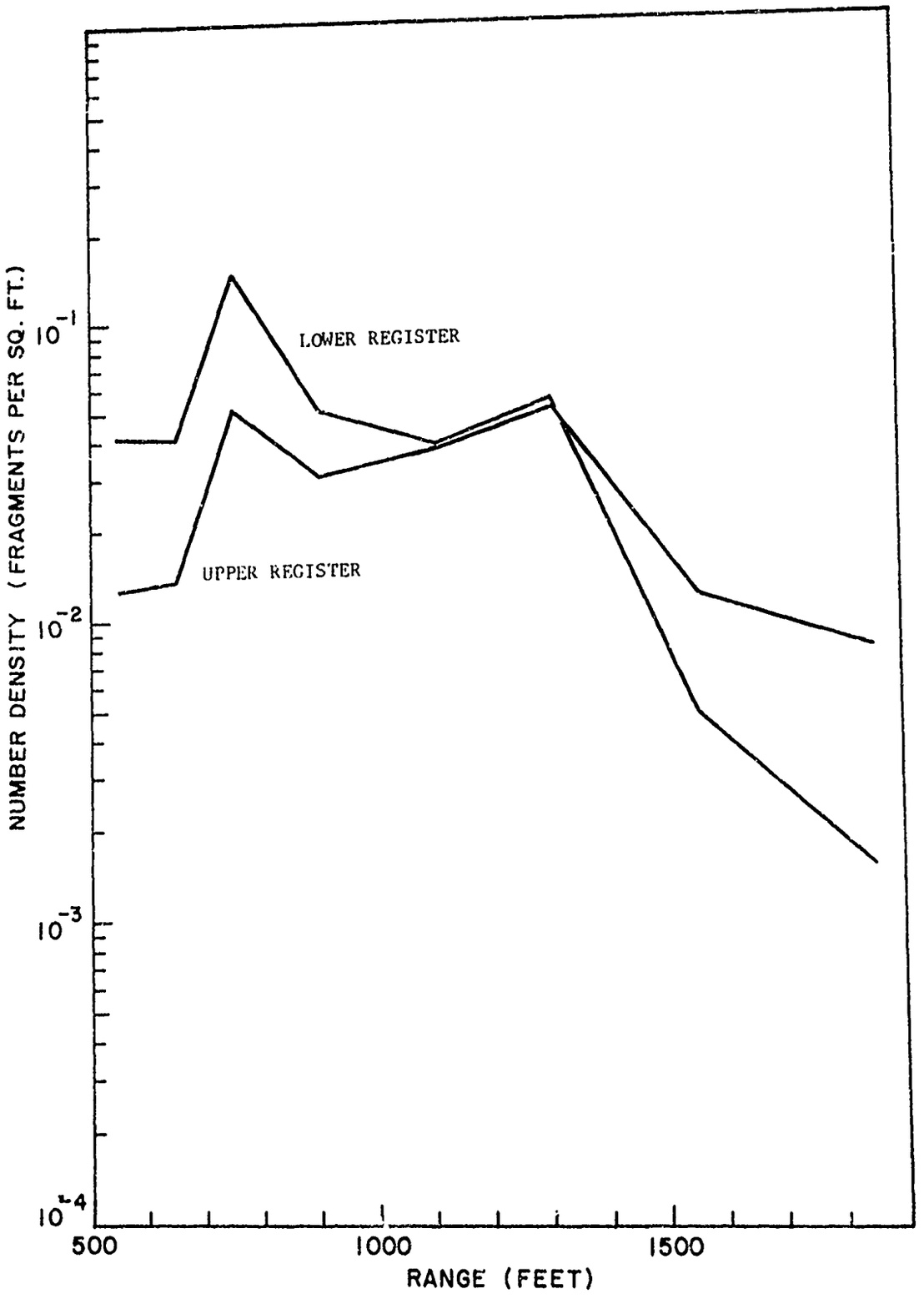

Figure 28 HAZARDOUS FRAGMENT NUMBER DENSITY FOR 11 ft-lb ENERGY CRITERIA - UPPER AND LOWER REGISTER CONTRIBUTIONS FOR RAY A

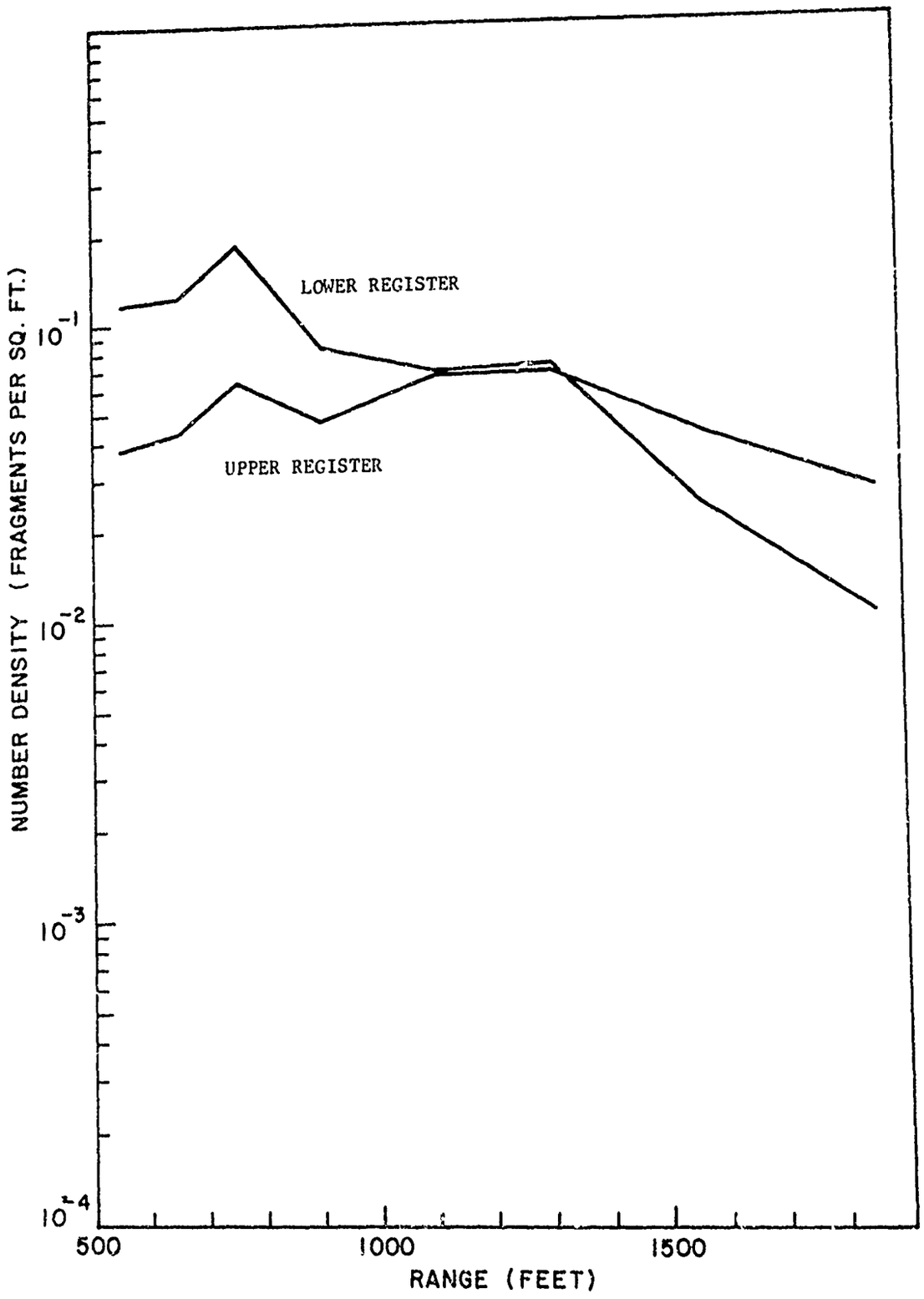

Figure 29 HAZARDOUS FRAGMENT NUMBER DENSITY FOR 11 ft-lb ENERGY CRITERIA - UPPER AND LOWER REGISTER CONTRIBUTIONS FOR RAY B

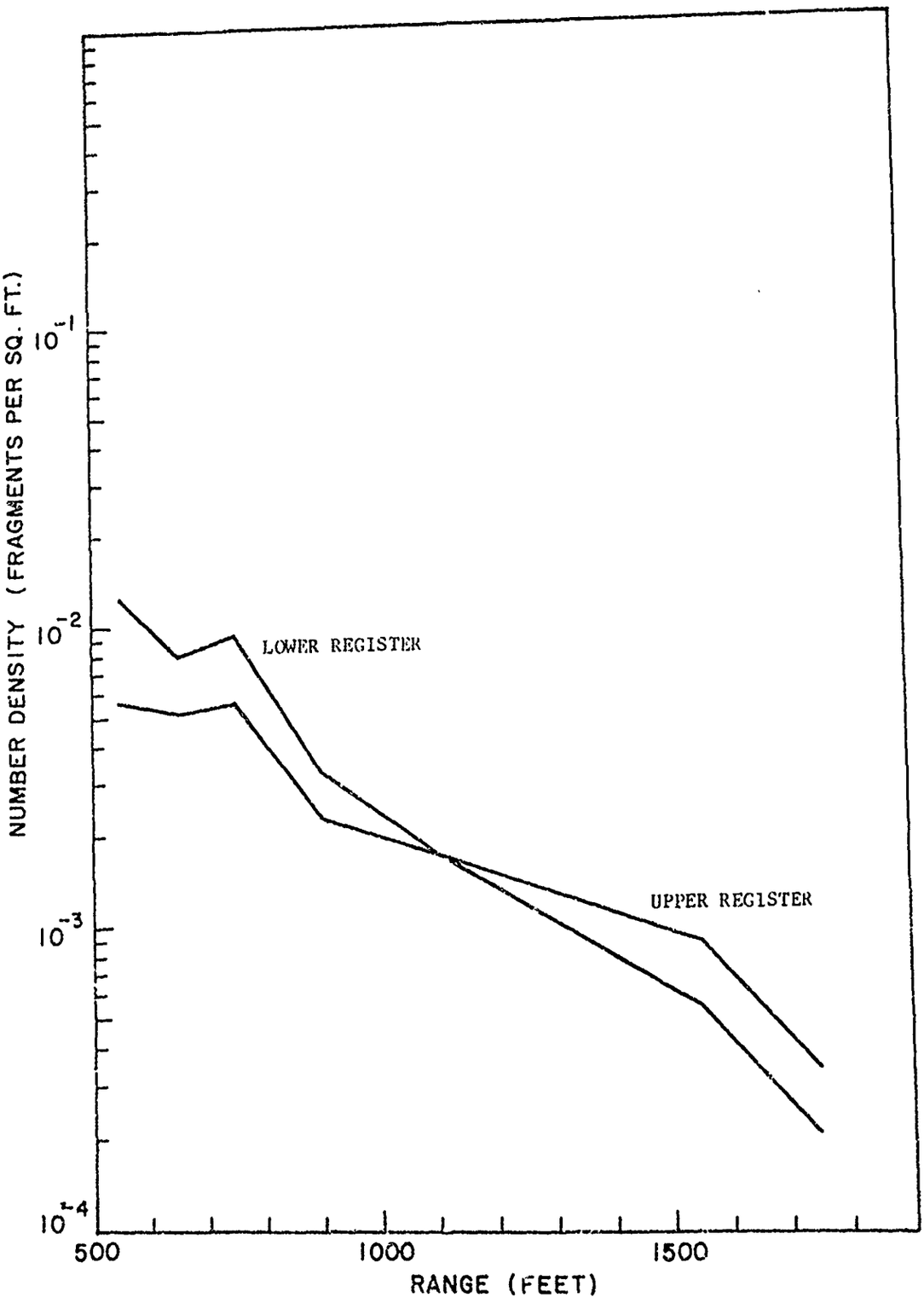

Figure 30 HAZARDOUS FRAGMENT NUMBER DENSITY FOR 11 ft-lb ENERGY CRITERIA - UPPER AND LOWER REGISTER CONTRIBUTIONS FOR RAY C

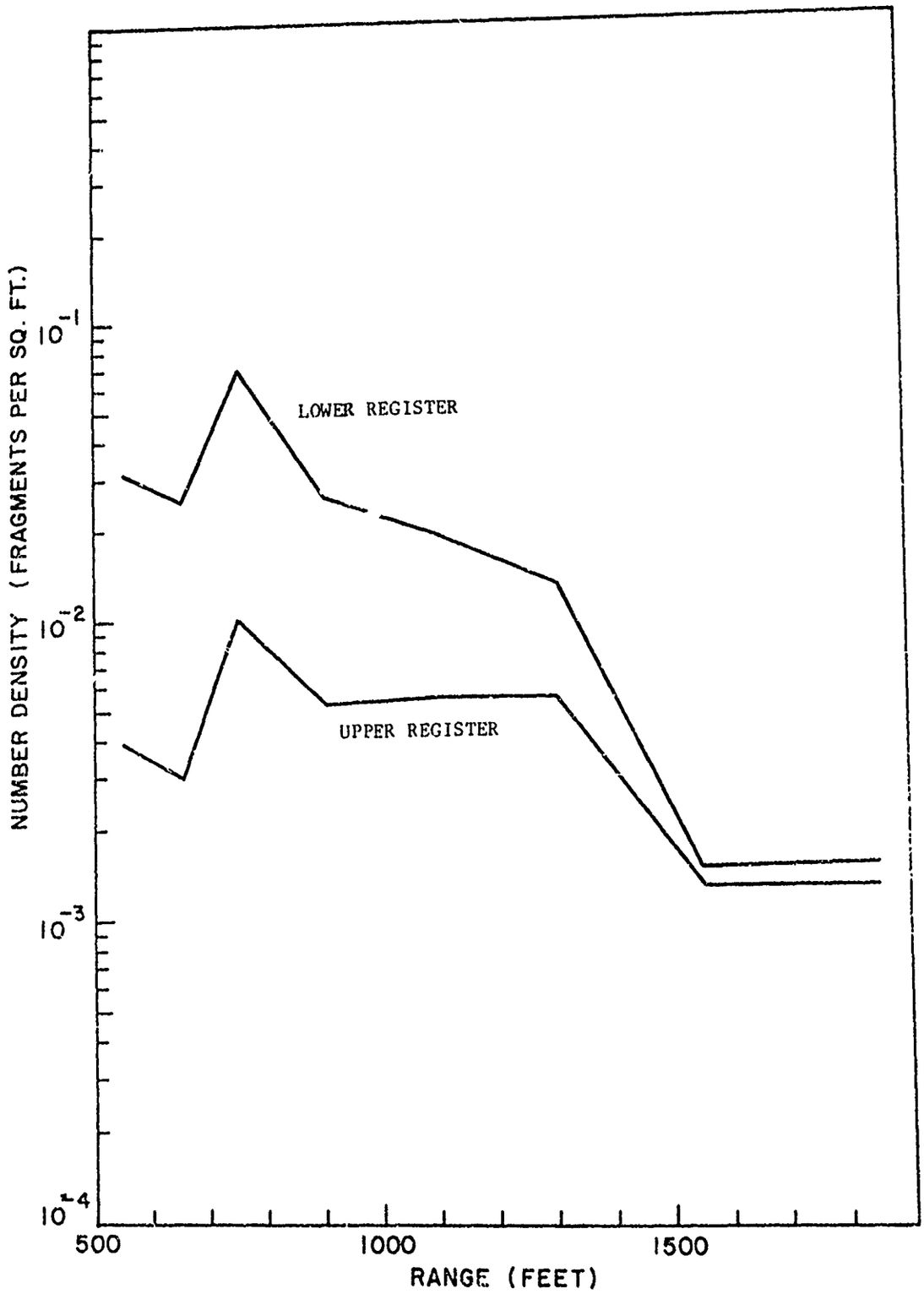

Figure 31 HAZARDOUS FRAGMENT NUMBER DENSITY FOR 58 ft-lb ENERGY CRITERIA - UPPER AND LOWER REGISTER CONTRIBUTIONS FOR RAY A

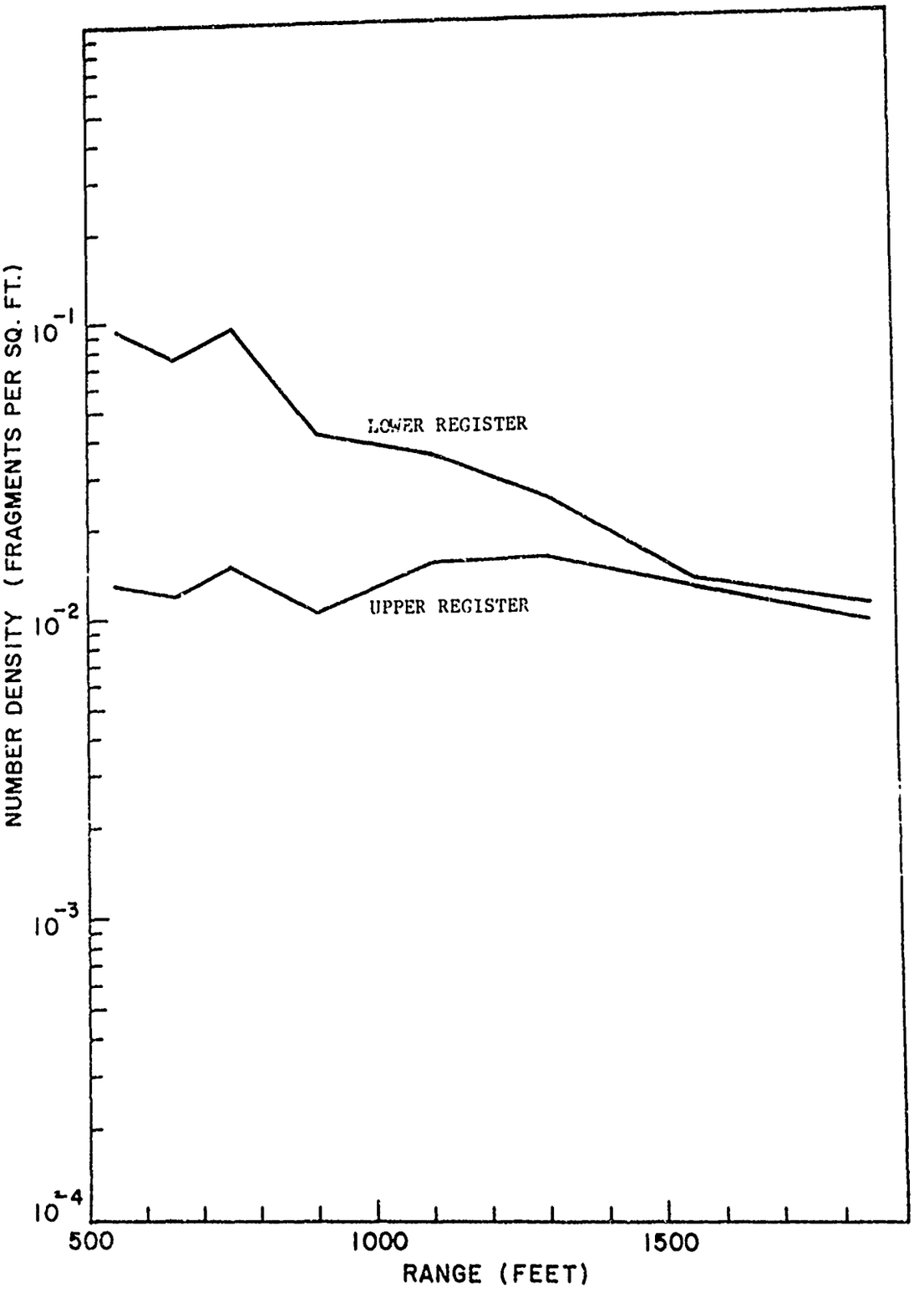

Figure 32 HAZARDOUS FRAGMENT NUMBER DENSITY FOR 58 ft-lb ENERGY CRITERIA - UPPER AND LOWER REGISTER CONTRIBUTIONS FOR RAY B

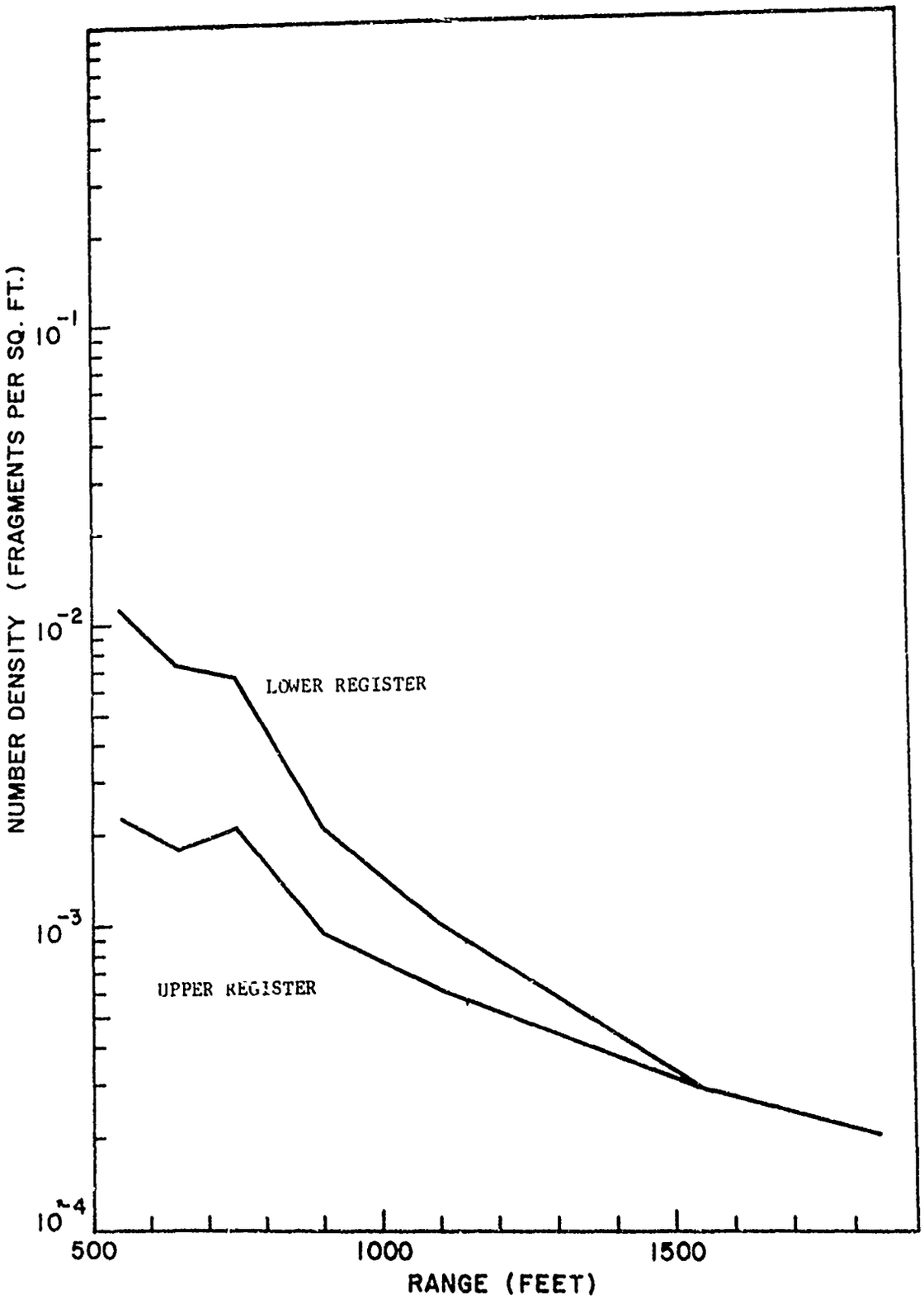

Figure 33 HAZARDOUS FRAGMENT NUMBER DENSITY FOR 58 ft-lb ENERGY CRITERIA - UPPER AND LOWER REGISTER CONTRIBUTIONS FOR RAY C

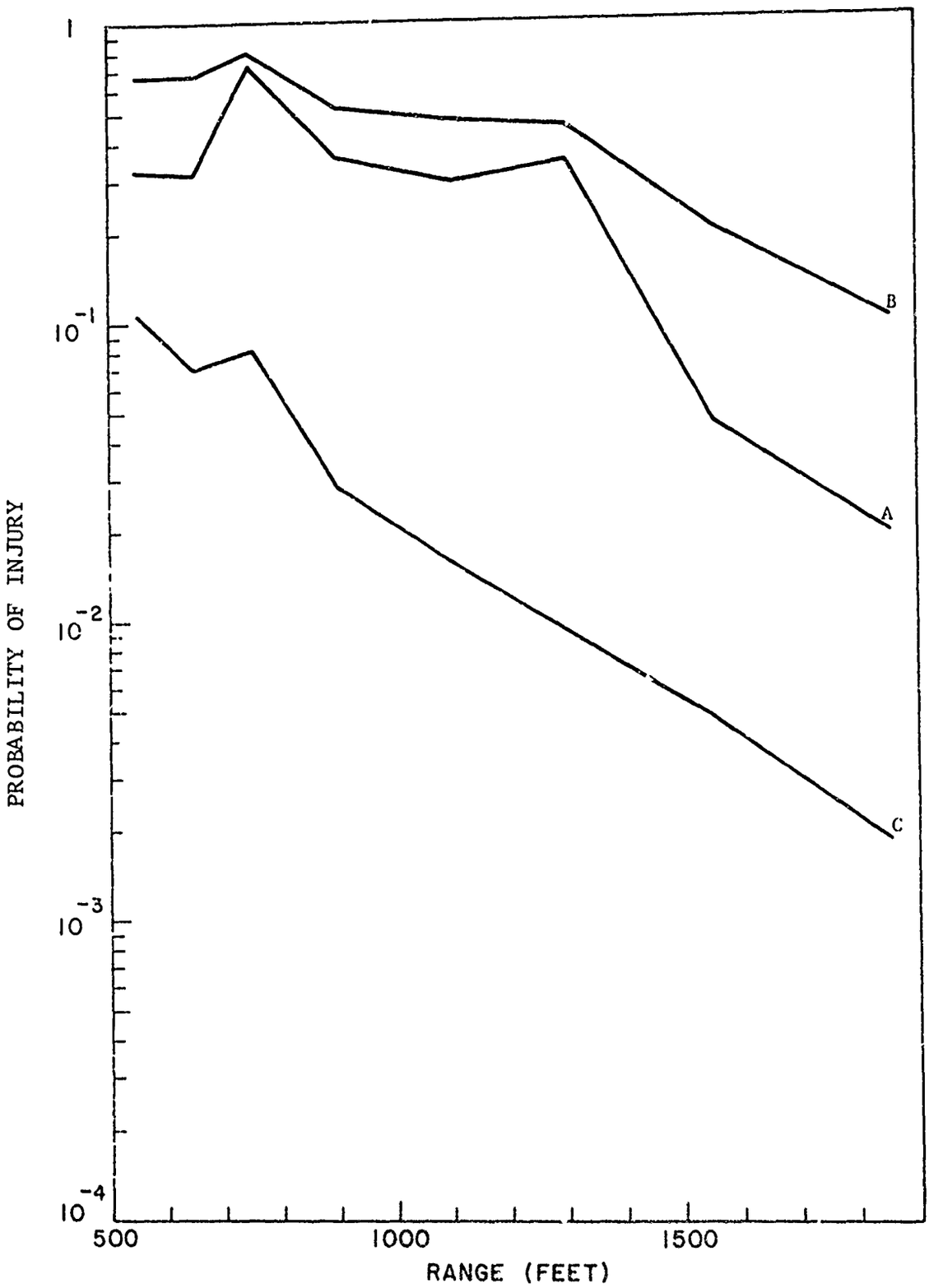

Figure 34 PERSONNEL FRAGMENT INJURY PROBABILITIES FOR 11 ft-lb ENERGY CRITERIA - RAYS A, B, C

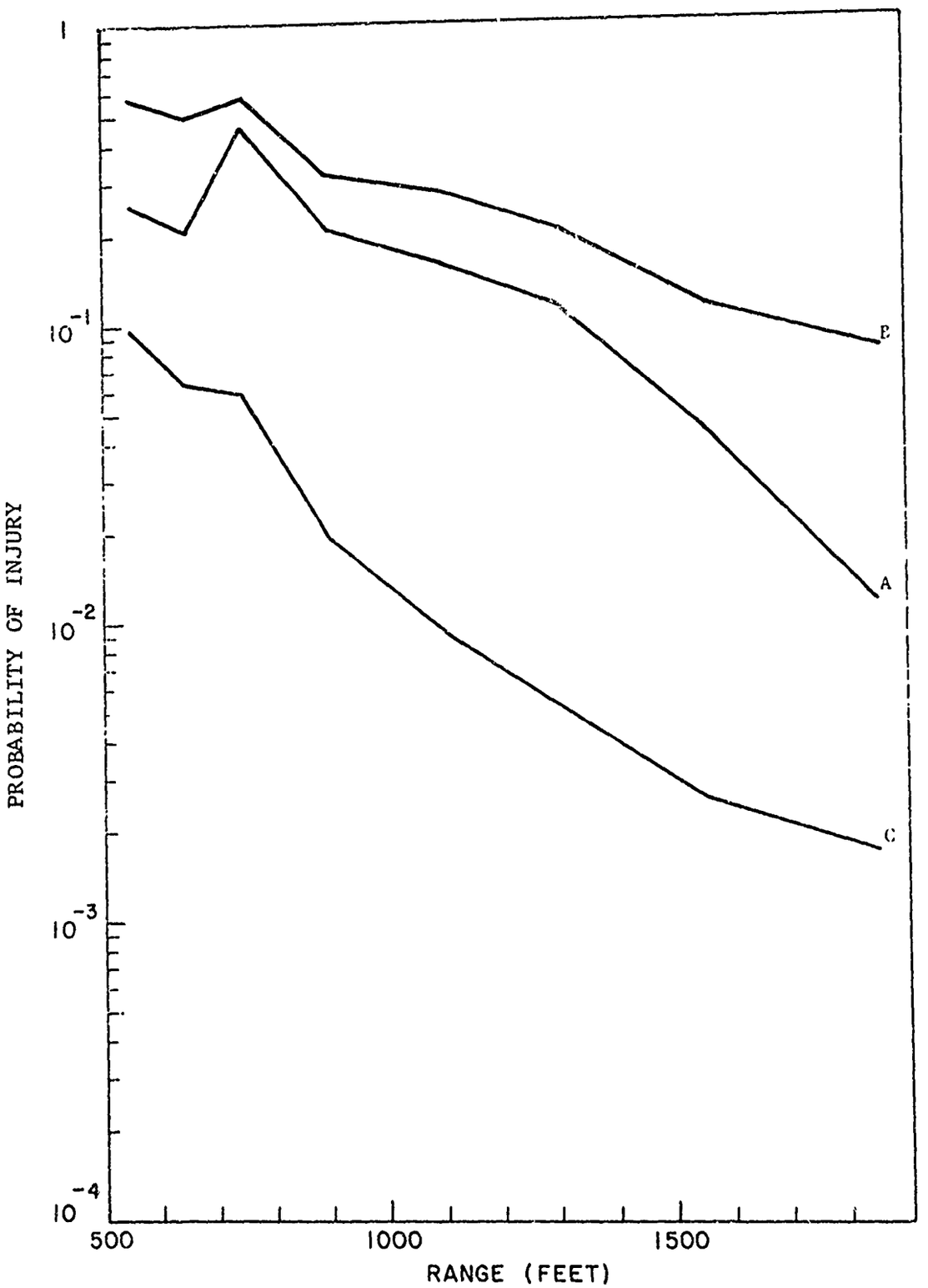

Figure 35 PERSONNEL FRAGMENT INJURY PROBABILITIES FOR 58 ft-lb ENERGY CRITERIA - RAYS A, B, C

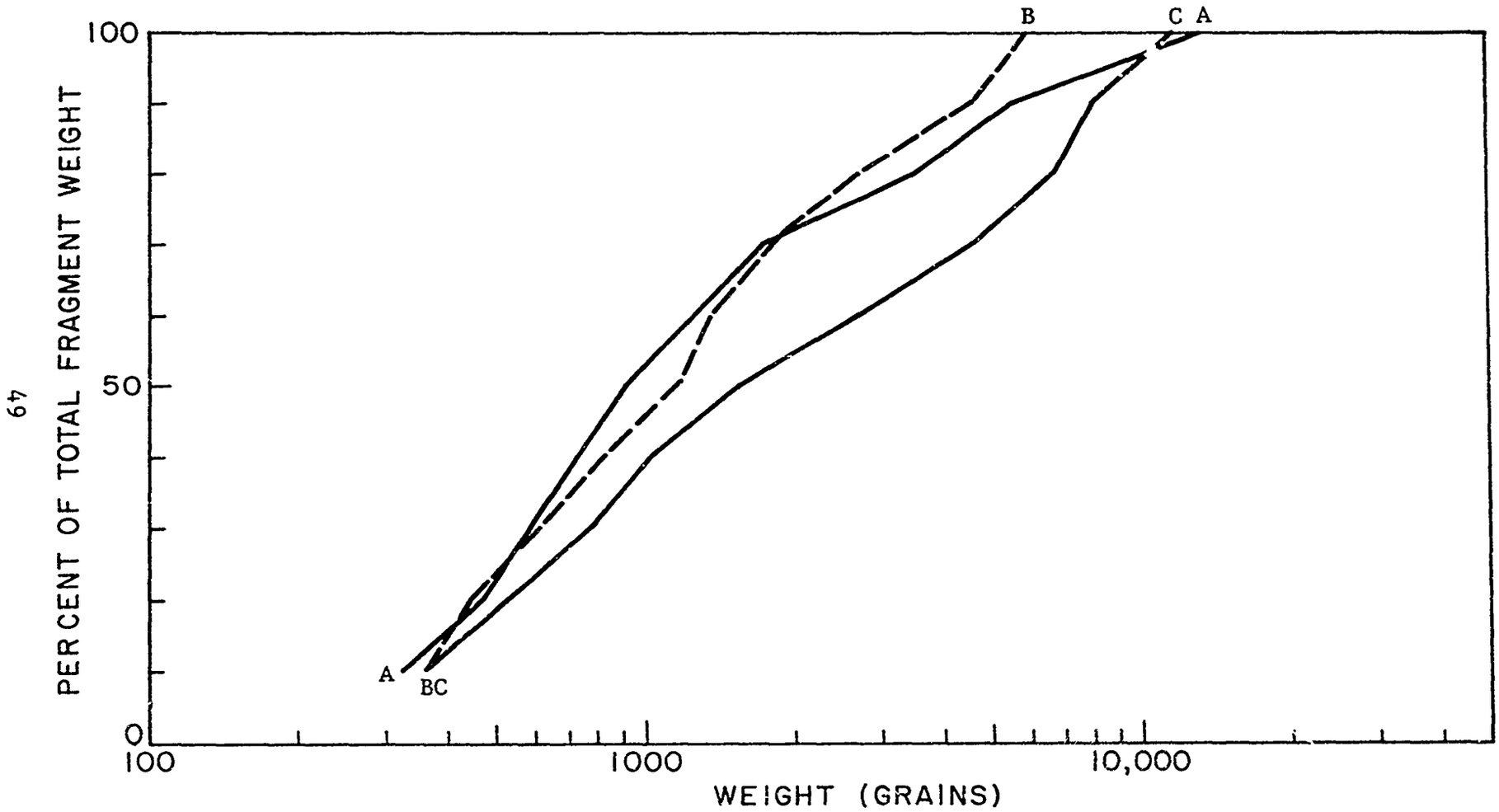

Figure 36 CUMULATIVE WEIGHT DISTRIBUTIONS FOR COLLECTION BAGS IN SECTOR A-4, BAGS A, B, C

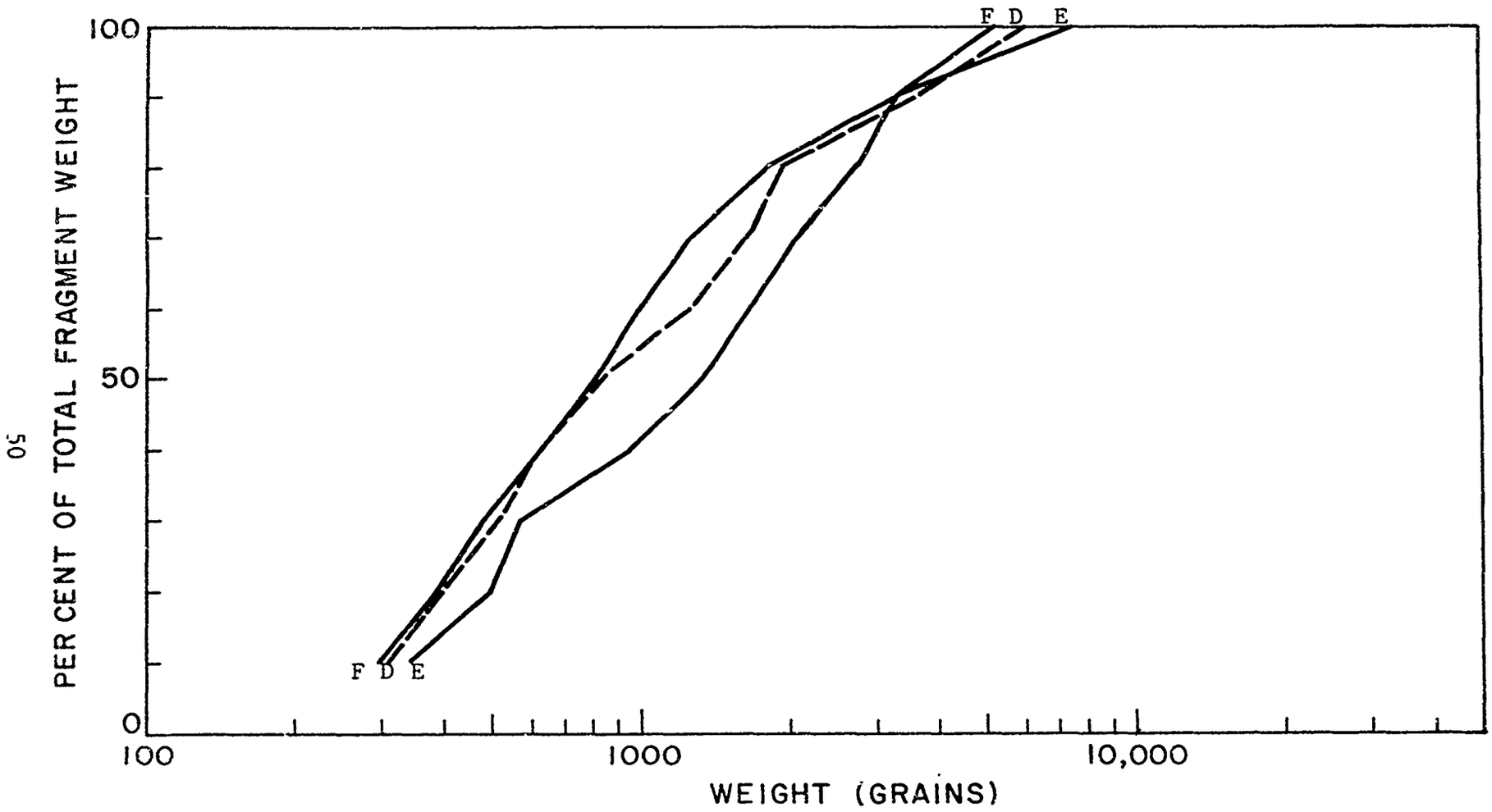

Figure 37 CUMULATIVE WEIGHT DISTRIBUTIONS FOR COLLECTION BACS IN SECTOR A-4, BAGS D, E, F

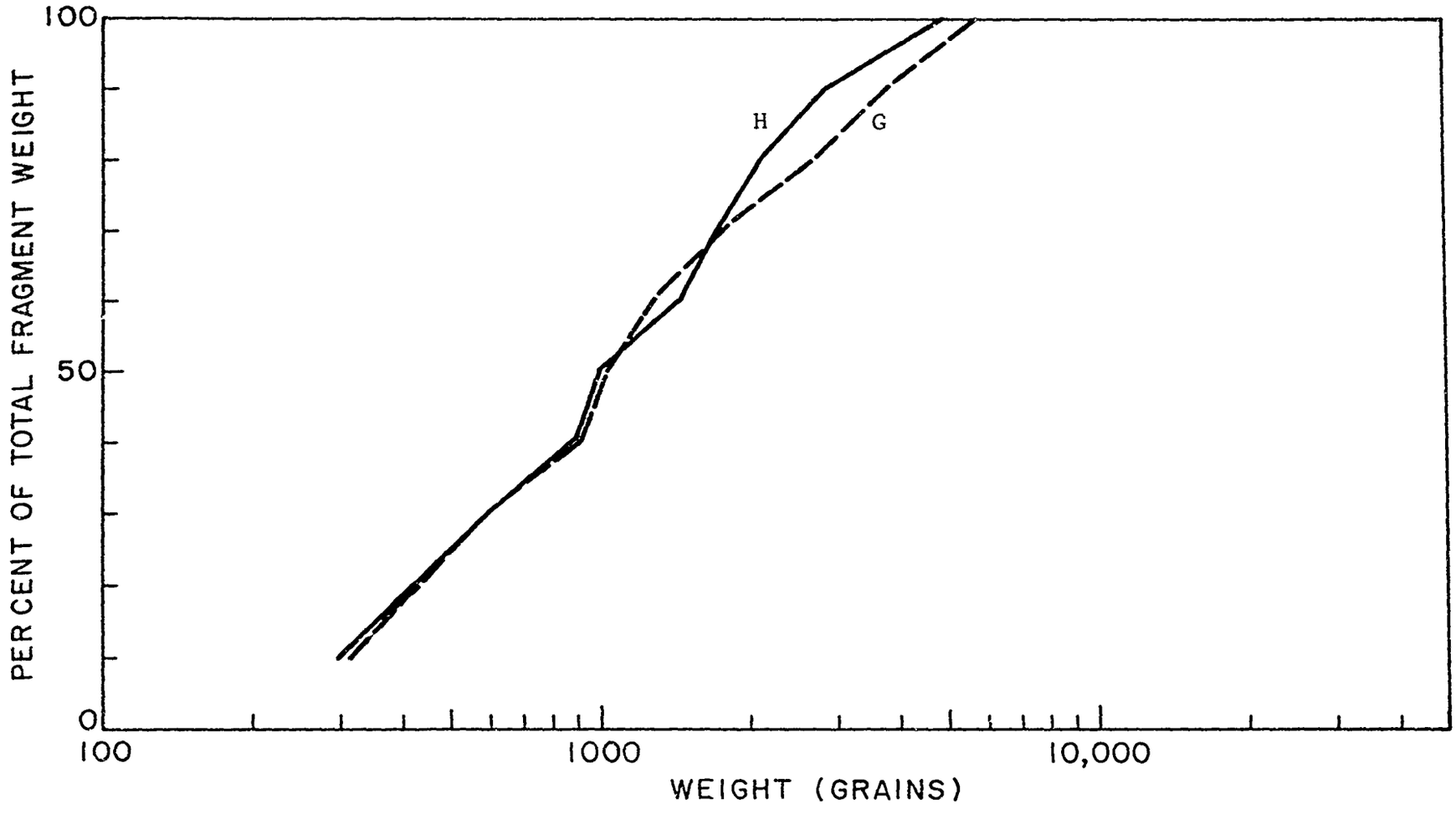

Figure 38 CUMULATIVE WEIGHT DISTRIBUTIONS FOR COLLECTION BAGS IN SECTOR A-4, BAGS G, H

5. YUMA RESULTS COMPARED WITH ESKIMO I RESULTS

Results obtained from NWC, China Lake, California have been placed in a similar format to the Yuma results in order to compare the two tests. That is, the cumulative number density as a function of fragment weight has again been compiled for all collected fragments, broken down by rays and then by sectors within rays. Also, the cumulative number density as a function of range, for all fragments remaining on the 5/8 in. sieve, has been prepared. Again this relationship has been developed for those fragments exceeding 11 and 58 ft-lbs and upper and lower register contributions noted.

5.1 Cumulative Number Density Versus Weight

Figures 39 through 43 correspond to their Yuma counterparts displayed in Figures 18 through 24. Figure 39 shows the total distribution of fragments collected at China Lake and, as might be expected, indicates an overall greater fragment density for all weight regimes than its Yuma counterpart (i.e., Figure 18). This was due to the much greater number of units detonated in the Eskimo I test. It is, however, interesting to note that the number of fragments per sq ft falls off at about the same rate, with increasing weight fragments, for both tests.

Figure 40 is a breakdown of Figure 39 by rays. It should be noted that the West (or side) ray, followed closely by the North (or front) ray, contained the greatest amount of fragments. The South (or rear) ray had considerably less fragments in it. It is interesting to note that the South ray of the Eskimo I test has essentially the same distribution as the base ray in the Yuma test.

Figures 41 through 43 give breakdowns of Figure 40 by sectors within rays. Here, fragment densities generally drop off with increasing distance from the detonation. This is in contrast to similar Yuma results shown in Figures 20 through 24 where there is a buildup and then general dropoff of fragment density as a function of range from detonation. The Yuma side ray results do, however, display similar results to Eskimo I sector results.

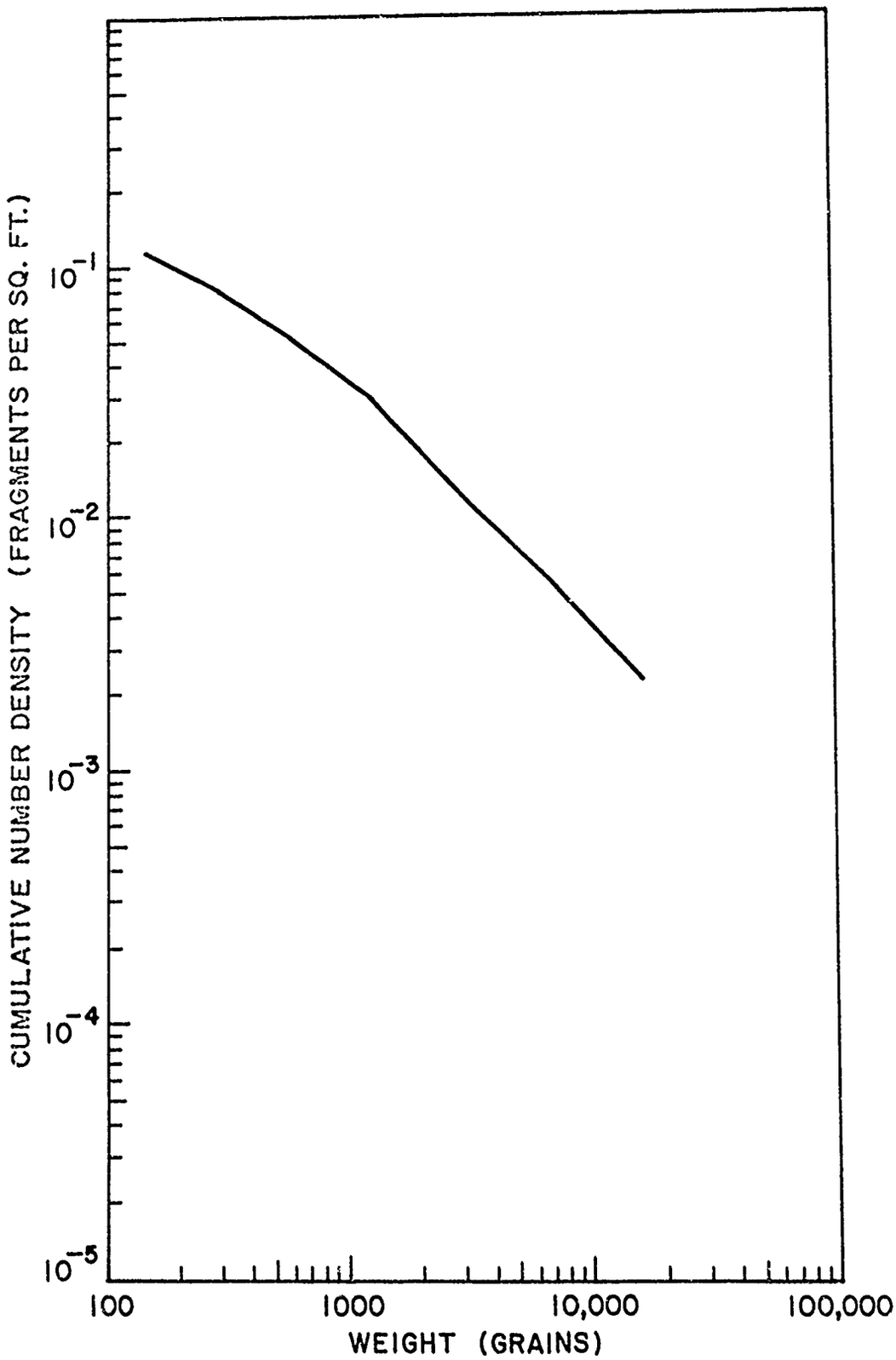

Figure 39 ESKIMO I FRAGMENT NUMBER DENSITY - ALL FRAGMENTS COUNTED

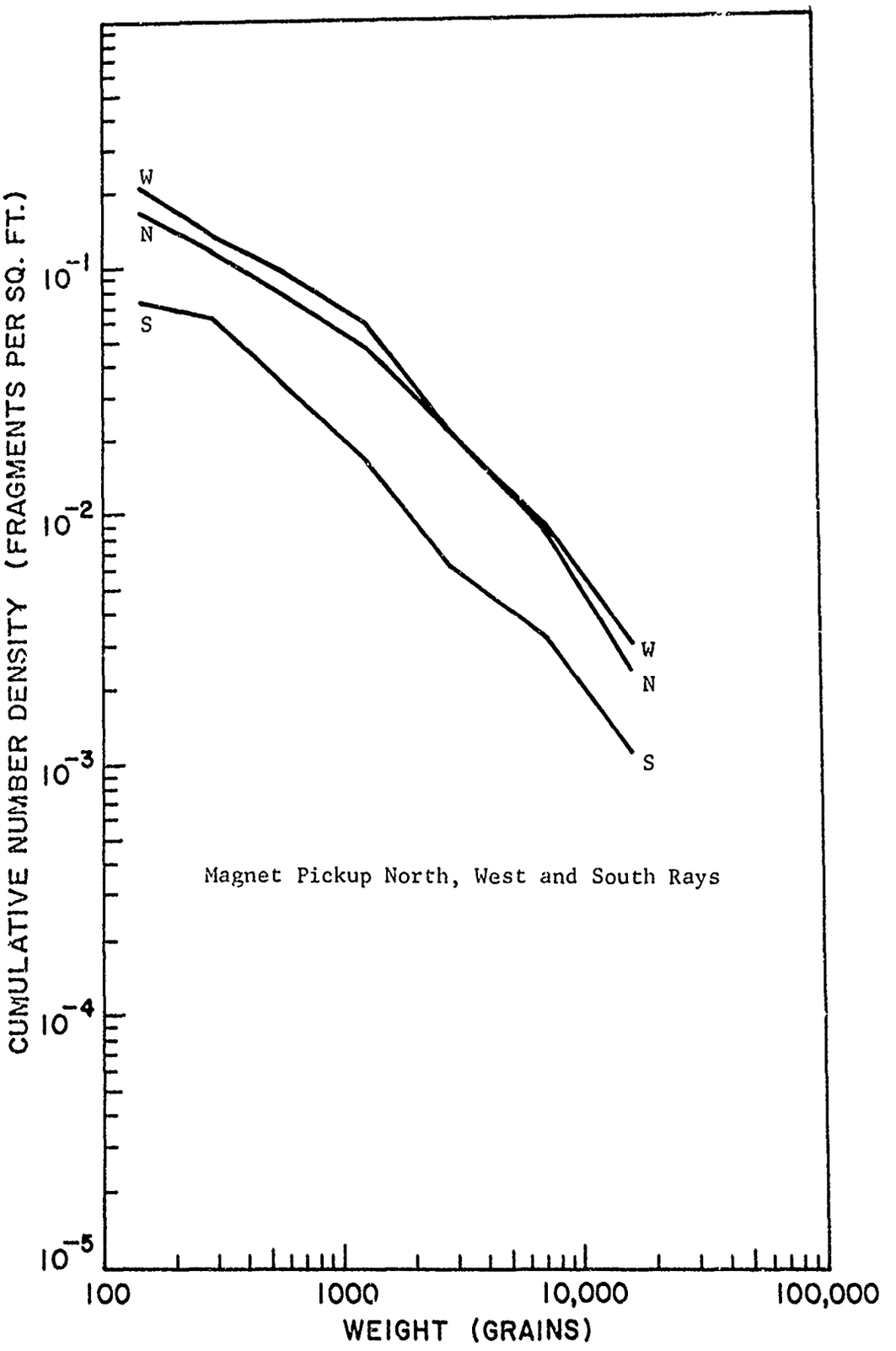

Figure 40 ESKIMO I FRAGMENT NUMBER DENSITY - RAYS W, N, S

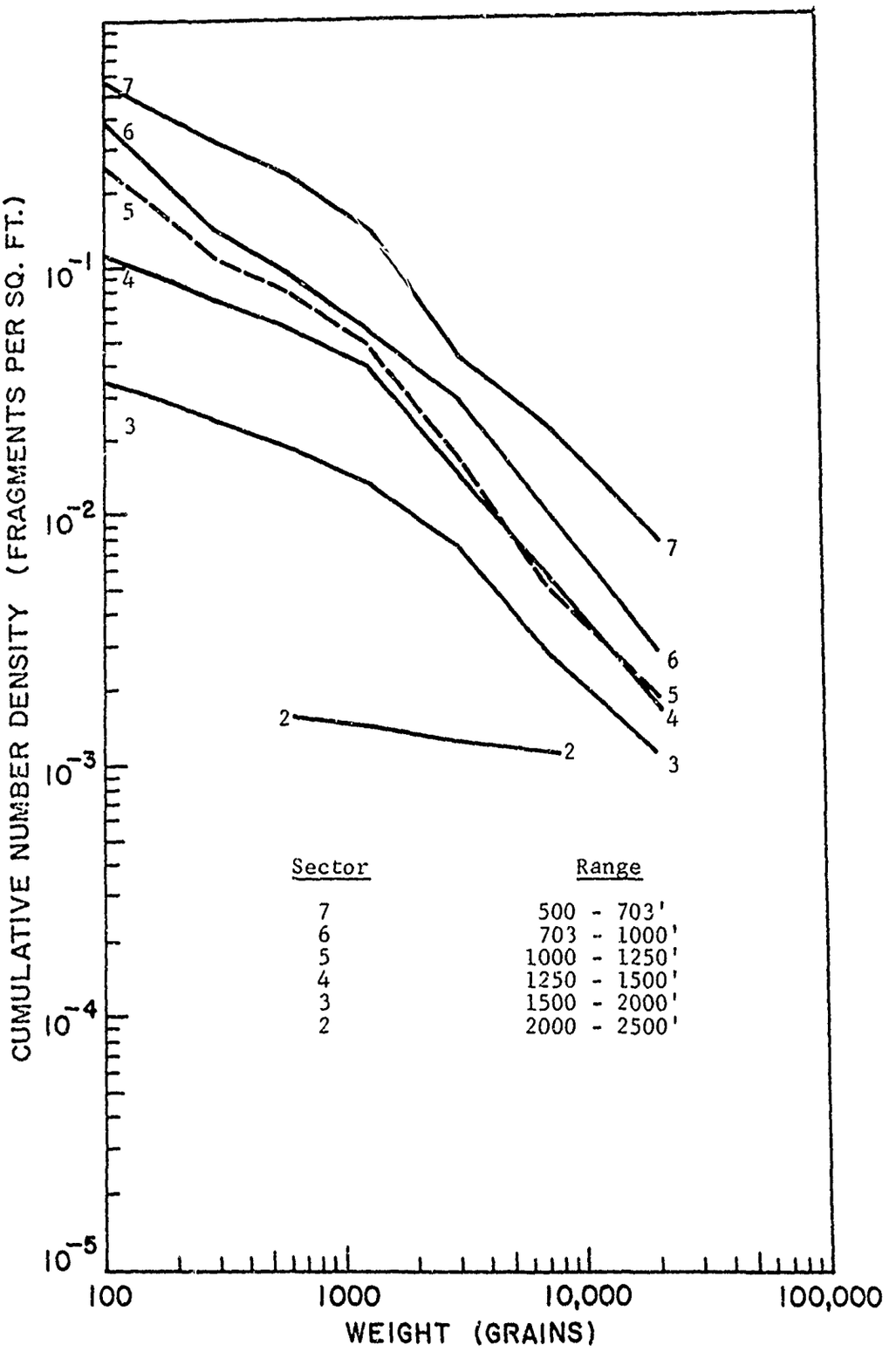

Figure 41 ESKIMO I FRAGMENT NUMBER DENSITY WEST RAY BY SECTOR

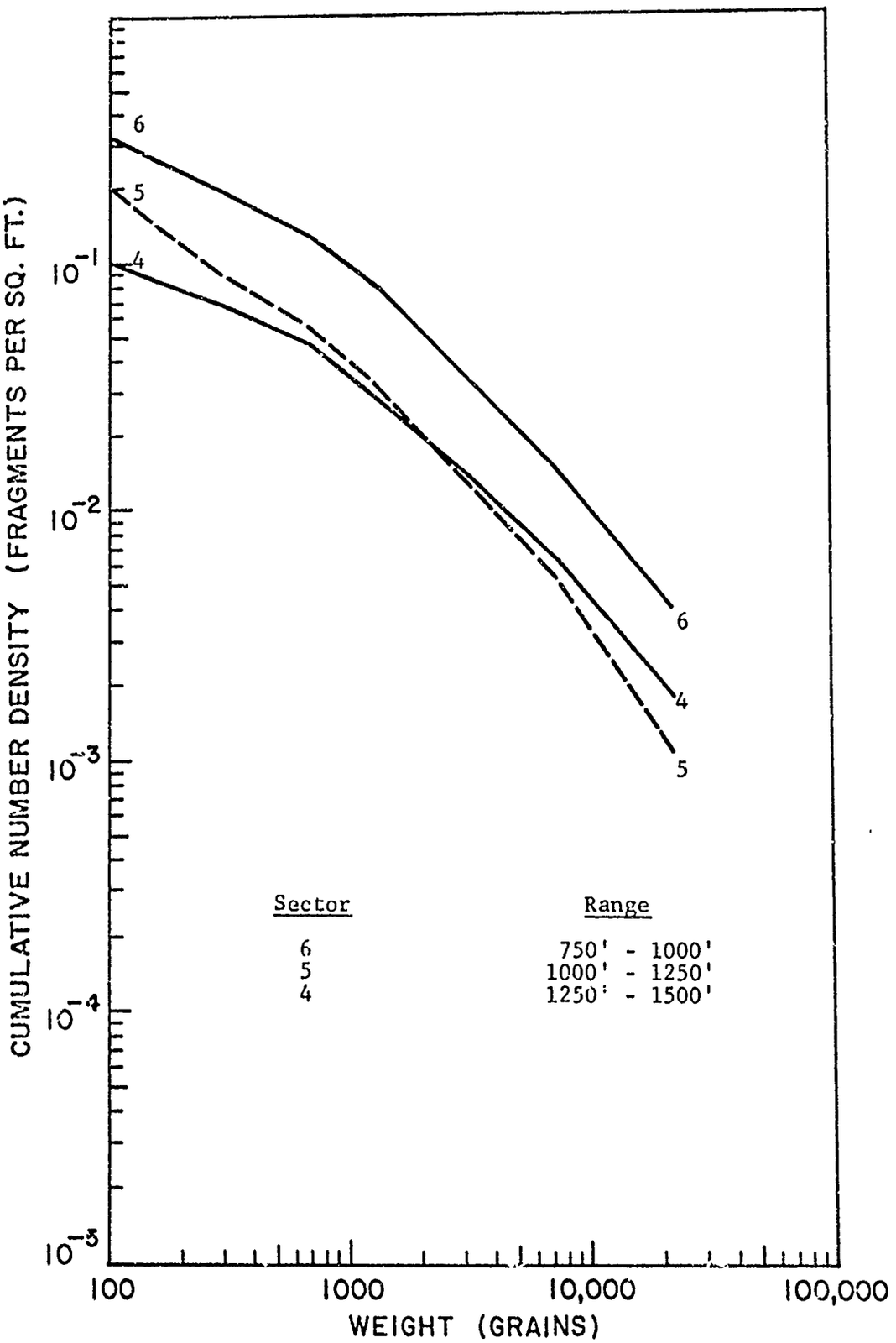

Figure 42 ESKIMO I FRAGMENT NUMBER DENSITY NORTH RAY BY SECTOR

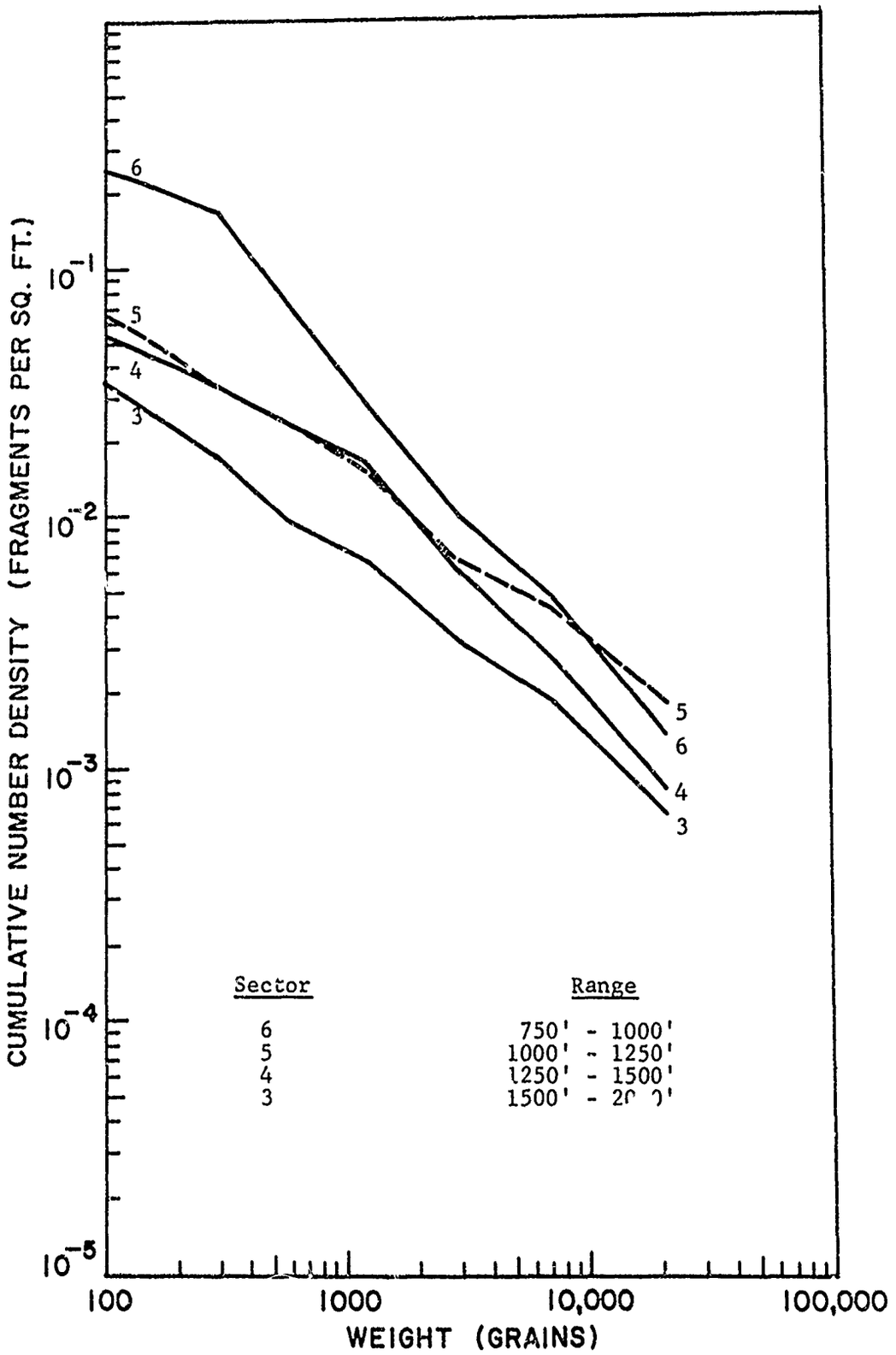

Figure 43 ESKIMO I FRAGMENT NUMBER DENSITY SOUTH RAY BY SECTOR

5.2 Number Density Versus Range

Figures 44 through 52 give number densities of all collected fragments as a function of range from the point of detonation for the Eskimo I test. These sets of figures correspond to their Yuma counterparts shown in Figures 28 through 33. The most interesting comparison here is the same marked falloff of fragment density with range which takes place in Eskimo I at about 1100 ft; the rate of falloff being similar. This is particularly apparent when comparing the fragment distributions along the base ray of Yuma with the distributions along the West ray of Eskimo I (i.e., the rays having the greatest density of fragments in their respective tests). It should also be noted that the lower register results displayed in Figures 47 through 50 were derived utilizing Figures 6 and 7 in conjunction with Figures 41 through 43.

5.3 Yuma Results Compared with Analytic Results

Previous effort has indicated that analytic results, obtained utilizing a computer model, compare favorably with experimental results involving stacks of 750 lb bombs obtained in the NWC-China Lake tests of March 1970. These results are illustrated in Figure 53. Here analytic results were generated for a single unit 750 lb bomb, multiplied by three and compared to multiple unit bomb stacks in 2 x 3 and 5 x 3 configurations. Thus, in this case, a simple multiple of the single unit result compared quite favorably with the multiple unit case.

Figure 54 provides a similar comparison of results between Yuma test results and analytic results obtained for a single unit 155-mm projectile. The single unit munition result, in this case, has been multiplied by a factor of 10 corresponding to there being 10 shells oriented in a similar direction to the single shell (i.e., with the longitudinal axis of the shell perpendicular to the side sector). At ranges of interest (i.e., beyond 1000 ft), agreement between analytic and experimental results is again quite good.

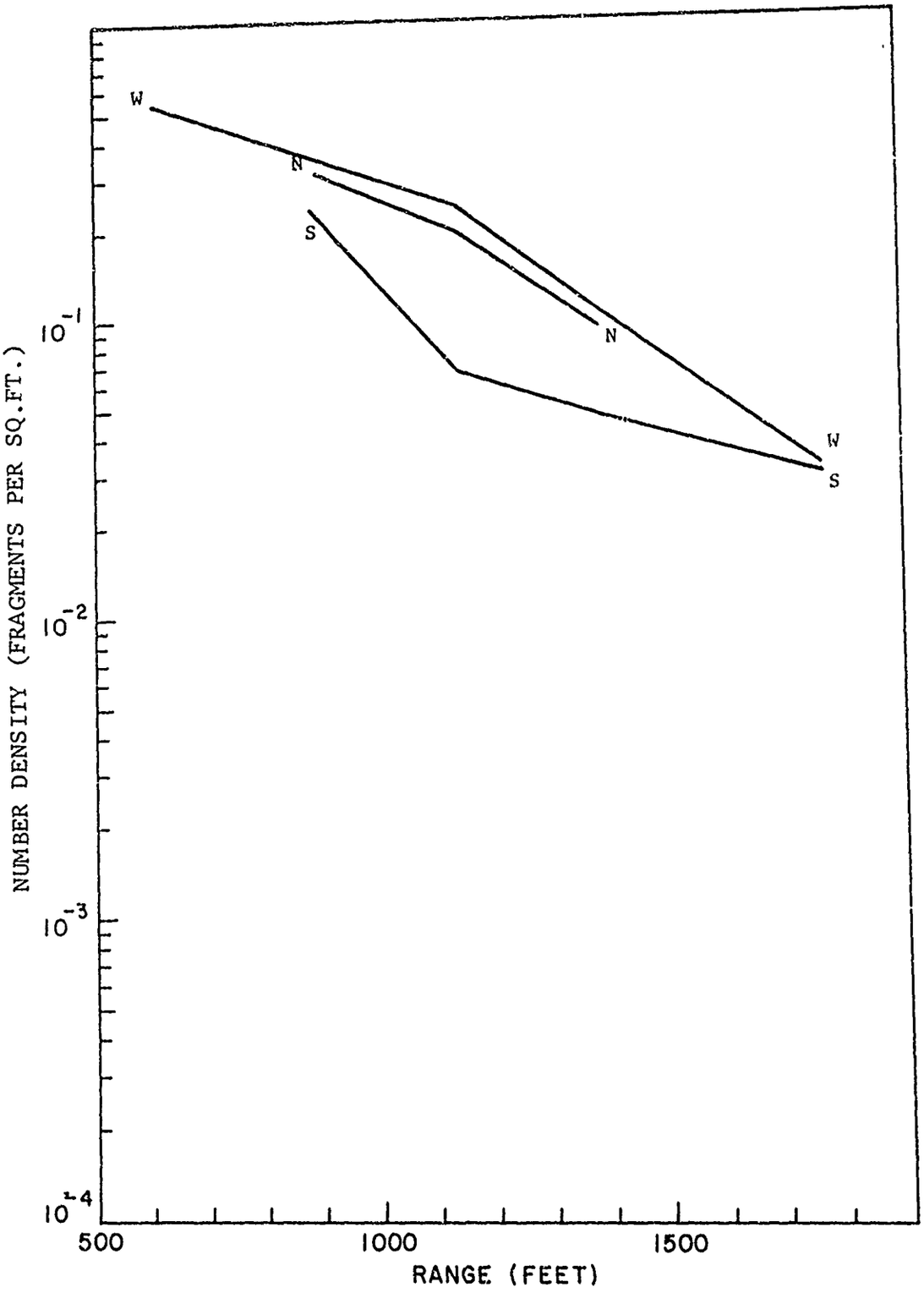

Figure 44 ESKIMO I FRAGMENT NUMBER DENSITY AS A FUNCTION OF RANGE, RAYS N, S, W

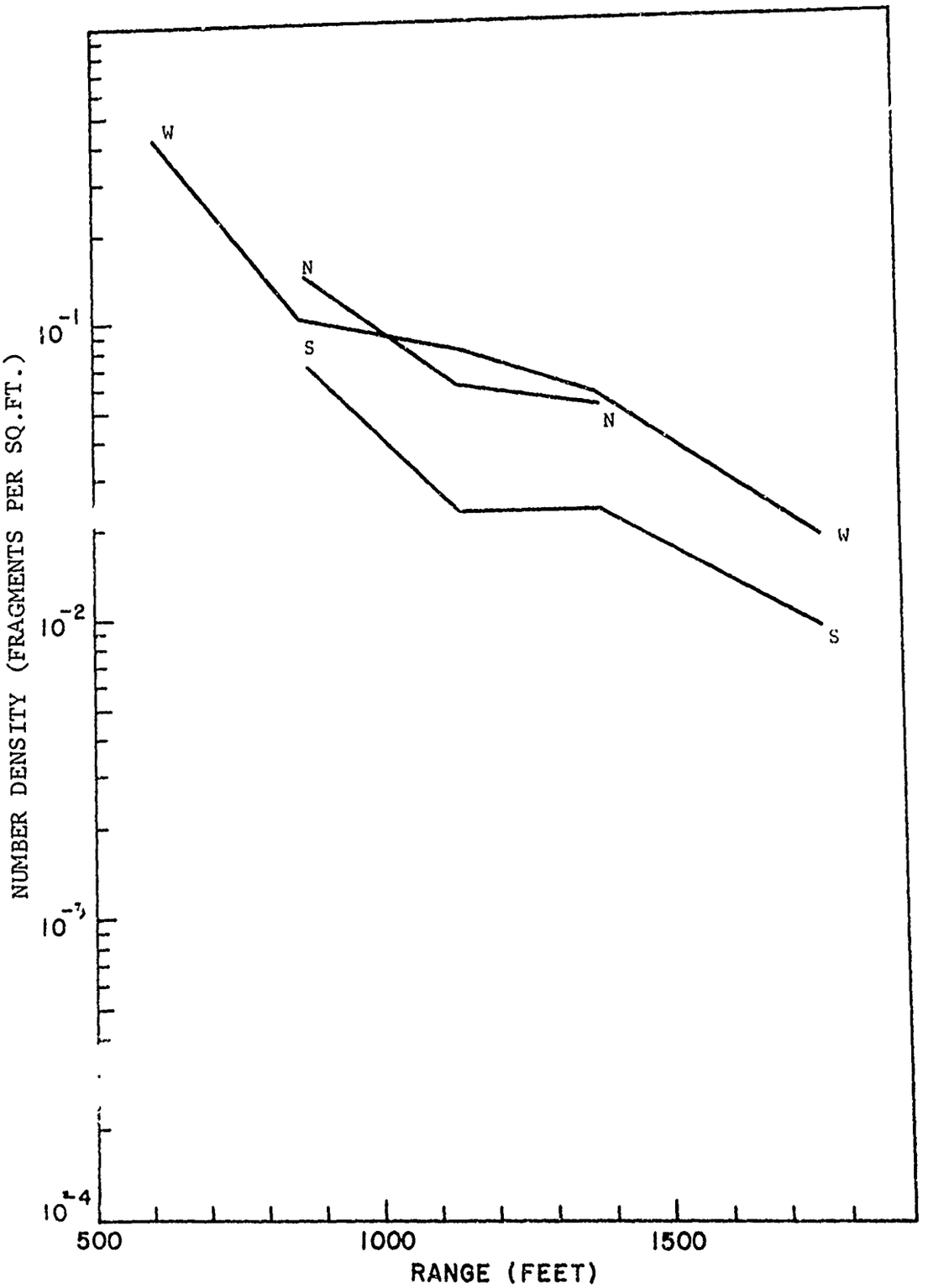

Figure 45 ESKIMO I HAZARDOUS FRAGMENT DENSITY AS A FUNCTION OF RANGE FOR 11 ft-lb ENERGY CRITERIA - RAYS N, S, W

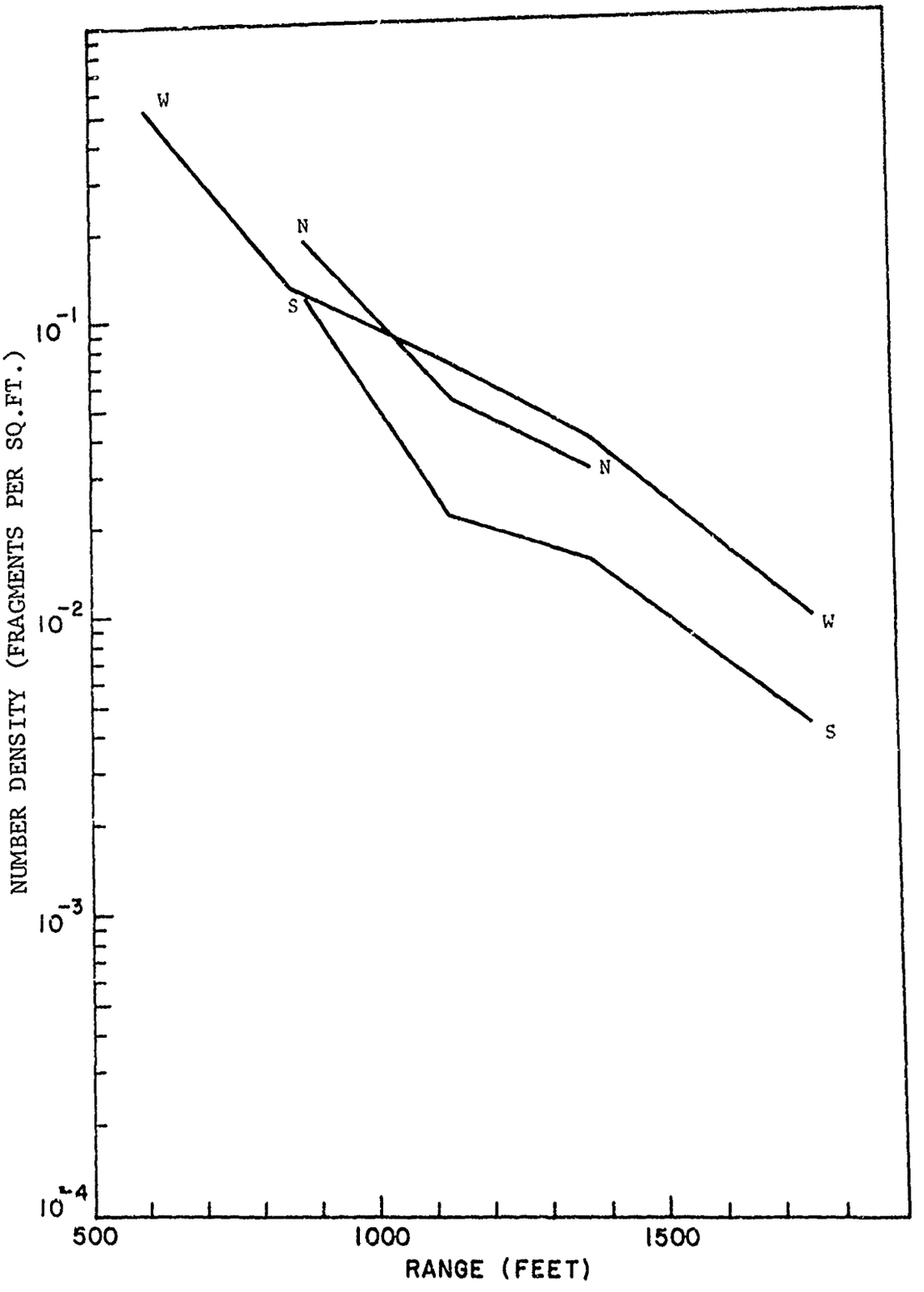

Figure 46 ESKIMO I HAZARDOUS FRAGMENT DENSITY AS A FUNCTION OF RANGE FOR 58 ft-lb ENERGY CRITERIA - RAYS N, S, W

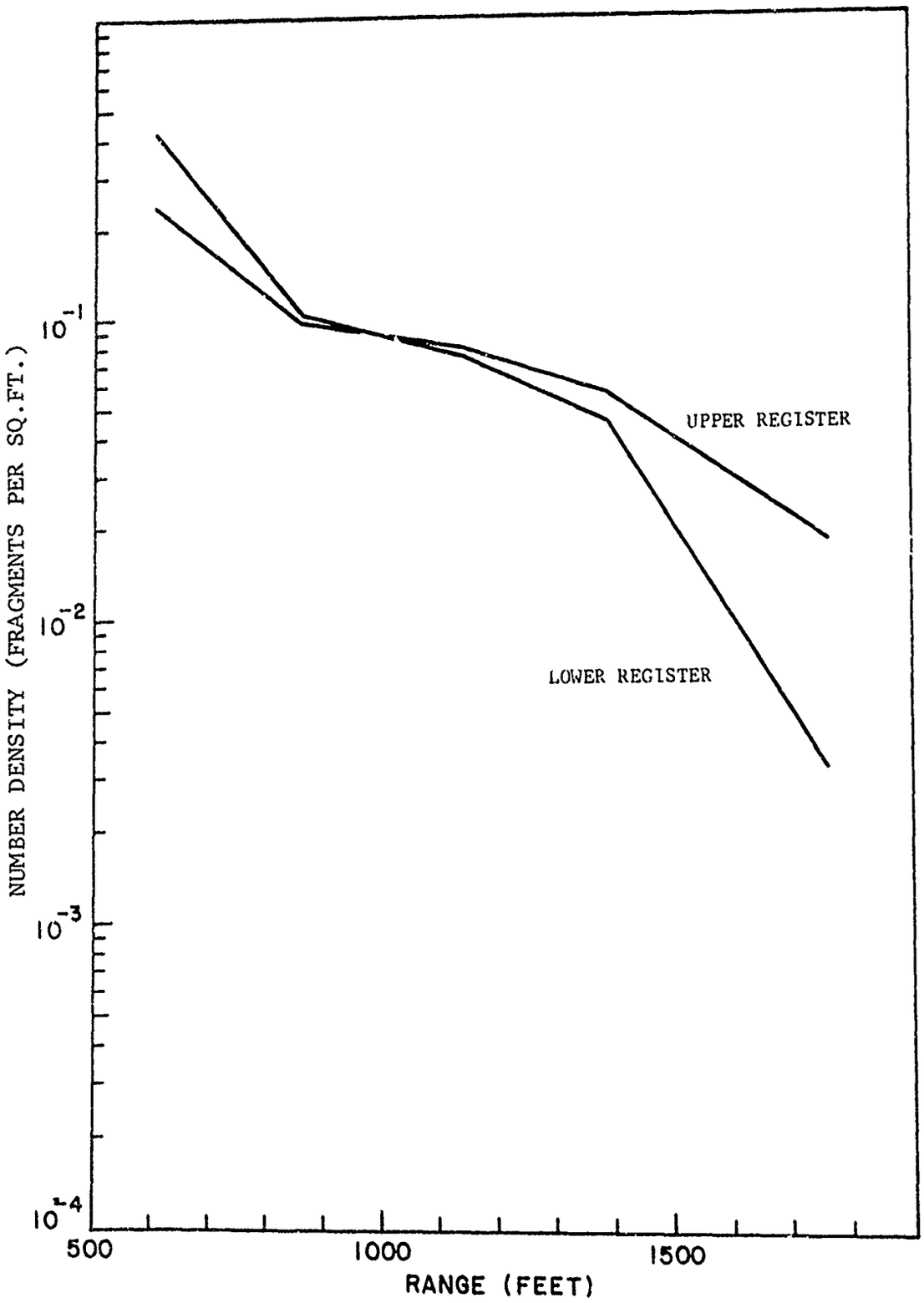

Figure 47 ESKIMO I HAZARDOUS FRAGMENT DENSITY CONTRIBUTIONS FROM UPPER AND LOWER REGISTER FOR 11 ft-lb ENERGY CRITERIA - WEST RAY

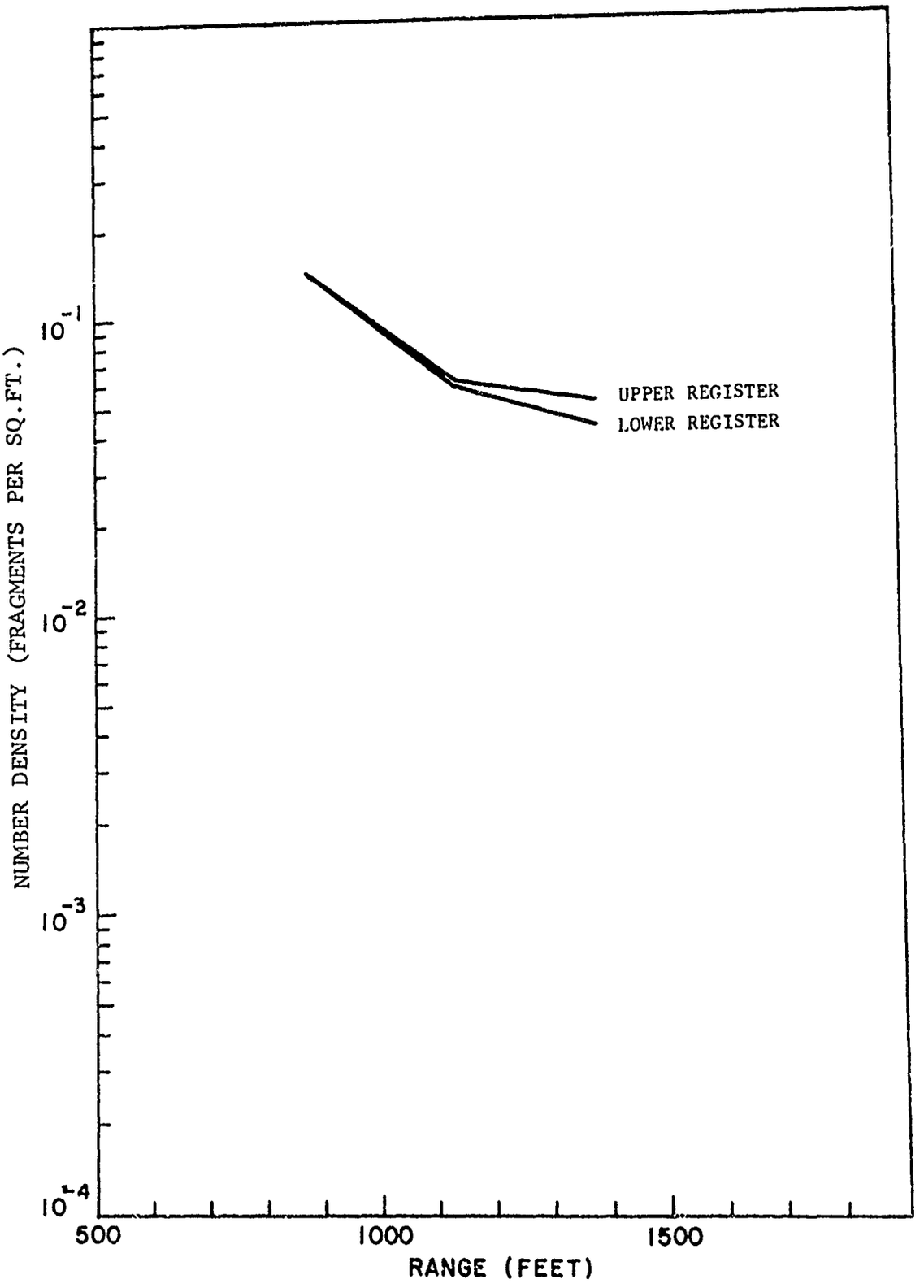

Figure 48 ESKIMO I HAZARDOUS FRAGMENT DENSITY CONTRIBUTIONS FROM UPPER AND LOWER REGISTER FOR 11 ft-lb ENERGY CRITERIA - NORTH RAY

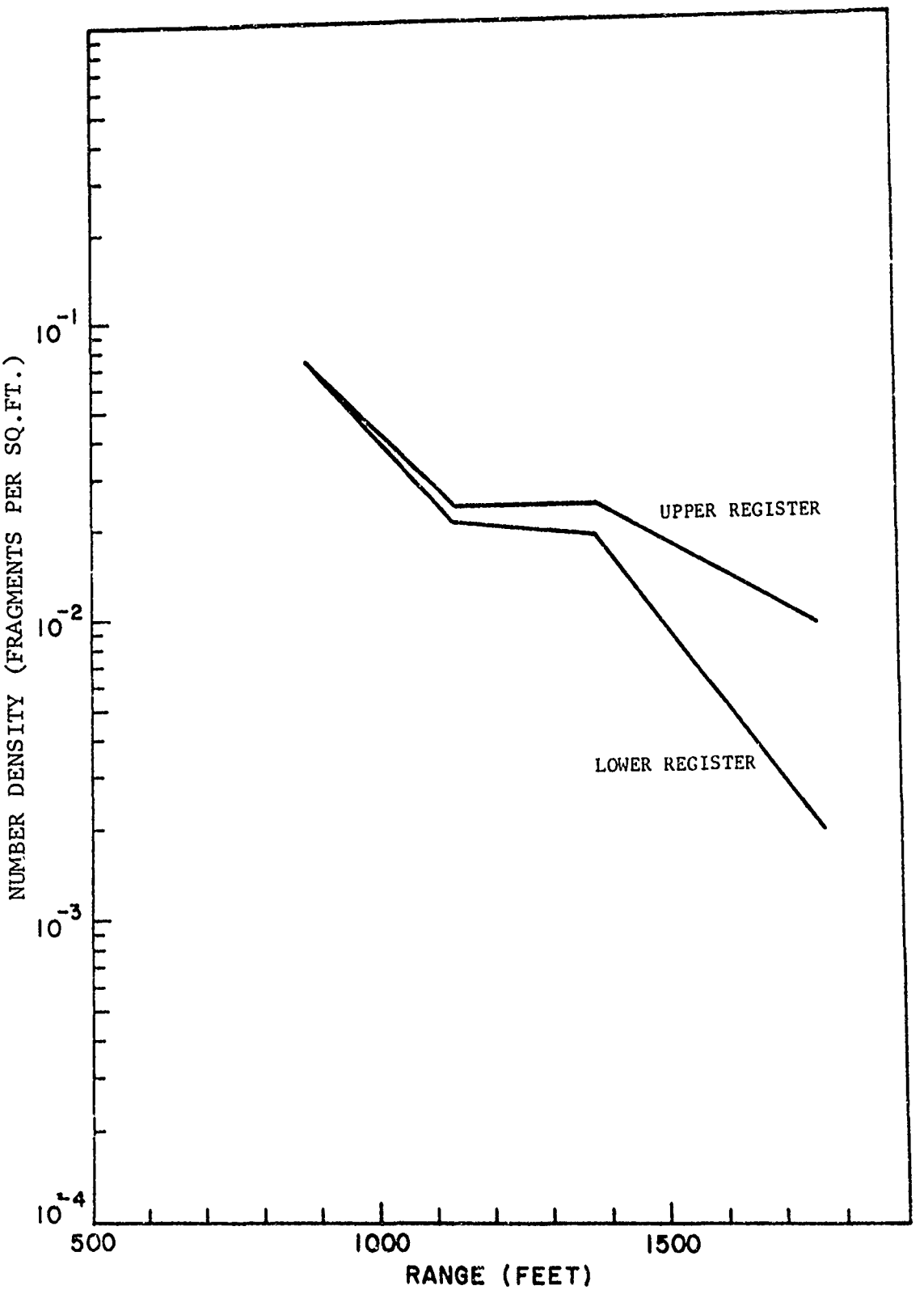

Figure 49 ESKIMO I HAZARDOUS FRAGMENT DENSITY CONTRIBUTIONS FROM UPPER AND LOWER REGISTER FOR 11 ft-lb ENERGY CRITERIA - SOUTH RAY

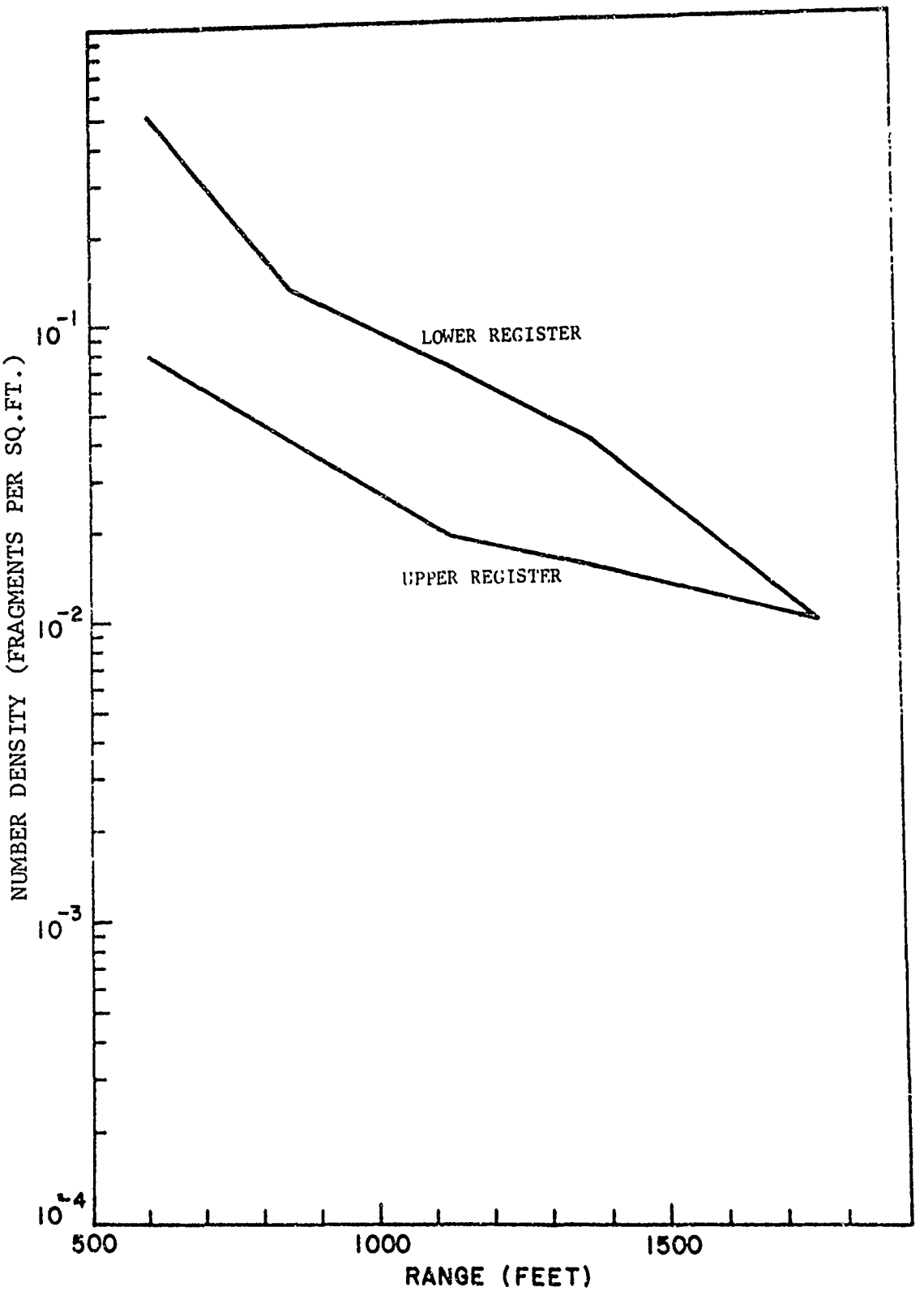

Figure 50 ESKIMO I HAZARDOUS FRAGMENT DENSITY CONTRIBUTIONS FROM UPPER AND LOWER REGISTER FOR 58 ft-lb ENERGY CRITERIA - WEST RAY

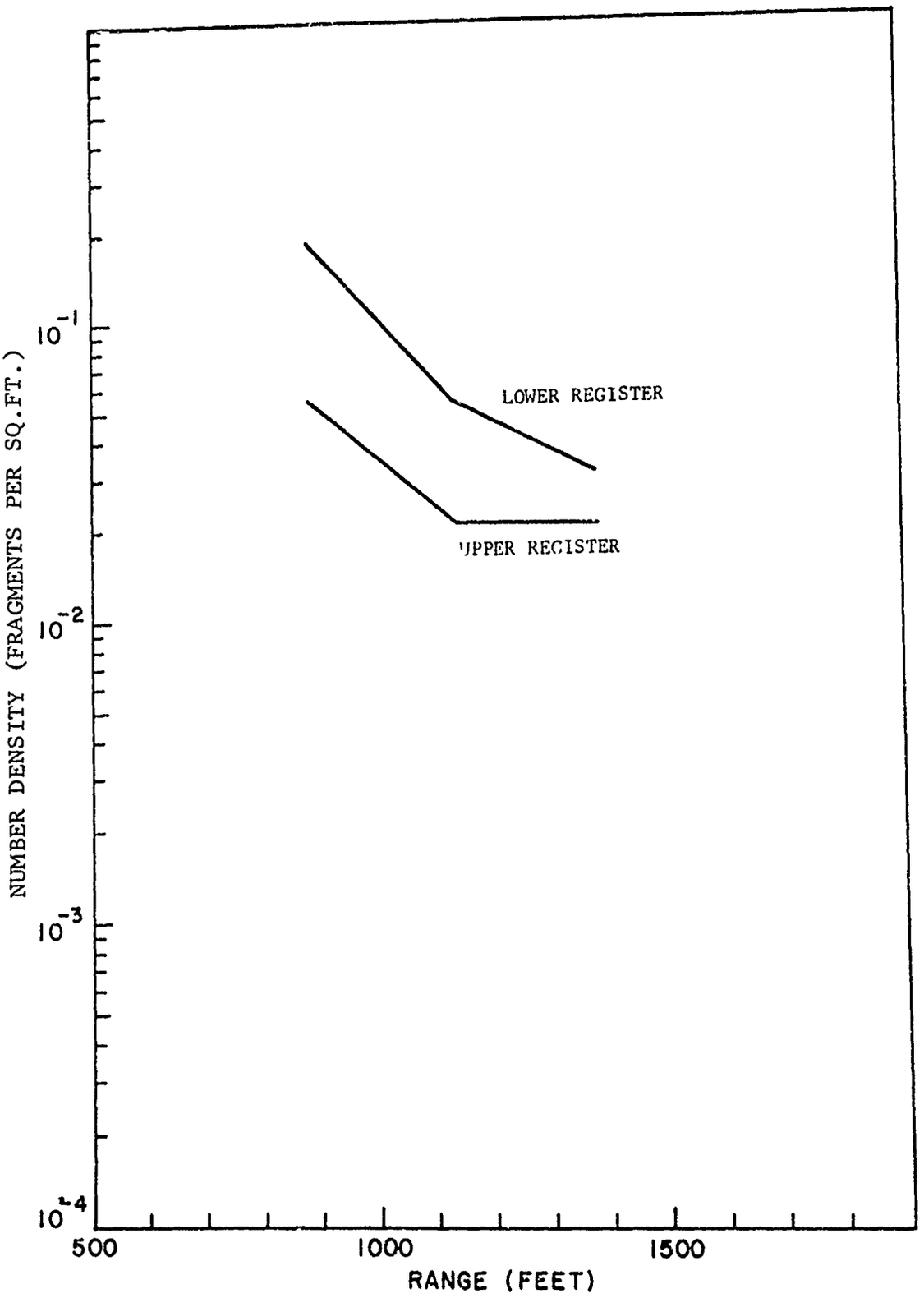

Figure 51 ESKIMO I HAZARDOUS FRAGMENT DENSITY CONTRIBUTIONS FROM UPPER AND LOWER REGISTER FOR 58 ft-lb ENERGY CRITERIA - NORTH RAY

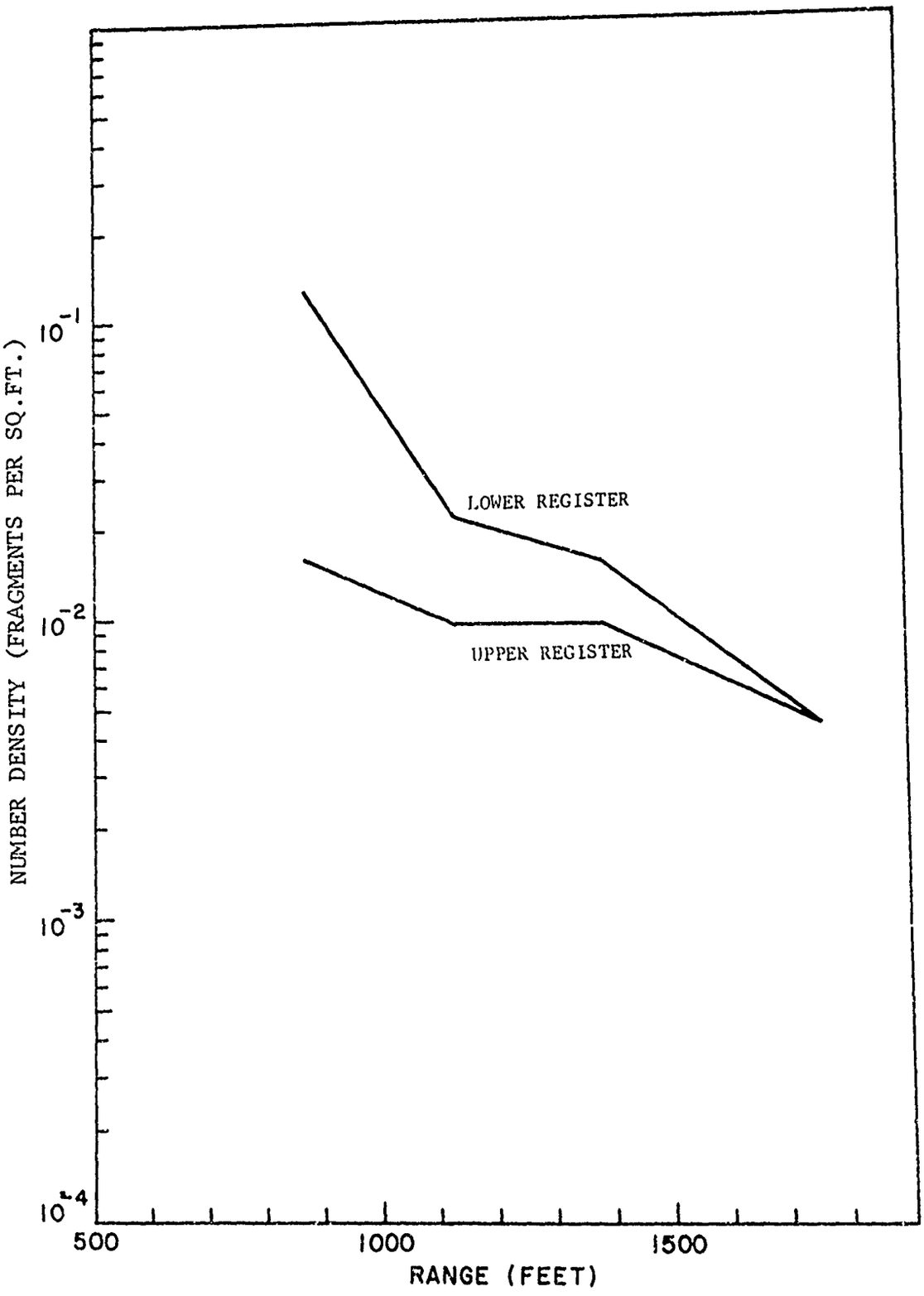

Figure 52 ESKIMO I HAZARDOUS FRAGMENT DENSITY CONTRIBUTIONS FROM UPPER AND LOWER REGISTER FOR 58 ft-lb ENERGY CRITERIA - SOUTH RAY

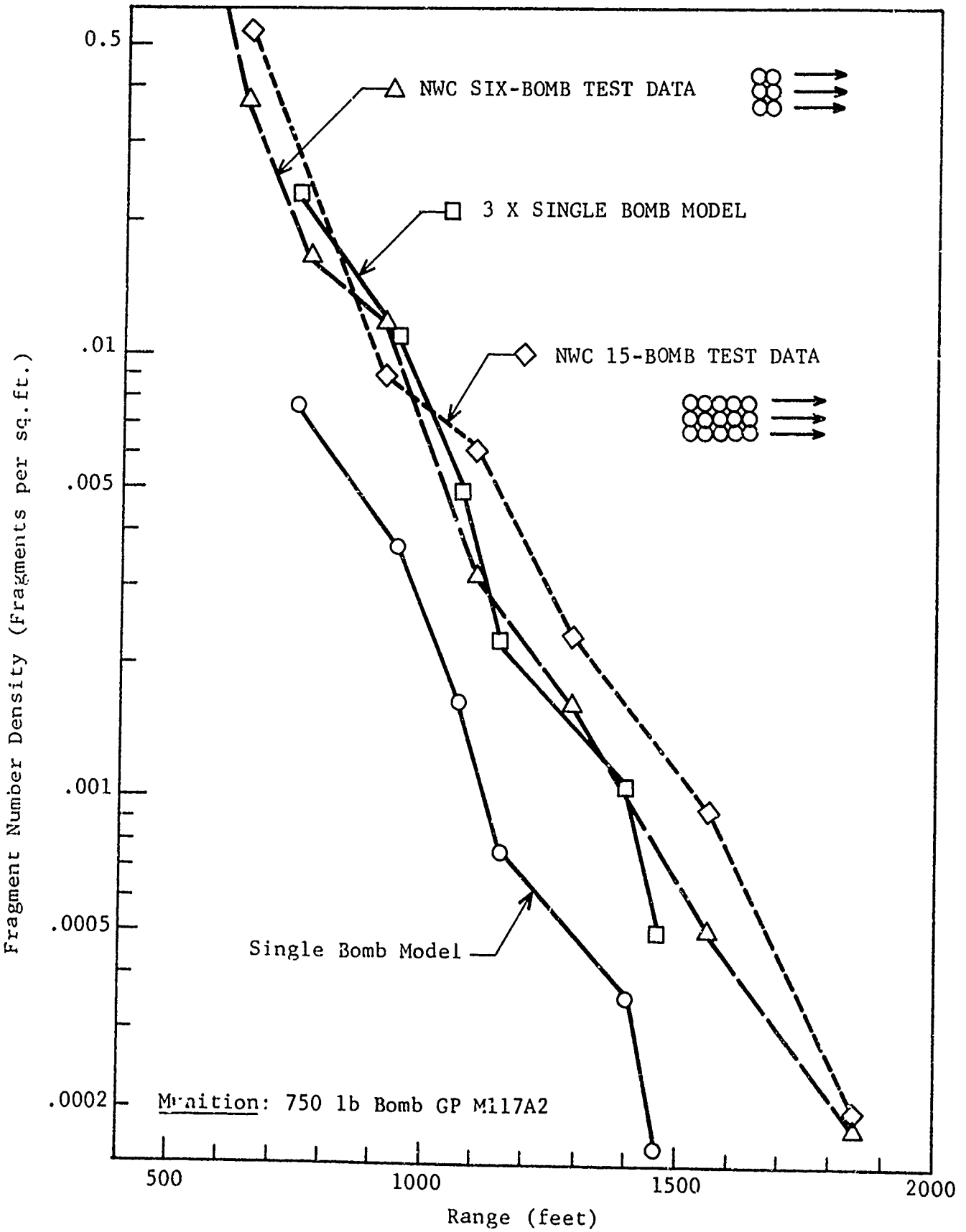

Figure 53 COMPARATIVE SIDE-SPRAY FRAGMENT DATA FOR ALL FRAGMENTS - 750 lb BOMBS

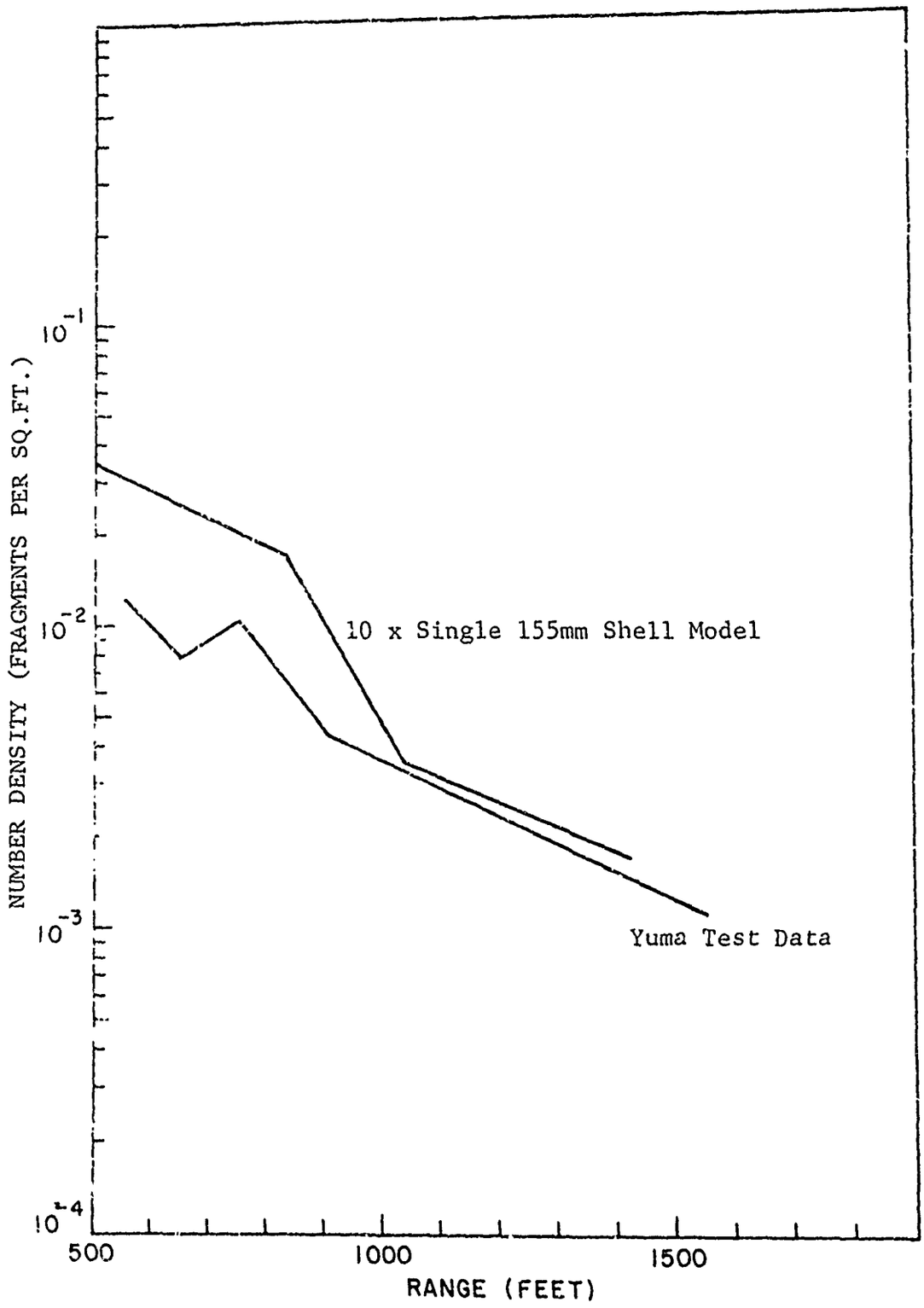

Figure 54 COMPARATIVE SIDE-SPRAY FRAGMENT DATA FOR ALL FRAGMENTS - 155mm SHELLS

This is especially true considering that the munition effectiveness data, used in generating the analytic result, have been shown to be quite different than the actual distribution of fragment sizes picked up at Yuma (e.g., Figure 17).

Similar comparisons with Eskimo I results are not, as yet, possible since changes must be made in the computer model to allow for initial shell orientations which correspond to the Eskimo I stack configuration (i.e., shells stacked nose up).

6. CONCLUSIONS AND RECOMMENDATIONS

Based upon the test results obtained in this study and their subsequent comparison with analytic results, one may conclude:

- Fragments failing to stay on a 5/8 in. sieve will not be hazardous to personnel at ranges of interest.
- Fragments can be counted, weighed, and recorded for subsequent machine processing at the rate of about 100 fragments per hour per man-machine utilizing the equipment developed in this study.
- Fragments emanating from multiple unit stacks of shells are considerably larger in size than those coming out of a single unit detonation.
- The density of Yuma fragments was greatest in the base ray, was less in the nose ray and was least in the side ray.
- The density of Yuma fragments showed a considerable falloff at about 1300 ft from the point of detonation which coincides with the point where upper register fragments begin to be more hazardous than lower register fragments.
- The effect of target size and its dependence upon fragment terminal elevation angle are responsible for a less rapid falloff of the probability of serious injury at ranges beyond 1300 ft from the Yuma test detonation point.
- While there is some similarity of fragment size distribution from individual magnet-truck pickup runs, there is also sufficient variability between runs to preclude anything but complete pickup within a sector.

- The fragment densities collected at the NWC-Eskimo I test were greater for all weight regimes than their counterpart fragment densities collected at Yuma.
- The number of fragments per sq ft falls off at about the same rate, with increasing weight fragments, for both the Eskimo I and Yuma tests.
- The Eskimo I results showed a dropoff of fragment density with increasing distance from detonation for all rays, while the Yuma test results showed a build-up in fragment density followed by a similar dropoff as in Eskimo I for the nose and base rays. The side ray of Yuma showed a similar dropoff in density with increasing distance from detonation. This might have been due to shielding of lower register fragments, at NWC, provided by adjacent acceptor igloos and the earth barricade in the north ray.
- There was a similar falloff of fragment density with range for both the Yuma and Eskimo I tests. This took place at about 1100 ft in the Eskimo I test and about 1300 ft in the Yuma test and the rate of fall-off beyond these distances was about the same.
- There was, as in the case of 750 lb bombs, close comparison between Yuma and analytic results which were generated based upon munition effectiveness data and a simple multiple of the single unit result.

From these conclusions the following recommendations are made:

(1) Future far-field fragment data should be processed, in total, counting and weighing all fragments which remain on a 5/8 in. sieve at ranges beyond 1000 ft. For closer range fragments, an analysis similar to the one made in section one of this study should be made to determine the minimum fragment size of interest. In addition, new pickup techniques other than the use of a magnet truck should be given consideration. Such a technique might include the random placement of 100 x 100 ft patches of wire screening material throughout the far-field (i.e., random over the entire test area and not just covering specific rays). Such a procedure would allow for rapid deployment of collection zones and the screening material could also serve as a container for the collected fragments.

(2) As a result of the many similarities between the Yuma and Eskimo I tests, in terms of similar hazards for two quite different multiple unit stack configurations, and the close comparison of Yuma results with computer generated results, a testing program should be initiated to develop empirical scaling relationships between analytically derived results for a single unit munition and an approximation of the hazard due to an arbitrary multiple unit configuration of the same munition. Such scaling relationships should consider stack configuration parameters and the detonation characteristics of the stack.

(3) Another testing program should be initiated aimed at characterizing the near-field distribution of fragments (i.e., munition effectiveness data) emanating from multiple unit sources since this is the input required by the computer model to compute the far-field hazard. Again, such a testing program should consider detonation characteristics as well as stack configuration.

(4) Minor changes should be made on the computer model so as to obtain the ability of generating results for a munition source whose longitudinal axis is oriented at an arbitrary angle with the ground. Presently, only an angle of zero is considered and munitions stacked on end cannot be considered.

(5) Finally, an interim technique for determining the fragment hazard of multiple-unit stacks should be developed. Based upon the similar results obtained in the Yuma and Eskimo I tests, there seems to be a characteristic distance at which hazardous fragment density begins to fall off rapidly regardless of stack configuration or the number of units in the stack. If this is so, then a conservative approach might be to adopt this distance adjusted by some factor of safety.

APPENDIX

TREATMENT OF YUMA TEST FRAGMENT DATA

After weighing and counting the 18,655 fragments of interest, the punched paper tape containing the weights of each fragment was converted to punch paper cards for ease of handling. These cards were checked for errors and placed on a magnetic disk file named OUTSET. Since the weighing process was divided into two phases (i.e., fragments remaining on a 1 in. sieve and those remaining on a 5/8 in. sieve), the first task was to merge these data into file OUTST1. This new file contained complete ordered data sets for the fragments counted and organized by collection bag. A cumulative weight distribution was derived for each bag in order to determine the similarity, if any, among bags of fragments collected within a given sector.

The data in file OUTST1 were merged into complete ordered data sets for each sector and this file was denoted OUTST2. This file was further merged into a complete ray data set, file OUTST3. Finally, a data set was generated for all fragments counted and labeled file OUTST4. Two sets of cumulative weight distributions were derived from files OUTST2, OUTST3, and OUTST4. The first set consisted of sector, ray and total distributions for all individually weighed fragments. The second set consisted of these distributions for the weighed fragments with the net weight of the unweighed fragments included. The derivation of these distributions was accomplished by adding fragment weights in ascending order until some percentile increment was exceeded.

Cumulative number (i.e., frequency) distributions were derived for each of the three data sets. Logarithmic weight increments were chosen and the total number of fragments weighing more than a given increment was computed. Since the fragment pickup was not accomplished within uniform areas, these distributions were normalized to 1 sq ft.

File OUTST5, the fragment trajectory data, was created from the merged sector data set. Lower register velocity was computed as a function of weight and range (i.e., assumed uniform in a

sector) by an iterated perturbation method (Ref. 4). The lower register launch and impact angles were also determined. Upper register velocity was determined as a function of weight by

$$V = (g/\beta)^{1/2} \qquad \text{(A-1)}$$

where g is the acceleration due to gravity and β is given by

$$\beta = C_D w/2(w'^2 W)^{1/3} \qquad \text{(A-2)}$$

where C_D is the drag coefficient (~1.28), w is the specific weight of air (.310 grains/in.^{3}), w' is the ballistic density of a fragment (~ 660 grains/in.^{3} for shell fragments and 590 grains/in.^{3} for bomb fragments), and W is the weight of the fragment. Equation (A-1) assumes a fragment in free fall with velocity in the downward vertical direction. Fragment energy was determined as

$$E = WV^2/2g \qquad \text{(A-3)}$$

where V was either the upper or lower register velocity. Finally, the target area for a person was determined. A standing man was considered to have 9 sq ft frontal area and 1.33 sq ft area normal to the ground. An upper register fragment was assumed to be falling normal to the ground and therefore the corresponding target area was always 1.33 sq ft. A lower register fragment impacted the target at some angle between 0 and -90 degrees. The target area was assumed to be the projection of the frontal and horizontal components of a target on a plane normal to the impact direction. A_T, the target area is given by

$$A_T = 9 \cos \alpha - 1.33 \sin \alpha \qquad \text{(A-4)}$$

where α is the terminal impact angle.

Using the data stored in OUTST5, hazardous fragment densities for 1 sq ft were computed. Two hazardous energy criteria were used (i.e., 11 and 58 ft-lbs) and the respective densities for these criteria were determined. A fragment was assumed to have the greater of its upper and lower register energies. These

densities were also computed for cases when all fragments were assumed lower register and when all fragments were considered upper register.

Finally, the target damage probability was computed for each sector as

$$q = 1 - \exp\ (N_L A_L + N_H A_H) \qquad \text{(A-5)}$$

where N_L is the number density of lower register hazardous fragments, A_L is the average lower register target area, N_H is the number density of upper register hazardous fragments and A_H is the upper register target area (i.e., 1.33 sq ft). Since 1.33 sq ft is the minimum target area produced by a standing person, a lower register fragment will always have a larger target than an upper register fragment. Hence, a hazardous lower register fragment will be more probable a cause of target damage than a hazardous upper register fragment. Therefore, in cases where both the upper and lower register energy of a fragment were above the hazardous threshold, the fragment was assumed to be lower register. The hazard was computed for both the 11 and the 58 ft-lb criteria.

REFERENCES

1. Zaker, T. A., et al., Fragmentation Hazard Study, Phases I and II, IITRI Final Report J6176 for the Armed Services Explosives Safety Board under Contract DAHC-04-69-C-0056, April 1970.

2. Feinstein, D. I., et al., Fragmentation Hazard Study, Fragment Hazards From Detonation of Multiple Munitions in Open Stores, Phase III, IITRI Final Report J6176 for the Armed Services Explosive Safety Board under Contract DAHC-04-69-C-0056, August 1971.

3. Feinstein, D. I., Fragmentation Hazards to Unprotected Personnel, IITRI Final Report J6176 for the Department of Defense Explosives Safety Board under Contract DAHC-04-69-C-0056, January 1972.

4. Zaker, T. A., Trajectory Calculations in Fragment Hazard Analysis, Minutes, Thirteenth ASESB Seminar, 101-115, September, 1971.

5. Feinstein, D. I., Fragmentation Hazards to Unprotected Personnel, Third Monthly Progress Report on IITRI Project J6176 for the Department of Defense Explosives Safety Board, October 1971.

6. Smith, H. C., Static Detonation Test (Special Study) of Separate-Loading 155mm Projectiles Containing 15000 lbs of TNT, Yuma Proving Grounds Project 489, July 1970.